ESD-TR-68-288

MTR-733

THE MODIFIED SPACE-A TRAJECTORY GENERATION PROGRAM

NOVEMBER 1968

W. L. Wallace

R. H. Wiggins

Prepared for

DIRECTORATE OF PLANNING AND TECHNOLOGY

ELECTRONIC SYSTEMS DIVISION
AIR FORCE SYSTEMS COMMAND
UNITED STATES AIR FORCE
L. G. Hanscom Field, Bedford, Massachusetts

Project 7070

Prepared by

THE MITRE CORPORATION
Bedford, Massachusetts

Contract AF19(628)-5165

THE MODIFIED SPACE-A TRAJECTORY GENERATION PROGRAM

NOVEMBER 1968

W. L. Wallace

R. H. Wiggins

Prepared for

DIRECTORATE OF PLANNING AND TECHNOLOGY

ELECTRONIC SYSTEMS DIVISION
AIR FORCE SYSTEMS COMMAND
UNITED STATES AIR FORCE
L. G. Hanscom Field, Bedford, Massachusetts

Project 7070

Prepared by

THE MITRE CORPORATION
Bedford, Massachusetts

Contract AF19(628)-5165

FOREWORD

The SPACE-A program described in this report is a modified version of the trajectory and observation generation portion of the Sequential Position and Covariance Estimation (SPACE) program originally acquired from NASA. This document contains a detailed analysis of the equations and models used by the program, a brief description of the routines used in the program, as well as instructions for its operation. The principal applications of SPACE-A are the prediction of space-vehicle trajectories and the generation of observational data plus other trajectory related information.

There have been numerous changes made in the original program in addition to its adaptation to the IBM 7030 and its subsequent debugging. The modified SPACE-A program is the result of the efforts of the authors and L. E. Wilkie. S. Schwartz aided in the debugging and rewriting of certain routines. Special thanks and appreciation are due to R. K. Squires, D. S. Woolston, and other members of the Special Projects Branch, Theoretical Division of the Goddard Space Flight Center from whom the SPACE program was obtained.

The work reported in this document was performed by The MITRE Corporation, Bedford, Massachusetts, for the Directorate of Planning and Technology, Electronic Systems Division, of the Air Force Systems Command under Contract AF 19(628)-5165.

REVIEW AND APPROVAL

Publication of this technical report does not constitute Air Force approval of the report's findings or conclusions. It is published only for the exchange and stimulation of ideas.

ANTHONY P. TRUNFIO
Technical Advisor, Development Engineering Div.
Directorate of Planning and Technology

ABSTRACT

This report describes the SPACE-A program presently available for operational use. SPACE-A is the trajectory and observation generation portion of the Sequential Position and Covariance Estimation Program (SPACE) which is currently under development. The document contains a detailed analysis of the equations and models used by the program, a brief description of routines used in the program, as well as instructions for its operations. The principal applications of SPACE-A are the prediction of the space-vehicle trajectories and the generation of observational data plus other trajectory related information.

TABLE OF CONTENTS

TABLE OF CONTENTS
(concluded)

LIST OF FIGURES

LIST OF TABLES

SECTION I
OBJECTIVES

INTRODUCTION

The SPACE trajectory determination program was originally developed for the Special Projects Branch, Theoretical Division, Goddard Space Flight Center by the Sperry Rand Systems Group. It was designed as a comprehensive trajectory determination and tracking program for both orbital and deep space flights. The original program consisted of three major modes of operation:

(1) SPACE-A, designed for trajectory and observation generation without statistical processing.

(2) SPACE-B1, designed for statistical estimation of the six state variables describing the position and velocity at prescribed points of the trajectory.

(3) SPACE-B2, designed for statistical estimation of the six state variables describing position and velocity plus up to 20 additional states selected from a group of variables which permit estimation of dynamic biases (parameters affecting orbital motion) or observational biases (affecting measurements).

The version of the SPACE program received by MITRE contained numerous errors in programming. SPACE-B1 and SPACE-B2 had never been debugged and many of the routines of SPACE-A were unworkable. In addition, the programming had to be made compatible with the IBM 7030. Therefore, a large effort was put into checking the theory, debugging the program, and revising or rewriting certain routines. Many checkout runs were necessary during and after the debugging of the program.

Since the SPACE-B2 mode includes the capabilities of the SPACE-B1 mode, the SPACE-B1 mode was not debugged. The original SPACE-B2 (which was not operational when received by MITRE) employed two different statistical estimation techniques:

(1) a minimum variance sequential filtering technique, the so-called "Kalman filter", and

(2) a non-recursive batch processing technique.

Because a number of trajectory estimation programs at MITRE already employ the batch processing technique, the second option of the SPACE-B2 mode was left in a non-operational status. The first option of SPACE-B2, which incorporates the Kalman filter in the trajectory estimation procedure, is presently being debugged and checked out. The theory, programming, and results of its operation will be published in a succeeding document. The theoretical development and much of the programming of the trajectory generation portion of SPACE-B2 is identical with that used in SPACE-A.

This document deals with the modified SPACE-A trajectory generation program written in Fortran IV and is presently operational on the IBM 7030 at MITRE. This report is based on the original documents[1,2,3] published by Sperry Rand for NASA.

Section I contains a brief discussion of the objectives and capabilities of SPACE-A. Section II discusses the theoretical background, as well as the equations and methods employed by the program. Section III consists of a user's guide for operating the program. Section IV gives the program structure and a brief description of the function of each subroutine.

The larger part of the report is contained in Section II since understanding or following the programming is really a matter of following the appropriate equations. Although parts of Section II are original, the contents of pertinent sections of the SPACE Analytic Manual[1] have been freely used or modified to fit the description of the present program. Sections III and IV closely follow the format of the original User's Manual[2] and Programmer's Manual[3]; however, since a number of changes in programming have been made, only Section III and Section IV of this report should be used in operating the modified SPACE-A trajectory generation program.

CAPABILITIES

The modified SPACE-A trajectory generation may be run in any of the following modes:

(1) Trajectory generation - the computation of position and velocity of the vehicle at regular time points along a trajectory.

(2) Observation generation - the computation of certain ground-based observations of the vehicle at regular time points.

(3) Simulated data - the computation and writing onto tape of the observations in a format suitable for processing data by SPACE-B2.

(4) Visibility computation - the time of initial view of the vehicle by a given station, the total time in sight by the station, and the observations while the vehicle is in sight.

The required input consists of the initial date and initial time of a particular run and the initial position and velocity of the vehicle. When the effect of drag is to be included which is usually the case, the effective area and mass of the vehicle and the magnitude of solar flux must be specified. When the effect of direct solar radiation is included, an effective area pertaining to solar radiation must be specified. For observation calculations, the specification of the station location on the surface of the Earth is necessary. The details of the units and format of these required inputs along with other optional input features are discussed in Section III. The types of output data, which consist primarily of trajectory and/or observation information, is also given in Section III.

The philosophy behind the modified SPACE-A trajectory generation program is that its primary use would be for Earth orbital trajectories. Toward this objective, its dynamic model includes the effects of the primary term and oblateness perturbations of the Earth's gravity, the solar, lunar, and planetary gravitational perturbations, the effect of direct solar radiation and drag, as well as such dynamic effects as precession, nutation, and the daily rotation of the Earth.

The model used for drag is a combination of the U.S. Standard Atmosphere 1962 and the Harris-Priester model for the upper atmosphere, which depends on the magnitude of solar flux. The model for Earth gravitational oblateness may include up to nine zonal harmonics, four sectorial harmonics, and twelve additional tesseral harmonics. The types of ground station observations that may be specified are given in Section II (see OBSERVATIONS).

Although the modified SPACE-A program is intended primarily for Earth orbital trajectories, it may be used for other types of missions. However, a number of options that were included in the original SPACE-A trajectory generation program are not presently operational. These options were a capability for modeling the perturbations due to thrust, a model for lunar libration, simple models for lunar gravitational oblateness perturbations, as well as models for the drag of Mars and Venus, and a capability for computing on-board observations from a vehicle. Although these options are not presently available in the modified SPACE-A program, with some effort they could also be included.

SECTION II
THEORY

GENERAL DESCRIPTION OF TRAJECTORY COMPUTATION

Orbit prediction or trajectory computation is the process of calculating the position and velocity of a vehicle at any time subsequent to some initial time, provided the initial position and velocity of the spacecraft are given.

To accomplish this prediction, one uses the laws of celestial mechanics embodied in the differential equations of motion. The forcing functions for the equations of motion are obtained from a dynamic model which accounts for the accelerations on the vehicle. A reference frame is erected to express the components of the various vector quantities, and the equations of motion are numerically integrated subject to the given initial conditions. Once the vehicle trajectory is determined, the program can then generate observations.

The coordinate system used in this program is based upon the position of the mean Earth's equator and equinox at 0^h 1 January of the year subsequent to the initial input time of the program. Coordinate directions of this frame are inertial with respect to the fixed stars; the center of origin of the system, however, may be transferred from one central body to another so that the spacecraft motion is specified relative to a point mass which itself has a proper motion. This reference frame is called the Base Date System or simply the inertial system.

Observations made from the Earth are necessarily in a system different from the Base Date System. To accomplish transfer between various coordinate systems, transformations are provided (see COORDINATE SYSTEMS AND TRANSFORMATIONS). These transformations include the dynamical effects of precession, nutation, and daily rotation of the Earth.

All accelerations acting on the vehicle are specified in the Base Date System. The gravitational attractions of bodies in the solar system are functions only of position with respect to the vehicle; consequently, the program employs an ephemeris giving planetary coordinates relative to the Sun, and lunar coordinates relative to the Earth, all in a Base Date System. A Base Date System is specified for overlapping two-year blocks of data, the date corresponding to the middle of the two-year file. Specifying an initial time causes the program to choose an ephemeris file having as its Base Date the beginning of the year following the initial input time of the program. In this way, at least one full year of ephemeris information is available before a change of reference system is necessary.

Another acceleration specified in the Base Date System without transformation is that arising from solar radiation pressure. Since this acceleration is a function of relative position between the Sun and the vehicle, its direction is given in the proper frame by using information from the ephemeris.

Other accelerations, such as perturbations due to Earth oblateness effects must be transformed through nutation and precession to the proper frame. All positions, velocities and accelerations are computed in canonical units (i.e., Earth radii (ER), Earth radii per hour (ER/hr), Earth radii per hour per hour (ER/hr^2), respectively) and appropriate constants are used to transform to other units of measure.

Vehicle motion is always computed relative to some reference body; a planet; the Moon; the Sun. Consequently, the equations of motion contain a term which accounts for the acceleration of the reference body on the vehicle. The remaining accelerations are usually, but not always, much smaller than this primary acceleration and are therefore called perturbations. In most cases, they can be regarded as giving rise to small disturbances in the orbit determined by the reference body and the initial conditions.

Reference bodies are changed during a trajectory calculation when the vehicle leaves the "region of influence" associated with a particular body. Regions of influence are computed for a body with respect to the object of which it is a satellite. Hence, each planet has a region of influence defined relative to the Sun, and the Moon has a similar region defined relative to the Earth. In transferring into or out of such a region, velocity as well as position with respect to the new reference body must be calculated.

Since no analytic solution exists for the equations of motion, numerical methods are employed to compute the components of position and velocity. In the program, a choice may be made between using straightforward integration and using Encke's method. The former technique, called Cowell's method, is conceptually simple, but suffers from precision and machine running time problems. Encke's method, although somewhat more complicated, gives dividends in both precision and machine efficiency. In this procedure, the Keplerian orbit arising from the reference body central force field is taken as a nominal trajectory. The perturbation accelerations are integrated and the resulting position and velocity increments are added to the Keplerian solutions. Naturally, Encke's method is most effective when the perturbations are small.

The present program has the capability to compute a number of ground-based observations. Corrections are provided for the refraction of an electromagnetic signal by the troposphere and by the ionosphere. Adjustments are computed for errors in elevation angle, range, and radial velocity; other angular corrections are calculated from the adjustment in elevation angle.

Description of the basic equations used by the program for the dynamic model now follows. It includes derivations of the accelerations due to the planets, Earth oblateness, drag, and direct solar radiation pressure. It also discusses the coordinate systems, numerical integration methods, and observation calculations including the

refraction model used by the program.

DYNAMIC MODEL

The equations of motion for a space vehicle are second-order differential equations which describe the accelerations arising from the forces acting on the vehicle. These forces can be classified as follows:

(1) Gravitational acceleration of the reference body - primary.

(2) Gravitational perturbations due to other bodies (e.g., planets).

(3) Gravitational perturbations due to reference body oblateness.

(4) Perturbations due to drag.

(5) Perturbations due to direct solar radiation pressure on the space vehicle.

For orbit determination the reference body primary gravitational force almost always predominates the perturbation forces given above. The only exception occurs during reentry of a vehicle into the atmosphere, when drag forces may be larger than the primary force of gravity. Another force which may exceed the primary force of gravity is that of vehicle thrust. Since this program is designed primarily for orbital computations, this force is not discussed here although it can be readily included if desired.

The simplest gravitational force field is that due to a single point mass or equivalently that due to a homogeneous ponderable body which is perfectly spherical. In this case the equations of motion of a vehicle with respect to the ponderable reference body are:

$$\ddot{\vec{R}} = -\frac{\mu \vec{R}}{R^3} \tag{1}$$

where

$\mu = G(M+m) \approx GM$, since $m << M$

G is the universal gravitational constant,

M is the mass of the reference body,

m is the mass of vehicle,

$\vec{R}$ is the vector position of the vehicle with respect to the reference body center.

With initial conditions $\vec{R}_0$ and $\dot{\vec{R}}_0$ Equation (1) defines a "two-body" or Keplerian orbit, which arises from the primary reference body central force field and which may be expressed in closed form in terms of its true or eccentric anomaly.

The above "two-body" dynamic model may be extended to include perturbational accelerations acting on the vehicle, in which case Equation (1) becomes:

$$\ddot{\vec{R}} = -\frac{\mu\vec{R}}{R^3} + \vec{P}_1 + \vec{P}_2 + \vec{P}_3 + \vec{P}_4 \qquad (2)$$

where

$\vec{P}_1$ is the summation of all the accelerations arising from planetary, lunar and solar attraction,

$\vec{P}_2$ is an acceleration arising from the oblateness of the reference body,

$\vec{P}_3$ is an acceleration arising from drag as derived from an appropriate model to be described later, and

$\vec{P}_4$ is an acceleration due to direct solar radiation upon the vehicle neglecting reflected sunlight from the reference bodies or planets.

The perturbational accelerations $\vec{P}_1$, $\vec{P}_2$, $\vec{P}_3$, and $\vec{P}_4$ are obtained from specific dynamical models whose details are described below.

PERTURBATIONS DUE TO PLANETARY ATTRACTIONS

The general expression for the perturbational acceleration, $\vec{P}_1$, of a space vehicle due to the gravitational influence of the Sun, Moon, and other planets (excluding the reference body) is given by:

$$\vec{P}_1 = \sum_j -\mu_j\left[\frac{\vec{R}_{vj}}{R_{vj}^3} - \frac{\vec{R}_{rj}}{R_{rj}^3}\right] \qquad (3)$$

where

$\mu_j = GM_j$

G is the gravitational constant,

M_j is the mass of the j^{th} body,

$\vec{R}_{vj}$ is the position of the vehicle with respect to the j^{th} body, (Figure 1)

$\vec{R}_{rj}$ is the position of the reference body with respect to the j^{th} body, (Figure 1)

$\Delta\vec{R}$ is the position of the vehicle with respect to the reference body (Figure 1).

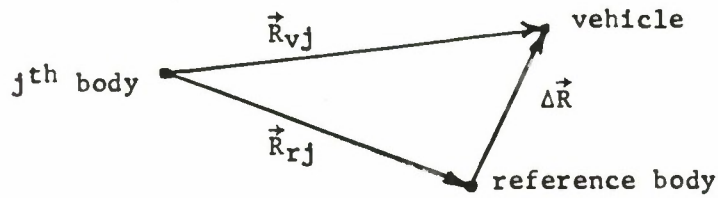

Figure 1. Vectors for Planetary Attractions

If the two terms of the bracketed expression in Equation (3) are very nearly equal, a loss of accuracy due to round-off errors by machine computations will occur. Equation (3) can be written in a more convenient form due to Battin[4] thereby eliminating this problem. Using Equation (3), and Equation (4) below and rearranging terms one obtains Equation (5).

$$\Delta\vec{R} = \vec{R}_{vj} - \vec{R}_{rj} \tag{4}$$

$$\vec{P}_1 = \sum_j \frac{\mu_j}{R_{vj}^3} \left[\vec{R}_{rj} \left(\frac{R_{vj}^3}{R_{rj}^3} - 1\right) - \Delta\vec{R}\right] \tag{5}$$

This latter form is used to achieve more computational accuracy. The actual programmed equations, which can readily be shown equivalent by substitution are:

$$\vec{P}_1 = \sum_j \frac{\mu_j}{R_{vj}^3} \left[\vec{R}_{rj} \left(f(U)\right) - \Delta\vec{R}\right] \tag{6}$$

where

$$f(U) = \frac{U[3 + U\ (3+U)]}{1 + (1+U)^{3/2}} \tag{7}$$

$$U = \frac{2(\vec{R}_{rj} + \Delta\vec{R}) \cdot \Delta\vec{R}}{R_{rj}^2} \tag{8}$$

The forces introduced by solar, lunar and planetary attractions in orbit prediction about the Earth are usually smaller by a factor of 10^{-7} than that of the primary attraction of the Earth's gravitational pull. Planetary perturbations (including solar and lunar perturbations) do have a significant effect on a vehicle trajectory over long time periods or for deep space probes.

PERTURBATIONS DUE TO EARTH OBLATENESS

The fact that the Earth is not a perfect sphere of uniform density gives rise to perturbational accelerations due to Earth oblateness. Formulas are derived below which the program uses to include these perturbations in the prediction of near-Earth trajectories. In a coordinate system attached rigidly to the Earth, the Earth oblateness perturbation may be treated as the acceleration of a conservative force derivable from a potential. Thus:

$$\vec{P}_2 = -\nabla U \tag{9}$$

The potential function is given by Equation (12) and the final form of the acceleration $\vec{P}_2$ is given by Equations (26)-(29) and Equation (32) below.

The Geopotential Function

The geopotential function can be derived from the basic property that the potential, U, satisfies Laplace's Equation[5, pp. 117, 118].

$$\nabla^2 U = 0. \tag{10}$$

In spherical coordinates, Equation (10) becomes

$$\nabla^2 U = \frac{1}{r^2 \cos\phi}\left[\frac{\partial}{\partial r}\left(r^2 \cos\phi \frac{\partial U}{\partial r}\right) + \frac{\partial}{\partial \phi}\left(\cos\phi \frac{\partial U}{\partial \phi}\right) + \frac{\partial}{\partial \lambda}\left(\frac{1}{\cos\phi}\frac{\partial U}{\partial \lambda}\right)\right] = 0 \tag{11}$$

Although the solution of Equation (11) is not elementary, the equation may be solved by applying the method of separation of variables and using Legendre polynomials[6, p.40]. The solution of Equation

(11) is given by:

$$U = -\frac{\mu}{r} \sum_{n=0}^{\infty} \left(\frac{R_e}{r}\right)^n \sum_{m=0}^{n} \left\{P_n^m (\sin \phi) \left[C_{n,m} \cos m\lambda + S_{n,m} \sin m\lambda\right]\right\} \qquad (12)$$

where

μ is the Earth's gravitational parameter,

R_e is the Earth's mean equatorial radius,

r, λ, ϕ are spherical coordinates (see Figure 2),

P_n^m is the associated Legendre function (spherical harmonics) of the first kind of degree n and order m, and

$C_{n,m}$ and
$S_{n,m}$ are numerical coefficients.

The Legendre polynomials, $P_n(x)$, are defined by

$$P_n(x) = \frac{1}{2^n\, n!} \frac{d^n}{dx^n} \left[(x^2 - 1)^n\right],$$

and the associated Legendre function $P_n^m(x)$ by

$$P_n^m(x) = (1 - x^2)^{\frac{m}{2}} \frac{d^m}{dx^m} P_n(x).$$

The spherical coordinates r, λ, ϕ are defined with respect to the fundamental planes determined by the true equator, and the Greenwich meridian (see Figure 2).

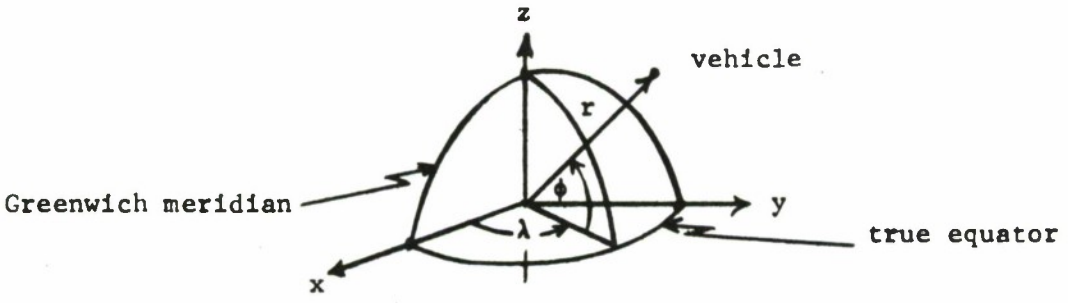

Figure 2. Spherical Coordinates

The fundamental term in the expression for U is given by $m = n = 0$. The terms in which $m = 0$ are called zonal harmonics. Inspection of Equation (12) shows that these terms vary only with latitude, and hence reflect deviations of the Earth's potential from a sphere of uniform density that are symmetric around the spin axis (e.g., a pear shaped Earth potential can be modeled with zonal harmonics). Evaluating the 2,0 term for U we have

$$- \frac{\mu}{r} \left(\frac{R_e}{r}\right)^2 P_2 (\sin \phi) \, C_{2,0} \tag{13}$$

and since

$$P_2(x) = \frac{1}{2} (3x^2 - 1)$$

Equation (13) becomes

$$- \frac{\mu}{r} \left(\frac{R_e}{r}\right)^2 \frac{1}{2} (3 \sin^2 \phi - 1) \, C_{2,0}.$$

The zeros of Equation (13) are at $\pm$ 35°.25.

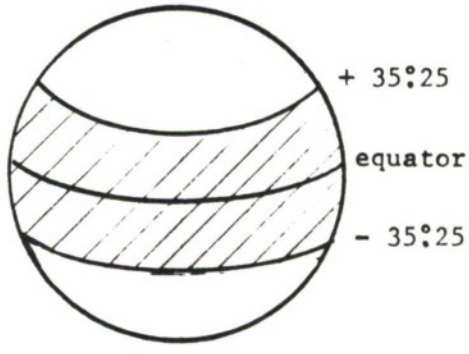

Figure 3. Zonal Harmonic for $n = 2$, $m = 0$

The sectorial harmonics arise when $m = n$. The zeros of the sectorial terms lie along lines of longitude. The remaining combinations are tesseral or square in that these terms vanish both along a number $(m - n)$ of parallels of latitude and a number $(2m)$ of meridians of longitude. Figure 4 provides an illustration of zonal,

sectorial, and tesseral harmonic variations for a sample set.

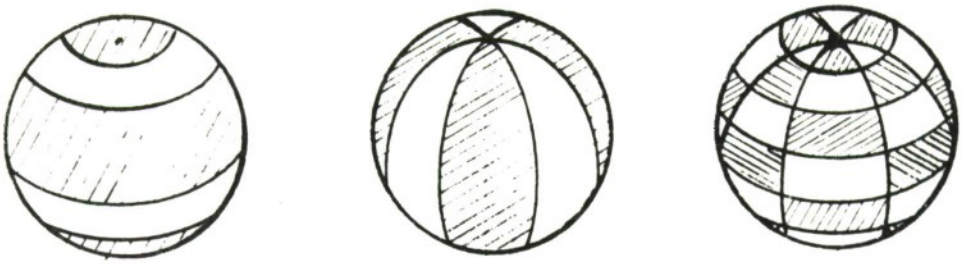

Zonal Harmonics	Sectorial Harmonics	Tesseral Harmonics
n = 4	n = 3	n = 8
m = 0	m = 3	m = 3

Figure 4. Variations

In summary, Equation (12) describes the Earth's gravitational potential at any point in space; the negative gradient of this potential gives the corresponding acceleration. Note should be made, however, that the acceleration obtained is in the Greenwich coordinate system, and hence must be transformed into the inertial system (the Base Date System) to be employed in trajectory computation.

Computation of Acceleration Due to Earth Oblateness

The components of gravitational acceleration are now expressed as the sum of terms which have the same general form for any m, n combination. First, it is necessary to develop expansions for $\cos m\lambda$ and $\sin m\lambda$ in terms of $\cos \lambda$ and $\sin \lambda$. From DeMoivre's theorem,

$$\cos m\lambda + i \sin m\lambda = (\cos \lambda + i \sin \lambda)^m$$

Now, expanding by the binomial theorem

$$\cos m\lambda + i \sin m\lambda = \sum_{k=0}^{m} \binom{m}{k} (\cos \lambda)^{m-k} (i \sin \lambda)^k .$$

For m an even number

$$\cos m\lambda + i \sin m\lambda = \sum_{k=0}^{\frac{m}{2}} \binom{m}{2k} (-1)^k (\cos \lambda)^{m-2k} (\sin \lambda)^{2k}$$

$$+ i \left\{ \sum_{k=0}^{\frac{m}{2}-1} \binom{m}{2k+1} (-1)^k (\cos \lambda)^{m-2k-1} (\sin \lambda)^{2k+1} \right\},$$

and for m an odd number

$$\cos m\lambda + i \sin m\lambda = \sum_{k=0}^{\frac{m-1}{2}} \binom{m}{2k} (-1)^k (\cos \lambda)^{m-2k} (\sin \lambda)^{2k}$$

$$+ i \left\{ \sum_{k=0}^{\frac{m-1}{2}} \binom{m}{2k+1} (-1)^k (\cos \lambda)^{m-2k-1} (\sin \lambda)^{2k+1} \right\}.$$

Equating real and imaginary parts above, we have

$$\cos m\lambda = \sum_{k=0}^{M} (-1)^k \binom{m}{2k} (\cos \lambda)^{m-2k} (\sin \lambda)^{2k} \tag{14}$$

$$\sin m\lambda = \sum_{k=0}^{M'} (-1)^k \binom{m}{2k+1} (\cos \lambda)^{m-2k-1} (\sin \lambda)^{2k+1} \tag{15}$$

where $\binom{m}{\ell} = \frac{m!}{\ell!(m-\ell)!}$

$$M = \begin{cases} \frac{m}{2} & \text{if } m \text{ is even} \\ \frac{m-1}{2} & \text{if } m \text{ is odd,} \end{cases}$$

and $$M' = \begin{cases} \frac{m}{2} - 1 & \text{if } m \text{ is even} \\ \frac{m-1}{2} & \text{if } m \text{ is odd.} \end{cases}$$

From the definition of spherical coordinates:

$$\left.\begin{aligned} \sin\phi &= \frac{z}{r} \\ \cos\phi\cos\lambda &= \frac{x}{r} \\ \cos\phi\sin\lambda &= \frac{y}{r} \end{aligned}\right\} \tag{16}$$

where x, y, and z are the coordinates of the vehicle in the Greenwich coordinate system.

Using Equation (16) in Equations (14) and (15), we have:

$$\cos m\lambda = \frac{1}{(r\cos\phi)^m} \sum_{k=0}^{M} (-1)^k \binom{m}{2k} (x)^{m-2k} (y)^{2k} \tag{17}$$

$$\sin m\lambda = \frac{1}{(r\cos\phi)^m} \sum_{k=0}^{M'} (-1)^k \binom{m}{2k+1} (x)^{m-2k-1} (y)^{2k+1} \tag{18}$$

Substitution of Equations (17) and (18) into Equation (12) yields:

$$U = -\frac{\mu}{r} \sum_{n=0}^{\infty} \left[\frac{R_e}{r}\right]^n \sum_{m=0}^{n} \frac{P_n^m(\sin\phi)}{(r\cos\phi)^m} G(x, y) \tag{12'}$$

where

$$G(x, y) = C_{n,m} \sum_{k=0}^{M} (-1)^k \binom{m}{2k} (x)^{m-2k} (y)^{2k} + S_{n,m} \sum_{k=0}^{M'} (-1)^k \binom{m}{2k+1} (x)^{m-2k-1} (y)^{2k+1}$$

From the definition of the associated Legendre function, we have

$$P_n^m(\tau) = \frac{(1-\tau^2)^{\frac{m}{2}}}{2^n\, n!} \frac{d^{m+n}}{d\tau^{m+n}} [(\tau^2 - 1)^n]. \tag{19}$$

Setting $\tau = \sin\phi$ and dividing Equation (19) by $\cos^m\phi$,

$$\frac{P_n^m(\sin\phi)}{\cos^m\phi} = \frac{1}{2^n\, n!} \frac{d^{m+n}}{d\tau^{m+n}} [(\tau^2 - 1)^n] \tag{20}$$

Setting $U = \sum_{n=0}^{\infty} \sum_{m=0}^{n} U_{m,n}$, and using Equation (20) we have

$$U_{m,n} = -\frac{\mu}{r}\left[\frac{R_e}{r}\right]^n \left[\frac{1}{r^m\, 2^n\, n!}\right] \frac{d^{m+n}}{d\tau^{m+n}} (\tau^2 - 1)^n\, G(x, y)$$

$$= \left[\frac{-\mu\, R_e^{\,n}}{r^{m+n+1}\, 2^n\, n!}\right] \frac{d^{m+n}}{d\tau^{m+n}} (\tau^2 - 1)^n\, G(x, y)$$

The gravitational acceleration is computed by taking the negative gradient of the potential function. The general derivative in the gradient will be taken with respect to ξ, where ξ takes on the values of x, y, and z.

Defining

$$A^{\xi}_{m,n} = -\frac{\partial U_{n,m}}{\partial \xi}$$

and carrying out the indicated operations using

$$\frac{\partial r}{\partial \xi} = \frac{\xi}{r} \quad \text{and} \quad \frac{\partial \tau}{\partial \xi} = \frac{\partial}{\partial \xi}\left[\frac{z}{r}\right] = \frac{1}{r}\left[\frac{\partial z}{\partial \xi} - \frac{z\xi}{r^2}\right]$$

yields:

$$A^{\xi}_{n,m} = -\frac{\mu\, R_e^{\,n}}{2^n\, n!\, r^{m+n+1}} \left[\frac{(m+n+1)\xi}{r^2} G(x,y) \frac{d^{m+n}}{d\tau^{m+n}} (\tau^2 - 1)^n \right.$$

$$- \frac{G(x, y)}{r}\left[\frac{\partial z}{\partial \xi} - \frac{z\xi}{r^2}\right] \frac{d^{m+n+1}}{d\tau^{m+n+1}} (\tau^2 - 1)^n$$

$$\left. - \frac{d^{m+n}}{d\tau^{m+n}} (\tau^2 - 1)^n \frac{\partial G(x, y)}{\partial \xi}\right] \qquad (21)$$

where

$$\frac{\partial G(x, y)}{\partial \xi} = C_{n,m} \sum_{k=0}^{M} \left[(-1)^k \binom{m}{2k}\left\{(m-2k)\, x^{m-2k-1}\, y^{2k} \frac{\partial x}{\partial \xi}\right.\right.$$

$$\left. + 2k\, x^{m-2k}\, y^{2k-1} \frac{\partial y}{\partial \xi}\right\}]$$

$$+ S_{n,m} \sum_{k=0}^{M'} \left[(-1)^k \binom{m}{2k+1}\left\{(m-2k-1)\, x^{m-2k-2}\, y^{2k+1} \frac{\partial x}{\partial \xi}\right.\right.$$

$$\left. + (2k+1)\, x^{m-2k-1}\, y^{2k} \frac{\partial y}{\partial \xi}\right\}]. \qquad (22)$$

It can be shown by applying the binomial theorem and induction that

$$\frac{d^{\ell}}{d\tau^{\ell}} (\tau^2 - 1)^n = \sum_{k=0}^{[n - \frac{1}{2}]} (-1)^k \binom{n}{k} \frac{(2n-2k)!}{(2n-2k-i)!} (\tau)^{2n-2k-i}$$

where $[n - \frac{1}{2}]$ indicates the integral part of $n - \frac{1}{2}$. Hence,

$$\frac{d^{m+n}}{d\tau^{m+n}} (\tau^2 - 1)^n = \sum_{k=0}^{[\frac{m-n}{2}]} (-1)^k \binom{n}{k} \frac{(2n-2k)!}{(n-2k-m)!} (\tau)^{n-2k-m} \tag{23}$$

and

$$\frac{d^{m+n+1}}{d\tau^{m+n+1}} (\tau^2 - 1)^n = \sum_{k=0}^{[\frac{m-n-1}{2}]} (-1)^k \binom{n}{k} \frac{(2n-2k)!}{(n-2k-m-1)!} (\tau)^{n-2k-m-1} \tag{24}$$

where $\tau = \sin \phi = \frac{z}{r}$. Therefore, Equation (21) may be rewritten as

$$A^{\xi}_{n,m} = \frac{-\mu R_e^n}{2^n\, n!\, r^{m+n+1}} \left[\left\{ \sum_{k=0}^{[\frac{m-n}{2}]} (-1)^k \binom{n}{k} \frac{(2n-2k)!}{(n-2k-m)!} \left(\frac{z}{r}\right)^{n-2k-m} \right\} \times \right.$$

$$\left\{ \frac{(m+n+1)}{r^2} \xi\, G(x, y) - \frac{\partial G(x,y)}{\partial \xi} \right\} -$$

$$\left\{ \sum_{k=0}^{[\frac{m-n-1}{2}]} (-1)^k \binom{n}{k} \frac{(2n-2k)!}{(n-2k-m-1)!} \left(\frac{z}{r}\right)^{n-2k-m-1} \right\}$$

$$\left. \times \left\{ \frac{G(x, y)}{r} \left[\frac{\partial z}{\partial \xi} - \frac{z\xi}{r^2} \right] \right\} \right] \tag{25}$$

By separately considering the case for $n-m$ odd and for $n-m$ even, it may be shown that Equation (25) reduces to the following expression:

$$A^{\xi}_{n,m} = -\frac{\mu R_e^n}{2^n\, r^{m+n+1}} \sum_{k=0}^{[\frac{n-m}{2}]} \left\{ (-1)^k \frac{(2n-2k)!}{k!\,(n-k)!\,(n-2k-m)!} \left(\frac{z}{r}\right)^{n-2k-m-1} \right\} \times \tag{26}$$

$$\left\{ \left((2n-2k+1) \frac{z\xi}{r^3} - \frac{(n-2k-m)}{r} \frac{\partial z}{\partial \xi} \right) G(x, y) - \frac{z}{r} \frac{\partial G(x, y)}{\partial \xi} \right\}$$

where

$$\frac{\partial x}{\partial \xi} = \begin{cases} 1 & \text{if } \xi = x \\ 0 & \text{if } \xi \neq x, \end{cases} \quad \frac{\partial y}{\partial \xi} = \begin{cases} 1 & \text{if } \xi = y \\ 0 & \text{if } \xi \neq y, \end{cases} \quad \frac{\partial z}{\partial \xi} = \begin{cases} 1 & \text{if } \xi = z \\ 0 & \text{if } \xi \neq z \end{cases} \tag{27}$$

and

$$G(x, y) = C_{n,m} \sum_{k=0}^{M} (-1)^k \frac{m!}{2k!\ (m-2k)!} (x)^{m-2k} (y)^{2k}$$

$$+ S_{n,m} \sum_{k=0}^{M'} (-1)^k \frac{m!}{(2k+1)!\ (m-2k-1)!} (x)^{m-2k-1} (y)^{2k+1} \tag{28}$$

$$M = \begin{cases} m/2 & \text{if } m \text{ is even} \\ \frac{m-1}{2} & \text{if } m \text{ is odd} \end{cases} \qquad M' = \begin{cases} \frac{m}{2} - 1 & \text{if } m \text{ is even} \\ \frac{m-1}{2} & \text{if } m \text{ is odd} \end{cases}$$

$$\frac{\partial G(x, y)}{\partial \xi} = C_{n,m} \sum_{k=0}^{M} \left[(-1)^k \frac{m!}{2k!\ (m-2k)!} \left\{ (m-2k)(x)^{m-2k-1} (y)^{2k} \frac{\partial x}{\partial \xi} \right.\right.$$

$$\left.\left. + 2k(x)^{m-2k} (y)^{2k-1} \frac{\partial y}{\partial \xi} \right\}\right]$$

$$+ S_{n,m} \sum_{k=0}^{M'} \left[(-1)^k \frac{m!}{(2k+1)!\ (m-2k-1)!} \right.$$

$$\left. \times \left\{ (m-2k-1)(x)^{m-2k-2} (y)^{2k+1} \frac{\partial x}{\partial \xi} + (2k+1)(x)^{m-2k-1} (y)^{2k} \frac{\partial y}{\partial \xi} \right\}\right] \tag{29}$$

It is important to note that when $z = 0$, a special procedure must be used since the term $\left(\frac{z}{r}\right)^{-1}$ arises in Equation (26) for $n-m$ even; and $\left(\frac{z}{r}\right)^{0}$, when $n-m$ is odd.

When $n-m$ is even, Equation (26) reduces to one term, when $z = 0$.

$$A^{\xi}_{n,m} = \frac{-\mu R_e^n}{2^n r^{m+n+1}} \left\{ (-1)^{\frac{n-m}{2}} \frac{(n+m)!}{\left(\frac{n-m}{2}\right)!\ \left(n-\frac{n-m}{2}\right)!} \right\} \left\{ \frac{(n+m+1)\xi}{r^2} G - \frac{\partial G}{\partial \xi} \right\}. \tag{30}$$

Similarly, when $n-m$ is odd, Equation (26) may be reduced

$$A^{\xi}_{n,m} = 0 \quad \text{for} \quad \xi = x, y$$

$$A^{z}_{n,m} = \frac{\mu R_e^n}{2^n r^{m+n+1}} \left\{ (-1)^{\left[\frac{n-m}{2}\right]} \frac{(n+m+1)!}{\left(\frac{n-m}{2}\right)! \left(n-\left[\frac{n-m}{2}\right]\right)!} \right\} \frac{\zeta}{r} \tag{31}$$

In summary, the program computes the acceleration of a vehicle due to the Earth in the Greenwich coordinate system by the formula:

$$\vec{P}_2 = \sum_{n=0}^{\infty} \sum_{m=0}^{n} \left(A^{x}_{n,m} \vec{I} + A^{y}_{n,m} \vec{j} + A^{z}_{n,m} \vec{k}\right) \tag{32}$$

where $\vec{I}$, $\vec{j}$, $\vec{k}$ are unit vectors in the Greenwich coordinate system.

In Equation (32) the range of indices (n,m) are restricted by SPACE-A to the following limits:

n	m
2	0, 1, 2
3	0, 1, 2, 3
4	0, 1, 2, 3, 4
5	0, 1, 2, 3
6	0, 1, 2
7	0, 1
8	0
9	0
10	0

The fundamental term is given by the (0, 0) combination and would be the only term present if the Earth were of uniform density and a perfect sphere. Since the center of the coordinate system is taken to be at the center of mass, it can be shown that the (1, 0) and (1, 1) combinations vanish[6,p.50].

In Equation (32), $A^{\xi}_{n,m}$ is given by (26) when $z \neq 0$, and when $z = 0$, by Equation (30) or Equation (31) depending on whether n-m is even or odd.

PERTURBATION DUE TO DRAG

Accurate simulation of an artificial satellite or other space vehicle trajectories requires consideration of vehicle deceleration resulting from atmospheric drag. A number of planets (e.g., Earth, Venus, Mars and Jupiter) have sufficiently dense atmospheres to retard the motion of a vehicle within their atmospheres; however, this discussion confines itself to the atmospheric model of the Earth.

An analysis of drag must take into account the particular mission of the vehicle, e.g., low eccentricity, orbit, reentry, or fly-by, since vehicle mission determines what portion of the atmosphere it is necessary to include in the model.

The following discussion describes the general equations used for drag computation, some of the problems involved in simulating the Earth's atmosphere, and the effects of certain simplifying assumptions.

Drag Equations

The program uses two different formulas for computing the vehicle deceleration, $\vec{P}_3$, due to drag. For a relatively dense atmosphere where the assumption of continuum flow is valid the following well known equation is used:

$$\vec{P}_3 = - C_1 \left[\frac{1}{2} \rho \frac{C_D S}{m}\right] V_a \vec{V}_a \qquad (33)$$

where

- ρ is the atmospheric density at the vehicle,
- C_D is the drag coefficient of the vehicle (dimensionless),
- S is the effective surface area of the vehicle,
- m is the mass of the vehicle,
- $\vec{V}_a$ is the vector of the velocity of the vehicle with respect to the local atmosphere,
- V_a is the magnitude of $\vec{V}_a$, and
- C_1 is a constant used to convert the above expression into the units used by the program.

Equation (33) is used to compute the acceleration of drag in the

lower atmosphere from 0 kilometers up to 120 kilometers, although the model for the lower atmosphere from which the values of ρ and C_D are obtained may be extended up to 210 kilometers with some loss of accuracy. The basic model used in the lower atmosphere is the U. S. Standard Atmosphere 1962[7] and its details are discussed below.

As the atmosphere becomes more diffuse, the mean free path length (average distance between impacts of air molecules) increases. At 110 kilometers, mean free path length is roughly one meter and at 130 kilometers may become as large as ten meters[7]. When the mean free path length exceeds the dimensions of the vehicle, the assumption of continuum air flow is no longer applicable. In such a diffuse atmosphere where all collisions are essentially two-body collisions, the air flow is referred to as free molecular flow.

Ketchum[8] has derived the following formula for the magnitude of drag deceleration in free molecular flow:

$$|\vec{P}_3| = \frac{\pi}{8}\left(1 + \frac{2R}{\lambda}\right)\left[\rho\ C_{av}\ \frac{S}{m}\right] V_a \qquad (34)$$

where

R the radius of the vehicle,

λ the mean free path,

C_{av} the average velocity of particles in the medium.

Ketchum is uncertain as to the validity of the $(1 + 2R/\lambda)$ term in Equation (34). In the high atmospheric region the assumption that $\lambda >> R$ is usually justified, except perhaps below 140 kilometers. Therefore, the program actually uses Equation (35) in computation of the drag in the high atmosphere.

$$\vec{P}_3 = - C_2\ \left[\frac{\pi}{8}\ \rho\ C_{av}\ \frac{S}{m}\right] \vec{V}_a \qquad (35)$$

where,

S is the effective surface area of the vehicle,

m is the mass of the vehicle,

ρ is the atmospheric density at the vehicle,

C_{av} is the average velocity of particles in the medium,

$\vec{V}_a$ is the vector of the velocity of the vehicle with respect to the surrounding atmosphere, and

C_2 is a constant used to convert the expression into the units used by the program.

Equation (35) is used to compute the deceleration of drag in the upper atmosphere from 100 kilometers up to 1,050 kilometers, although the model for the upper atmosphere may be extended up to 2,000 kilometers. The basic model used for the upper atmosphere is that due to Harris & Priester[9]. The values of ρ and C_{av} used in Equation (35) are derived from this model, the details of which are also discussed below.

Notice in both Equations (33) and (35) that the direction of the drag force is in a direction opposite to the velocity with respect to air. In addition, both formulations assume zero lift and assume that the angle of attack of the vehicle is zero, i.e., that the vehicle velocity relative to the air mass is in line with the vehicle longitudinal axis.

It is readily seen that the formula for drag in the upper atmosphere, Equation (35), differs from the equation of drag in the lower atmosphere, Equation (33). Furthermore, in the region between 100 kilometers and 120 kilometers there are disagreements between the two models. For example, the value of density predicted by the low atmospheric model (U. S. Standard Atmosphere 1962) at 120 kilometers is 34% higher than that predicted by the high atmospheric model (Harris-Priester) at the same height.

The present program achieves a compromise between these two models by treating the region from 100 to 120 kilometers as a transition region in which a weighted average is taken between the drag values computed by the two methods and gradually slides the weight from unity for free molecular flow and zero for continuum flow at 120 kilometers to unity for continuum flow and zero for free molecular flow at 100 kilometers.

Because of the uncertainties in the atmospheric models and because of the approximations made in the analysis the computation of drag deceleration is probably accurate to $\pm$ 5% in the lower atmosphere and is less accurate in the upper atmosphere.

Variables Used in Drag Computation

Vehicle Mass

In the most general case, the vehicle mass in the drag equations should be considered as variable with time. In the orbiting case or the fly-by case, a step change in mass representing the separation of a landing craft is conceivable. A long-term steady-state mass flow rate, however, would probably be small.

For the reentry case, if the reentry vehicle is of the heat-sink type, the mass would be constant. For an ablative nose cone (i.e., one which loses mass when moving at high speeds due to friction) the mass flow rate is a function of the drag. For ballistic missile applications, this mass change is usually ignored. In any event, such changes in mass represent a small error in the location of the impact point. Therefore, the program treats the mass as an input constant.

Surface Area

The effective surface area term S in the drag equation is not simply the cross-sectional area of the vehicle. The vehicle, in passing through the air, produces a shock wave which skirts the missile thereby placing the effective cross-sectional area at a point somewhat close to the nose. Since the shock wave changes with air speed, so does the effective cross-sectional area. In practice, S is made constant and any variation with speed is included in the coefficient of drag.

Velocity with Respect to Air

The velocity of the vehicle is available in an inertial coordinate system (Base Date System).

The vehicle velocity with respect to the moving air mass, $\vec{V}_a$,

in the same coordinate system, is obtained by subtracting the velocity of the air mass from the vehicle velocity. A good first approximation to the velocity of the air mass is obtained by assuming the air mass to be rigidly attached to the rotating planet.

From these considerations we have:

$$\vec{V}_a = \dot{\vec{R}} - \vec{\Omega}' \times \vec{R} \tag{36}$$

where

$\vec{V}_a$ is the velocity with respect to surrounding atmosphere,

$\vec{R}$ is the position vector of the vehicle in the inertial frame,

$\dot{\vec{R}}$ is the velocity vector of the vehicle in the inertial frame, and

$\vec{\Omega}'$ is the vector of angular rotation of Earth expressed in the inertial frame.

A better approximation could be obtained by including the effects of wind velocity. The purely local effects have to be neglected, but the long-term horizontal effects are known as a function both of position on the Earth's surface and of altitude. The effects of the wind velocity's direction (independent of altitude but dependent on latitude and longitude) and magnitude (strongly dependent on altitude, less strongly on latitude, and least on longitude) would have to be included. The error made by neglecting Earth winds is about 1,500 feet at impact for a typical ICBM mission. It should be noted that winds are of importance only in the Earth's lower atmosphere, mainly for the reentry case. In the present program the effect of winds is neglected.

Drag Coefficient

The drag coefficient, C_D, is sometimes considered to be a constant. Very often the ballistic coefficient, $B = \frac{C_D S}{m}$, is used in analysis in place of the drag coefficient, mass, and effective surface area. A much more accurate representation for C_D is obtained by considering it to be a function of Mach number. Mach number is

defined to be:

$$M = \left| \frac{\vec{V}_a}{c} \right| \tag{37}$$

where,

M is the Mach number,

$|\vec{V}_a|$ is the speed with respect to the surrounding air, and

c is the speed of sound in the surrounding air.

The speed of sound is a function of altitude obtained from the low atmospheric model (see below). It should be noted that as altitude increases, the atmosphere becomes rarified to the point that the speed of sound loses its physical significance.

In the program C_D is tabulated for about 40 different Mach numbers. These numbers are denser for speeds below Mach 2 than those above and are very dense in the region around Mach 1. For intermediate values of Mach number, linear interpolation is used.

Inadequate knowledge of the drag coefficient is one of the major sources of inaccuracy in the simulation of drag. Since drag coefficient is a function of Mach number, drag coefficient data has been obtained by wind tunnel measurements made at a range of Mach numbers.

Air Density

In the region below 120 kilometers the air density, ρ, is a function of altitude obtained from the low atmospheric model and is computed from a stored table (see below).

In the high atmosphere ρ is obtained from the upper atmospheric model of Harris-Priester and is considered to be a function of altitude, local solar time, solar flux, and latitude. Tables are provided in the program for its computation (see below).

Mean Particle Velocity

The mean particle velocity, C_{av}, is of importance only when the vehicle is in the upper atmosphere where the assumption of free molecular flow is valid. From Equations I.3.4-1 and I.2.6-1 of

Reference [7], C_{av} is given by

$$C_{av} = k\sqrt{\frac{T}{m}}\left(\frac{km}{sec}\right) \tag{38}$$

where

T is the absolute temperature of particles (°K),

m is the mean molecular weight of medium (gm),

k is a constant of proportionality (.145).

The values of T and m are given in the Harris-Priester model of the upper atmosphere. C_{av} can, therefore, be obtained directly from stored tables.

Lower Atmospheric Model

Drag in the lower atmosphere (below 120 kilometers) can be large and a vehicle entering this region will usually be slowed down sufficiently to be quickly captured by the Earth. Thus, the lower atmosphere is primarily of concern in the reentry case.

Data for an average model have been well established for the lower atmosphere. There are five sources for these data: U. S. Standard Atmosphere 1962; COSPAR International Reference Atmosphere (CIRA), 1961; COESA Table for Tropical Latitudes, 1962; ARDC Model Atmosphere 1956, 1959. Table I shows the density deviation (in percent), as a function of altitude, of each of the others from the U. S. Standard Atmosphere values. From the table, it is evident that, except for the COESA tables, there is good agreement between the various tables at low altitudes. Note that the U. S. Standard Atmosphere and CIRA tables are in excellent agreement all the way to 120 km. (400,000 feet).

The lower atmosphere is characterized by seasonal, diurnal, and latitude variations; however, none of these is sufficiently well documented. The only effect of omitting them is that the impact point of a re-entering body would be slightly different. It was estimated in 1958 that the standard deviation for a heat-sink type nose cone used in the ICBM application is only about 0.5 nm.

Table I

Comparison of Sources of Density Data

Altitude		U. S. Standard Atmosphere Density Values (Reference)	Percent Deviation from Reference			
km.	ft.	slugs/ft^3	ARDC 1956	ARDC 1959	CIRA 1961	COESA 1962
0	0	2.38^{-3}	0	0	0.55	-4.77
3.0	10,000	1.76^{-3}	0	0	-0.91	-5.32
5.5	18,000	1.36^{-3}	0.04	0	1.85	-1.67
10.1	33,000	7.97^{-4}	0.05	0	1.68	1.92
14.6	48,000	4.00^{-4}	0.09	0	2.36	15.5
20.4	67,000	1.61^{-4}	3.28	0.16	0.48	6.80
29.0	95,000	4.20^{-5}	0.59	-2.36	0.10	0.46
32.5	110,000	2.07^{-5}	-3.13	-3.13	0.68	2.53
48.8	160,000	2.32^{-6}	4.77	4.77	0.77	8.93
67.1	220,000	2.50^{-7}	15.0	15.5	1.30	8.10
91.4	300,000	4.62^{-9}	31.2	-10.8	0.11	- -
121.9	400,000	3.62^{-11}	81.5	-35.0	1.17	- -

Three tables with 32 values each are stored in the program for the lower atmospheric model. The first contains 32 values of altitudes in kilometers, the second contains 32 values of the logarithm (base 10) of the density, ρ, in gm/km^3, and the third contains 32 values of the speed of sound, c, in km/sec. The n^{th} entry in the altitude table corresponds to the n^{th} entry in the table for $\log_{10}\rho$ and c. Intermediate values are obtained by linear interpolation.

These three tables are obtained from the U. S. Standard Atmosphere 1962, in which densities and speed of sound at altitudes below 90 km are listed. Above 90 km the speed of sound was calculated from temperature and mean molecular weight data which are directly available.

The value of altitude (in Earth radii) above an ellipsoidal Earth is obtained using a formula found in Baker[10].

$$h = r - 1 + f \sin^2 \phi + \frac{f^2}{2} \left(\frac{1}{r} - \frac{1}{4}\right) \sin^2 2\phi \tag{39}$$

where

h is the height of the vehicle (ER),

r is the distance of the vehicle from the geocenter (ER),

ϕ is the geocentric latitude of the vehicle,

f is the flattening constant of the Earth = $\frac{1}{298.3}$.

For programming purposes Equation (39) is put into the more convenient form:

$$h = R - 1 + z^2 \frac{\left[1 + \left(\frac{2}{r} - \frac{1}{2}\right)\left(\frac{x^2 + y^2}{298.3\ R^2}\right)\right]}{298.3\ R^2} \tag{40}$$

where,

h is the altitude of the vehicle (ER),

x,y,z are the position coordinates of the vehicle in the Greenwich coordinate system (ER),

$R = \sqrt{x^2 + y^2 + z^2}$ is the distance of the vehicle from the geocenter (ER).

The position coordinates of the vehicle are available from the program and h is multiplied by 6378.165 to convert its units into kilometers.

After h is obtained, ρ ($\rho = 10^{\log_{10}\rho}$) and c are obtained from the low atmosphere tables. Then the air velocity, $\vec{V}_a$ and the drag coefficient, C_D, are computed as described above. Finally, $\vec{P}_3$ is computed according to Equation (33).

Upper Atmospheric Model

Models of the Earth's upper atmosphere (above 100 kilometers) must take into account solar activity. There is evidence that solar activity occurs cyclically at periods of 27 days, 6 months, 1 year and 11 years.

Theoretical models do not exist for the 27-day, 6-month, and 1-year cycles. Diurnal variations, if any, of the models for these cycles are not known. Investigation of the 11-year cycle (corresponding to the sunspot period) in solar flux led to the Harris-Priester model of the upper atmosphere. This model[9,11] has diurnal and solar flux variations.

The Harris-Priester model[9] lists the density, absolute temperature, and mean molecular weight of the atmosphere as a function of altitude, solar flux and local solar time. The mean particle velocity can be found by use of Equation (38). Note that at the North and South Poles local solar time is undefined.

The upper atmosphere has a delaying effect on solar radiation. It takes several hours for the Sun's heat to pass through the atmosphere and reach the Earth's surface. The Harris-Priester model is based on densities computed at the Earth's equator. Intuitively, it is expected that it will take longer for the solar flux to reach the poles as opposed to the equator. Therefore, it is considered that there is an effective variation of solar flux with latitude. This variation is implemented in the program by applying the Harris-Priester model <u>at the equator</u> and a stored table of "twilight" densities <u>at the poles</u>. The cosine of the latitude of the vehicle is used as a weighting factor to interpolate between the two sets of data.

The Harris-Priester upper atmospheric model has been incorporated in the program by means of a table look-up procedure. Two tables are used in the program.

The first table lists the logarithm to the base 10 of the density in gm/km^3 times the mean particle velocity in km/sec ($\log_{10}\rho C_{av}$) at the equator as functions of altitude (km), solar flux ($watts/m^2$ - Hz at a wavelength of 10.7 cm) and local solar time (hrs). These values have been tabulated for 16 values of altitude, 4 values of solar flux and 13 values of local solar time. Hence, this table has 832 entries.

The second table lists $\log_{10} \rho C_{av}$ in the same units at "twilight" for the modeling of the polar region as a function of altitude and solar flux. This table has 16 entries for altitude, 4 entries for solar flux, or 64 entries.

For intermediate values of the input variables (altitude, solar flux, local solar time) a linear interpolation is used to obtain the output, $\log_{10} \rho C_{av}$. This method gives fairly accurate results since ρC_{av} is nearly exponential. The value of solar flux is determined by input data. The value of altitude is computed according to Equation (40). The value of local solar time is computed from the x and y coordinates of the vehicle and the Sun in the inertial (Base Date) coordinate system (see Figure 5).

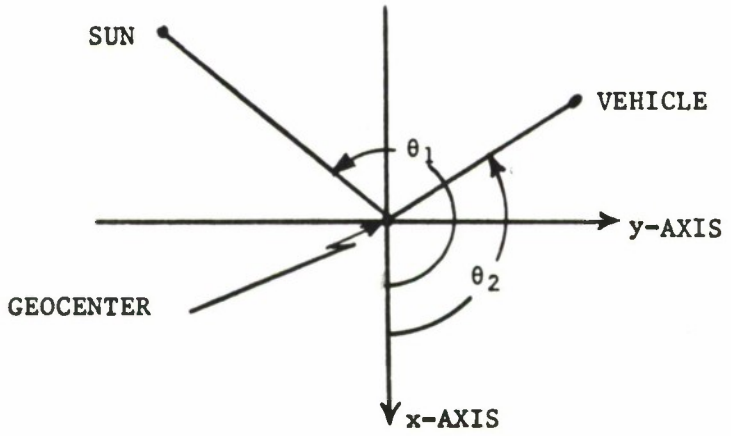

Figure 5. View of x-y Plane from Above

Thus we have:

$$\text{local solar time} = \left\{(\theta_2 - \theta_1 + \pi)\,\frac{180^\circ}{\pi} + 720^\circ\right\} (\text{mod } 360^\circ)$$

where

$$\theta_1 = \tan^{-1}\left(\frac{y_s}{x_s}\right) \quad \text{where} \quad \pi \leq \theta_1 \leq -\pi$$

$$\theta_2 = \tan^{-1}\left(\frac{y_v}{x_v}\right) \quad \text{where} \quad \pi \leq \theta_2 \leq -\pi$$

x_v, y_v are the vehicle coordinates in the inertial system,

x_s, y_s are the Sun's coordinates in the inertial system.

Local solar time given above is then divided by 15 to convert its units to hours.

After a value of $\log_{10} \rho C_{av}$ has been obtained from both the equatorial table and the "twilight" polar table an interpolation is done to obtain the final value of ρC_{av} using the cosine of latitude as a weighting function. Hence:

$$L = Lp + \cos \phi \, (L_E - Lp) \tag{42}$$

$$\cos \phi = \sqrt{\frac{x^2 + y^2}{x^2 + y^2 + z^2}} \tag{43}$$

$$\rho C_{av} = 10^L \tag{44}$$

where

- L is the final value of $\log_{10} \rho C_{av}$,
- Lp is the value of $\log_{10} \rho C_{av}$ obtained from the twilight table,
- L_E is the value of $\log_{10} \rho C_{av}$ obtained from the equatorial table,
- x, y, z are the coordinates of the vehicle in the inertial (Base Date) system and ϕ is the latitude of the vehicle.

Once ρC_{av} has been found, the vehicle area and mass (S and m, standard program inputs) as well as air velocity $\vec{V}_a$ (see Equation (36)), are obtained and the value of drag deceleration is finally computed according to Equation (35).

PERTURBATION DUE TO DIRECT SOLAR RADIATION

Solar radiation exerts a pressure on the intercepting surface of a vehicle. Orbiting planetary vehicles, having a large area to mass ratio are subject to noticeable perturbations due to solar radiation pressure. In fact, for orbits above 500 miles the solar radiation

perturbation is usually more significant than that due to drag[12]. The vehicle acceleration due to solar radiation pressure depends on the area to mass ratio of the vehicle as well as the intensity of the Sun's incident power at the vehicle and the fraction of solar illumination on the vehicle. The illumination factor is considered in three distinct regions in the following analysis: full sunlight, penumbral illumination, and no illumination (i.e., umbral region).

In computing the solar radiation perturbation, $\vec{P}_4$, this analysis neglects the dispursive effects of planetary atmospheres which complicate the geometry of the umbra and penumbra. The analysis also neglects the effects of reflected sunlight from the reference body or any other planet.

Acceleration Due to Solar Radiation Pressure

An expression for the acceleration due to solar radiation pressure given in Wolverton[12] is:

$$\vec{P}_4 = p\ q\ \left(\frac{A}{m}\right)\left(\frac{L_0}{4\pi c}\right)\frac{\vec{R}_{sv}}{R_{sv}^3} \tag{45}$$

where,

- p is the illumination factor,
- q is the reflectivity coefficient,
- A is the area of vehicle pertaining to solar radiation pressure,
- m is the mass of vehicle,
- $L_0 = 3.86 \times 10^{26}$ watts, the total power output of the Sun ($\pm$ 3%),
- c is the speed of light,
- $\vec{R}_{sv}$ is the vector from the Sun to the vehicle.

The SPACE program assumes a reflectivity coefficient equal to unity. This assumption may be altered by changing the area, A, by an appropriate factor. Simplifying Equation (45) and putting the above variables into units used by the program, one obtains:

$$\vec{P}_4 = p\ \left(\frac{A}{m}\right)\ C_P\ \frac{\vec{R}_{sv}}{R_{sv}^3} \tag{46}$$

where,

p is the illumination factor, $0 \leq p \leq 1$,

A is the area pertaining to radiation pressure (ft^2),

m is the mass pertaining to radiation pressure (lb-masses),

$\vec{R}_{sv}$ is the vector from the Sun to the vehicle (ER),

$Cp = 1.04819 \times 10^3 \left(\frac{ER^3\text{-lb}}{HR^2\text{-ft}^2}\right)$ and is a constant used to convert the expression into units used by the program and to account for the $\frac{L_0}{4\pi c}$ factor of Equation (45).

Equation (46) is the basic equation used by the program for computing the solar radiation perturbation acceleration.

The illumination factor, p, is obtained from the relative geometry of the vehicle with respect to the Sun, the Moon and the planets:

$p = 1$ in full sunlight,

$p = 0$ in the umbral region,

$0 < p < 1$ in the penumbral region.

It is possible that a vehicle may lie within the penumbral region of two bodies at the same time, e.g., the Earth and the Moon. In this case, only the penumbral illumination factor due to the reference body is computed. Errors introduced by this assumption are extremely small: first, because for most vehicles of interest the solar radiation perturbation is itself small (usually less than 10^{-5} times the acceleration of the reference body except for low density balloons); second, because only a short time is spent in the penumbral region of the reference body by an orbiting vehicle; and third, because the incidence of simultaneous penumbral obscuration is rare.

Since the geometry used in calculating the illumination factor is the same as that used for eclipse information, the portion of the program which computes the solar radiation pressure perturbation also computes the times at which the vehicle enters or leaves the umbra or penumbra of the celestial bodies. The geometry used in calculating the vehicle illumination factor, p, is described below.

Vehicle Illumination Factor

Figure 6 illustrates the geometry of vehicle illumination, neglecting the effects of atmospheric refraction. By similar triangles it is seen that the height of the umbral cone (h_u) and penumbral cone (h_p) are respectively given by:

$$h_u = \frac{R_{sp}}{\frac{R_s}{R_p} - 1} \tag{47}$$

$$h_p = \frac{R_{sp}}{\frac{R_s}{R_p} + 1} \tag{48}$$

where,

R_{sp} is the distance from the center of the Sun to the center of the reference body,

R_s is the radius of the Sun, and

R_p is the radius of the reference body.

Next, criteria are developed to see in which region the vehicle lies, i.e., full sunlight, umbra, or penumbra. First, consider Figures 7 and 8 and the definitions and relations below.

$\vec{R}_{sp}$ is the vector from the center of the Sun to the center of the reference body,

$\vec{R}$ is the vector from the center of the reference body to the vehicle.

$$\vec{P} = h_u \frac{\vec{R}_{sp}}{R_{sp}} \tag{49}$$

$$\vec{Q} = - h_p \frac{\vec{R}_{sp}}{R_{sp}} \tag{50}$$

From Figure 7 we get the following:

$$\cos A = \sqrt{1 - \left(\frac{R_p}{h_u}\right)^2} \tag{51}$$

$$\cos \alpha = - \frac{(\vec{R} - \vec{P}) \cdot \vec{R}_{sp}}{|\vec{R} - \vec{P}| \, R_{sp}} \tag{52}$$

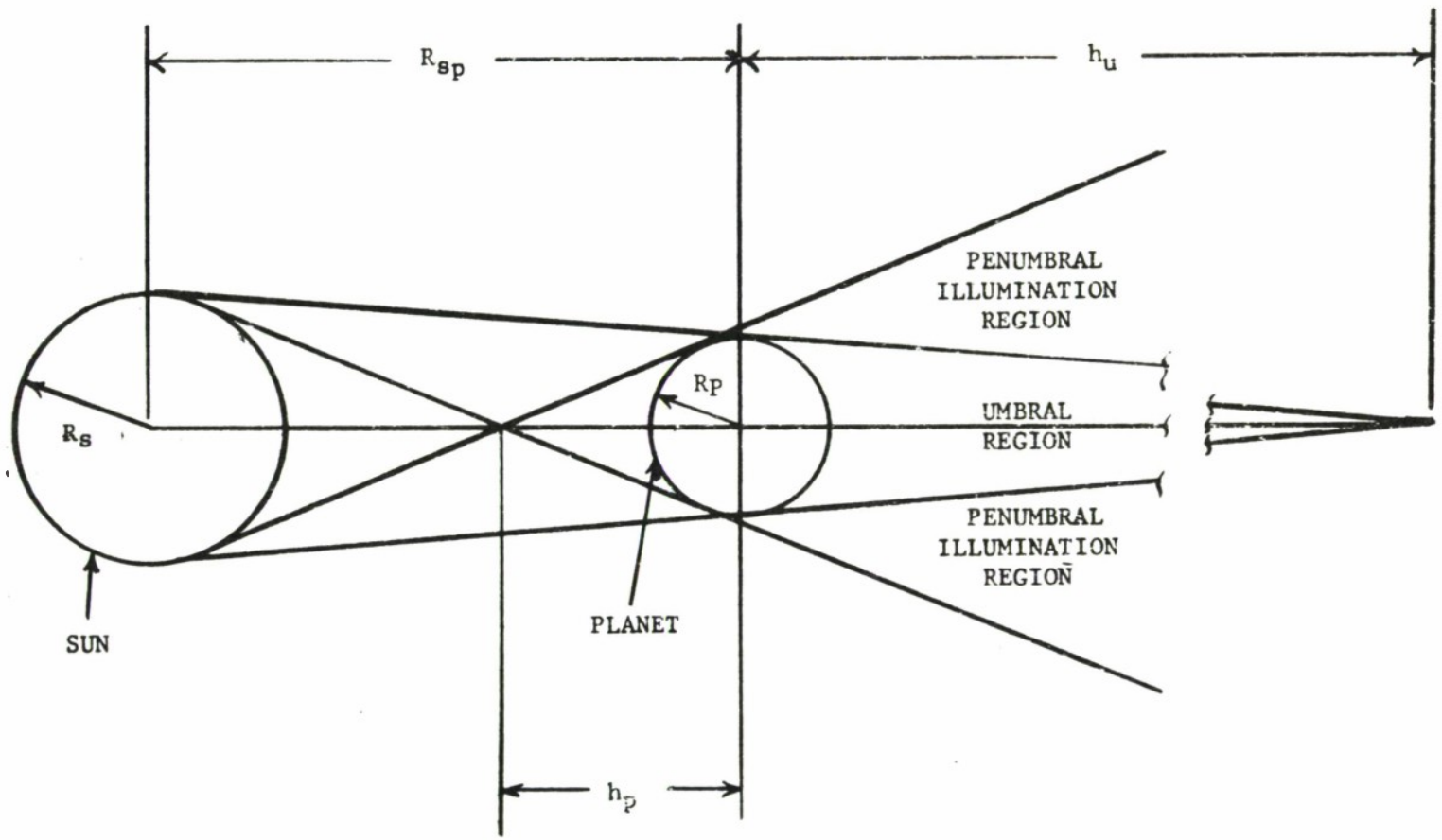

Figure 6. Vehicle Illumination

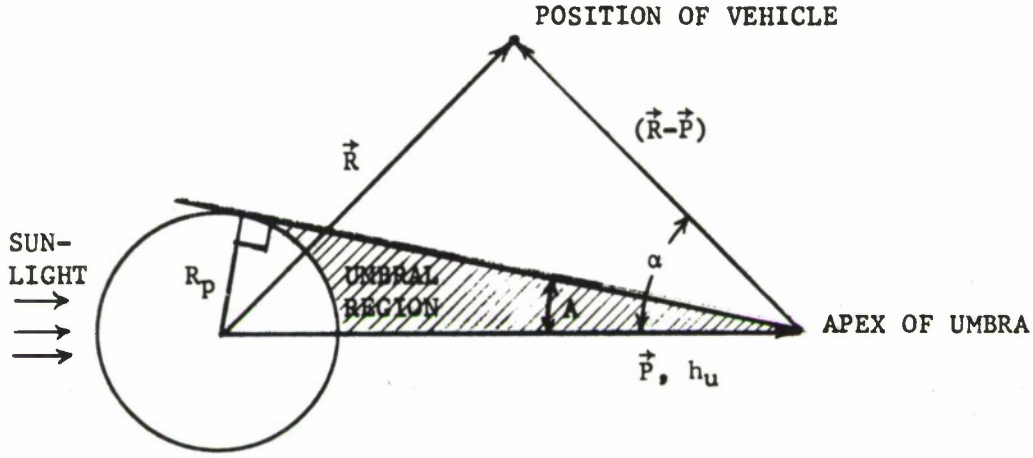

Figure 7. Umbral Region Geometry

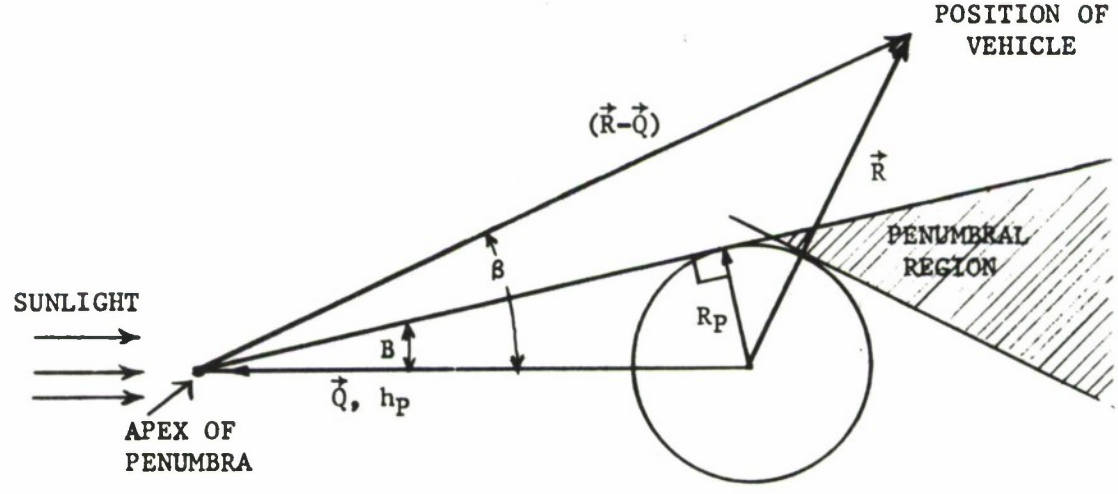

Figure 8. Penumbral Region Geometry

From Figure 8 we get:

$$\cos B = \sqrt{1 - \left(\frac{R_p}{h_p}\right)^2} \tag{53}$$

$$\cos \beta = \frac{(\vec{R} - \vec{Q}) \cdot \vec{R}_{sp}}{|\vec{R} - \vec{Q}| \, R_{sp}} \tag{54}$$

Now, if the scalar product $\vec{R} \cdot \vec{P}$ is positive, then the vehicle lies on the side of the reference body away from the Sun. In this case, if $\cos \alpha > 0$ and if $\alpha \leq A$, the vehicle or satellite lies in the umbra and p is set equal to zero. Another test is:

$$\text{if} \quad |\cos \alpha| \geq |\cos A| \tag{55}$$

$$\text{then} \quad p = 0,$$

i.e., the vehicle lies in the umbra.

If the vehicle does not lie in the umbral region one can test to see if it lies in the penumbra. Thus, if $\cos \beta > 0$ and $\beta \leq B$ the vehicle lies in the penumbra, or equivalently:

$$\text{if} \quad |\cos \beta| \geq |\cos B| \tag{56}$$

$$\text{then} \quad 0 < p < 1$$

(i.e., the vehicle lies in the penumbra).

If the vehicle does not lie in either the umbral or penumbral region, then the reference body does not obscure the Sun's rays. A check can then be made to see whether any other celestial body blocks or partially blocks the solar radiation; and if not, the illumination factor is set equal to one, $p = 1$.

Penumbral Illumination Factor

If the tests of Equations (55) and (56) above indicate that the vehicle lies in the penumbral region, then the illumination factor, p, is computed according to the formula:

$$p = \frac{A_{EX}}{\theta_S} \tag{57}$$

where A_{EX} is the angular area subtended by the exposed portion of the solar cap at the vehicle position, and

θ_S is the total angular area of the solar cap at the vehicle position.

The general approach used by the SPACE program for computing the penumbral illumination factor is somewhat more detailed than that given in most references. It consists in projecting the solar disc (or cap) and the cap of the obscuring planet (or moon) on to a great imaginary sphere whose center is at the vehicle position. The relative angular areas of the caps are computed and the illumination factor is given according to Equation (57). While the theoretical development is somewhat involved, it leads to simple closed form algebraic expressions convenient for use on a computer.

First, consider Figure 9 which shows a sphere of radius R, representing the Sun or a planet, and a point P at a distance $\ell + R$ from the center of the sphere. The apparent angular area of the sphere as seen from point P is equivalent to the angular area of the sphere's cap projected onto a projection sphere of radius a. Therefore the following is true:

$$\text{angular area } \theta = 2\pi\,[1 - \cos\psi]$$

$$= 2\pi \left[1 - \frac{\sqrt{\ell(\ell + 2R)}}{\ell + R}\right] \tag{58}$$

$$= 2\pi \frac{H}{a}\,. \tag{59}$$

where a is the radius of the projection sphere, and

H is the height of the projected cap.

The total angular area of a planet (θ_P) or of the Sun (θ_S) at the position of a vehicle can be obtained by substituting the appropriate values of ℓ and R into Equations (58) and (59) and simplifying. Thus, we have:

$$\theta_P = 2\pi \left[1 - \frac{\sqrt{h(h + 2R_P)}}{h + R_P}\right] = 2\pi \frac{H'}{a} \tag{60}$$

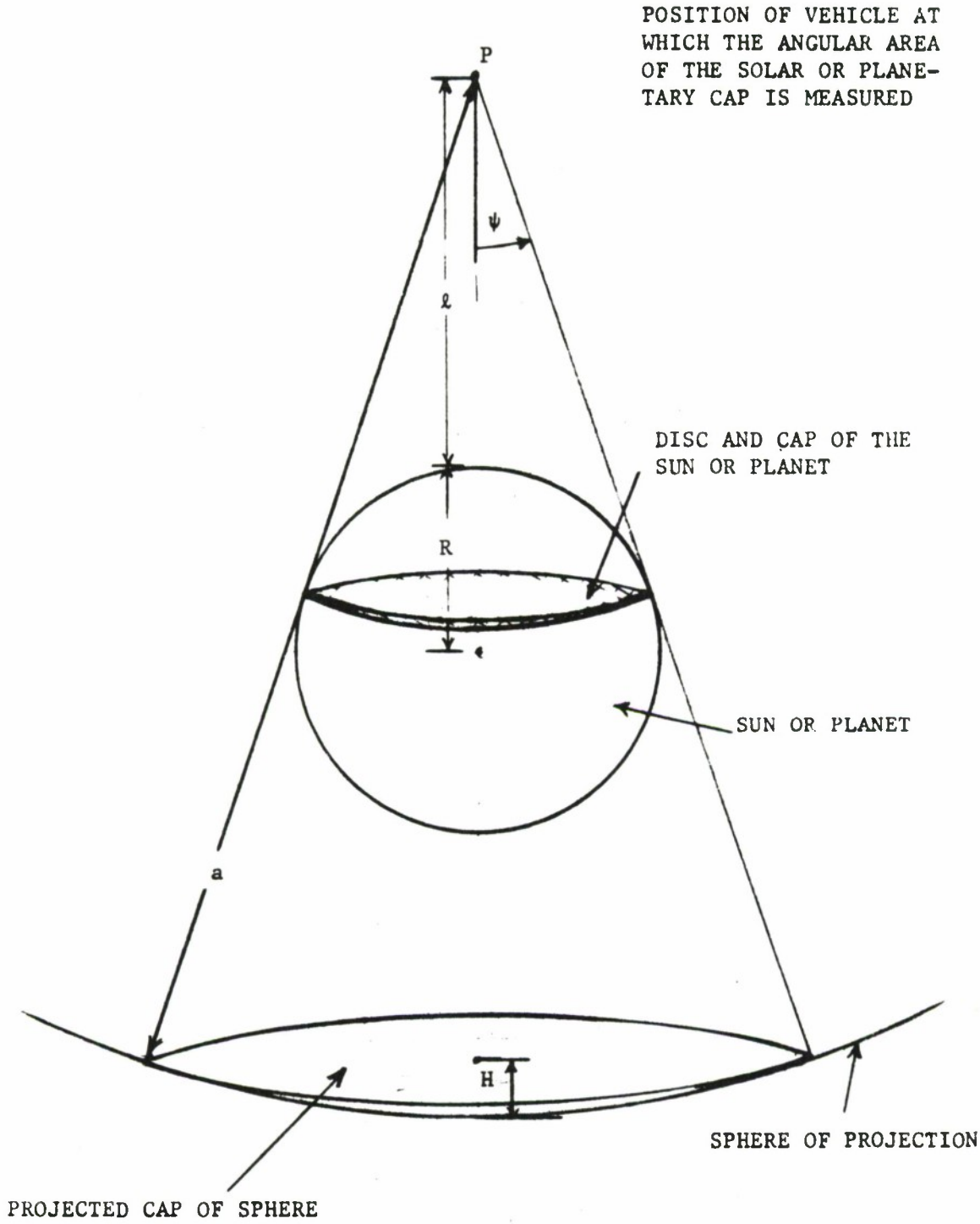

Figure 9. Geometry Used to Measure the Angular Area of the Solar or Planetary Cap

$$\theta_S = 2\pi \left[1 - \sqrt{1 - \frac{R_S^2}{R_{SV}^2}} \right] = 2\pi \frac{H}{a} \tag{61}$$

where

θ_p is the angular area of the planet (or moon) at the vehicle position,

h is the height of the vehicle above the planet's surface,

Rp is the radius of the planet,

θ_S is the angular area of the Sun at the vehicle position,

R_{SV} is the distance from the center of the Sun to the vehicle,

R_S is the radius of the Sun,

H is the height of the solar cap,

H' is the height of the planetary cap,

a is the radius of the imaginary sphere of projection.

Equations (60) and (61) establish the relative size of the solar and planetary caps as seen from the vehicle.

Next, it is desired to determine the angular area of the exposed solar cap A_{EX}. To do this, consider Figure 10. In this figure the vehicle is positioned at the center of a great imaginary projection sphere of arbitrary radius, a. The relative positions of the Sun and the obscuring body or planet are shown as well as the projections of the solar and planetary caps onto the great sphere. The equator of the great sphere is constructed to be coplanar with the vehicle, the center of the Sun, and the center of the planet. A great circle is also constructed perpendicular to the equator and passing through the intersection of the caps; this circle will be used to define one of the limits of integration in the computation of the angular area of the two lunes which are formed by the great circle.

For the calculations to follow, three coordinate systems are defined and illustrated in Figures 10 and 11. The coordinate systems employed are:

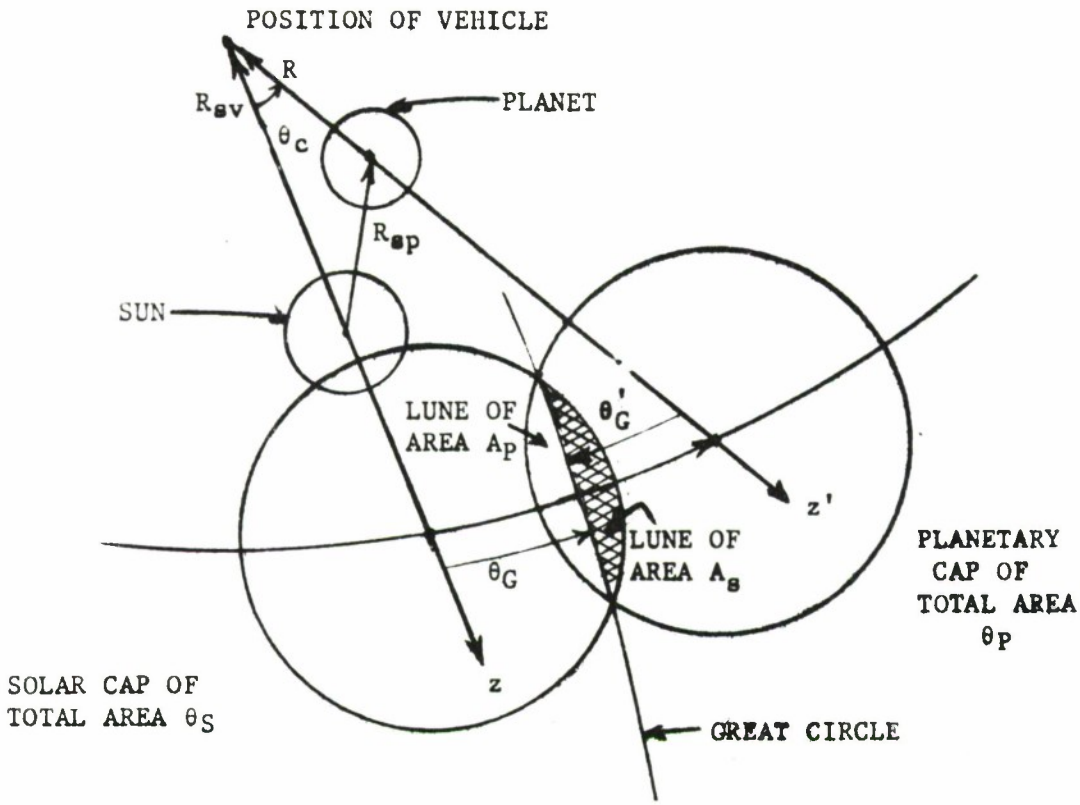

Figure 10. Geometry of the Intersection of the Solar and Planetary Caps

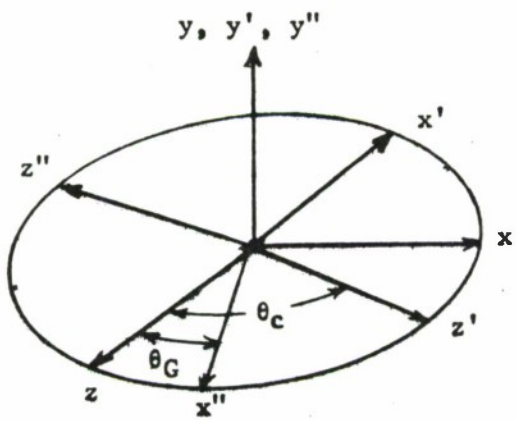

Figure 11. Definition of Coordinate System

(1) A system (x,y,z) for the solar cap.

(2) A system (x',y',z') for the planetary cap.

(3) A system (x'',y'',z'') for the great circle.

All three coordinate systems are orthogonal and have, in common, the same y axis. The relations between the coordinates are given in Equations (62) and (63):

$$\begin{bmatrix} x' \\ z' \\ y' \end{bmatrix} = \begin{bmatrix} \cos\theta_C & -\sin\theta_C & 0 \\ \sin\theta_C & \cos\theta_C & 0 \\ 0 & 0 & 1 \end{bmatrix} \begin{bmatrix} x \\ z \\ y \end{bmatrix} \tag{62}$$

$$\begin{bmatrix} x'' \\ z'' \\ y'' \end{bmatrix} = \begin{bmatrix} \sin\theta_G & \cos\theta_G & 0 \\ -\cos\theta_G & \sin\theta_G & 0 \\ 0 & 0 & 1 \end{bmatrix} \begin{bmatrix} x \\ z \\ y \end{bmatrix} \tag{63}$$

where

θ_C is the angle from the center of the solar cap (z-axis) to the center of the planetary cap (z'-axis),

θ_G is the angle from the center of the solar cap (z-axis) to the great circle (x"-axis).

By inspection of Figure 10 one finds that:

$$\boxed{\cos\theta_C = \frac{\vec{R} \cdot \vec{R}_{sv}}{R \; R_{sv}}} \tag{64}$$

where

$$0 < \theta_C \leq \frac{\pi}{2}$$

Next find the points of intersection of the planetary and solar caps $x = x_p$, $y = y_p$, and $z = z_p$. Referring to Figures 9 and 10 one sees that the equation of the small circle of the solar caps (having a cap height of H) is:

$$x^2 + y^2 + z^2 = a^2$$

$$z = a - H \tag{65}$$

$$\therefore\ x^2 + y^2 = H\,(2a - H) \tag{66}$$

Similarly, the equation of the small circle of the planetary cap having height H' is:

$$(x')^2 + (y')^2 + (z')^2 = a^2$$

$$z' = a - H' \tag{67}$$

$$x'^2 + y'^2 = H'\,(2a - H') \tag{68}$$

Using Equation (62) we can write Equations (67) and (68) in terms of the (x,y,z) coordinates.

$$z' = x \cos\theta_C + z \sin\theta_C = a - H' \tag{69}$$

$$x'^2 + y'^2 = (x \cos\theta_C - z \sin\theta_C)^2 + y = H'(2a - H') \tag{70}$$

From Equations (65) and (69) we find:

$$\boxed{x = x_p = \frac{(a - H') - (a - H)\cos\theta_C}{\sin\theta_C}} \tag{71}$$

Using this result and Equation (65), Equation (70) gives:

$$\boxed{y^2 = y_p^2 = \frac{H'(2a - H')\sin^2\theta_C - [(a - H')\cos\theta_C - (a - H)]^2}{\sin^2\theta_C}} \tag{72}$$

And, of course, Equation (65) can be rewritten:

$$\boxed{z = z_p = a - H} \tag{73}$$

Equation (72) requires some interpretation. Figure 10 illustrates a case where the solar and planetary caps intersect. It is possible that the caps are tangent or that the planetary cap lies within the

solar cap. To determine whether an intersection exists, the value of y_p^2 of Equation (72) may be used as a discriminant.

(1) If $y_p^2 > 0$, two intersections exist.

(2) If $y_p^2 = 0$, the caps are tangent.

(3) If $y_p^2 < 0$, the caps do not intersect and the exposed solar angular area is given by $A_{EX} = \theta_S - \theta_p$.

For the great circle passing through the intersection of the caps $z'' = 0$, $z = z_p$, $x = x_p$. Hence, Equation (63) gives:

$$z'' = -x \cos \theta_G + z \sin \theta_G = 0 \tag{74}$$

$$\text{or} \qquad \frac{x}{z} = \frac{x_p}{z_p} = \tan \theta_G \tag{75}$$

thus from Equations (71) and (73)

$$\boxed{\tan \theta_G = \frac{(a - H') - (a - H) \cos \theta_C}{(a - H) \sin \theta_C}} \tag{76}$$

In a similar manner we may also find the equation for θ_G', the angle between the center of the planetary cap and the great circle,

$$\tan \theta_G' = \frac{x'}{z'} \tag{77}$$

everywhere on the great circle.

Using Equation (62) evaluated at $x = x_p$ and $z = z_p$ we finally obtain:

$$\boxed{\tan \theta_G' = \frac{(a - H') \cos \theta_C - (a - H)}{(a - H') \sin \theta_C}} \tag{78}$$

In computing A_{EX}, there are five cases of interest and these cases are illustrated in Figure 12. If $y_p^2 < 0$ one obtains case V where $A_{EX} = \theta_S - \theta_p$. If $y_p^2 > 0$, however, the caps intersect; and before A_{EX} can be determined, one must calculate A_s and

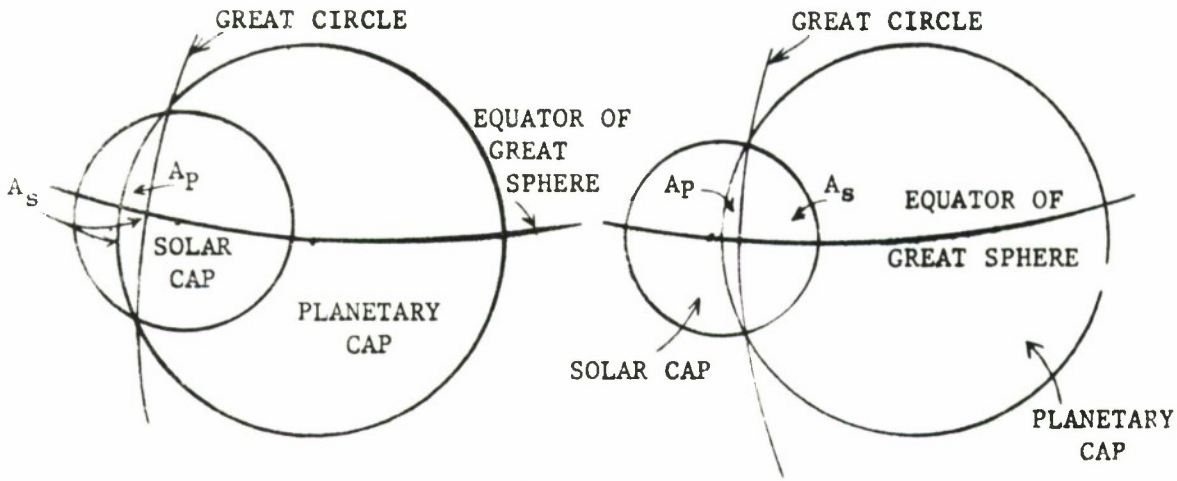

Case I. $A_{EX} = A_S - A_P$ Case II. $A_{EX} = \theta_S - A_S - A_P$

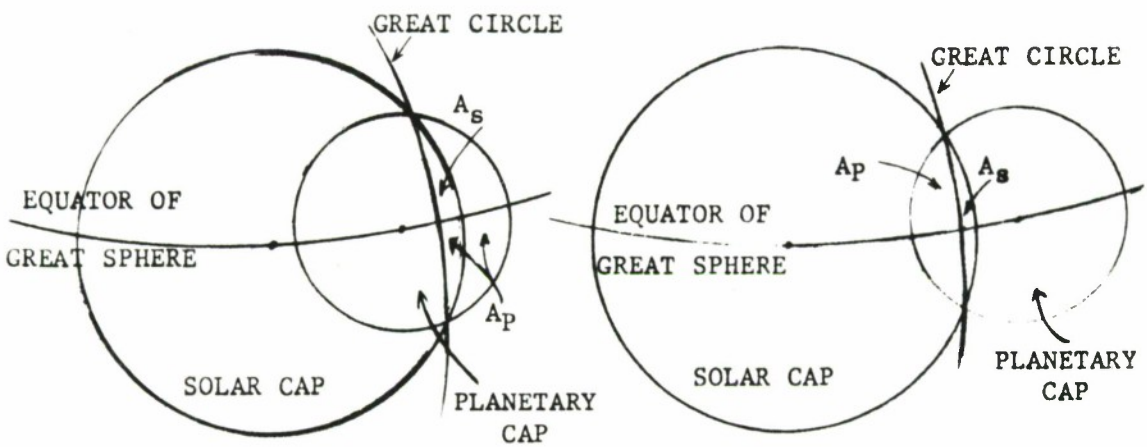

Case III. $A_{EX} = \theta_S - \theta P + Ap - A_S$ Case IV. $AEX = \theta_S - A_S - Ap$

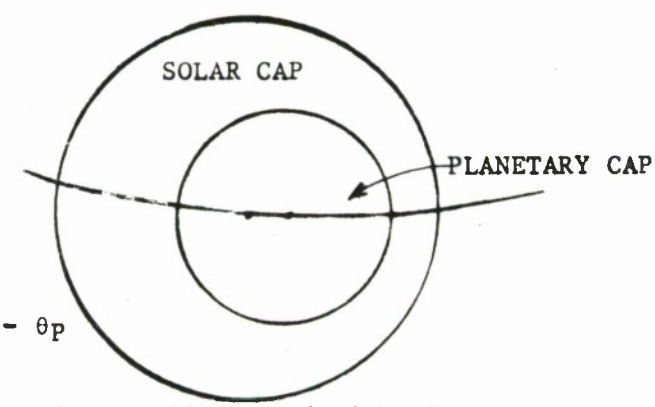

Case V. $A_{EX} = \theta_S - \theta P$

Figure 12. Possible Penumbral Configurations

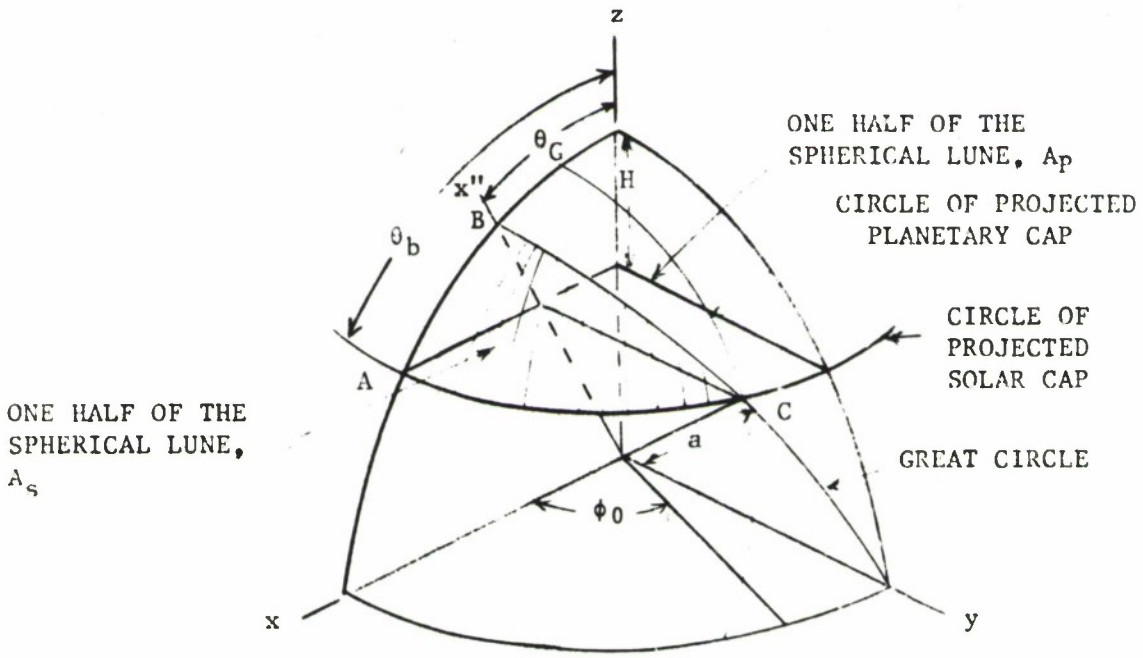

Figure 13. Area of Spherical Lune, A_s

Ap, where A_s is the angular area of the smaller lune formed by the solar cap and the great circle, and Ap is the angular area of the smaller lune formed by the planetary cap and the great circle.

Figure 13 illustrates the geometry and the variables used to compute A_s. The method of computing Ap is identical except that all computations are done in the (x', y', z') coordinate system instead of the (x, y, z) coordinate system.

The area of the surface $\overline{ABC}$ of Figure 13 is given by:

$$\text{area of } \overline{ABC} = \int_0^{\phi_0} a\, d\phi \int_{\theta_a(\phi)}^{\theta_b(\phi)} a \sin\theta\, d\theta, \quad 0 < \phi_0 < \frac{\pi}{2} \tag{79}$$

To get the angular area, A_s, one must double the area of $\overline{ABC}$ and divide the result by a^2. Thus,

$$A_s = 2 \int_0^{\phi_0} d\phi \int_{\theta_a(\phi)}^{\theta_b(\phi)} \sin\theta\, d\theta \tag{80}$$

or

$$A_s = 2 \int_0^{\phi_0} \{\cos[\theta_a(\phi)] - \cos[\theta_b(\phi)]\, d\phi \tag{81}$$

where

ϕ is the angular displacement in the x-y plane, positive counterclockwise,

$\theta_a(\phi)$ is the angular displacement of side BC (an arc of the great circle) from the z-axis, positive counterclockwise,

$\theta_b(\phi)$ is the angular displacement of side AC (an arc of the small circle of the solar cap) from the z-axis, positive counterclockwise.

Before Equation (81) can be evaluated, expressions for $\cos[\theta_a(\phi)]$ and $\cos[\theta_b(\phi)]$ must be found. The equation of the small circle of

the solar cap is:

$$x^2 + y^2 = H\ (2a - H). \tag{82}$$

Using the following transformation:

$$\begin{aligned} x &= a \sin\theta \cos\phi \\ y &= a \sin\theta \sin\phi \\ z &= a \cos\theta \end{aligned} \tag{83}$$

Equation (82) becomes:

$$a^2\ (\sin^2\theta \cos^2\phi + \sin^2\theta \sin^2\phi) = H\ (2a - H)$$

$$\text{or} \qquad a^2\ (1 - \cos^2\theta) = H\ (2a - H) \tag{84}$$

For the small circle of the solar cap, $\theta = \theta_b$, and Equation (84) becomes

$$\boxed{\cos\theta_b = \frac{a - H}{a}} \tag{85}$$

The equation of the great circle is

$$(x'')^2 + y^2 = a^2 \tag{86}$$

and using Equation (53) for x'' we obtain:

$$(x \sin\theta_G + z \cos\theta_G)^2 + y^2 = a^2. \tag{87}$$

From Equation (75) we note that everywhere on the great circle

$$z \tan\theta_G = x, \tag{88}$$

Hence, after substitution of Equation (88) into Equation (87) we have

$$(z \tan\theta_G \sin\theta_G + z \cos\theta_G)^2 + y^2 = a^2. \tag{89}$$

Inserting the polar coordinate relations from Equation (83), yields after some reduction:

$$\cos^2\theta\ (1 - \cos^2\theta_G \sin^2\phi) = \cos^2\theta_G \cos^2\phi \tag{90}$$

or, since $\theta = \theta_a(\phi)$ along the great circle

$$\boxed{\cos\theta_a(\phi) = \frac{\cos\theta_G \cos\phi}{\sqrt{1 - \cos^2\theta_G \sin^2\phi}}} \tag{91}$$

Now we can evaluate A_s of Equation (61) using the value of $\cos\theta_a$ and $\cos\theta_b$ above.

$$A_s = 2\int_0^{\phi_0}\left[\frac{\cos\theta_G \cos\phi}{\sqrt{1 - \cos^2\theta_G \sin^2\phi}} - \frac{a - H}{a}\right] d\phi \tag{92}$$

Rearranging we have:

$$A_s = 2\int_0^{\phi_0}\frac{\cos\phi\, d\phi}{\sqrt{\sec^2\theta_G - \sin^2\phi}} - 2\int_0^{\phi_0}\left(1 - \frac{H}{a}\right) d\phi$$

Letting $\sin\phi = x$, $c^2 = \sec^2\theta_G$

$$A_s = 2\int_0^{\sin\phi_0}\frac{dx}{\sqrt{c^2 - x^2}} - 2\left(1 - \frac{H}{a}\right)\phi_0$$

$$= 2\sin^{-1}\left[\frac{\sin\phi_0}{\sec\theta_G}\right] - 2\left(1 - \frac{H}{a}\right)\phi_0$$

$$\boxed{A_s = 2\sin^{-1}\left[\sin\phi_0 \cos\theta_G\right] - 2\phi_0\left(1 - \frac{H}{a}\right)} \tag{93}$$

From Equation (82) and Figure 13, it is evident that

$$\cos\phi_0 = \frac{x_p}{\sqrt{x_p^2 + y_p^2}} = \frac{xp}{\sqrt{H\,(2a - H)}} \tag{94}$$

$$\boxed{\sin\phi_0 = \frac{y_p}{\sqrt{x_p^2 + y_p^2}} = \frac{y_p}{\sqrt{H\,(2a - H)}},\ y_p > 0} \tag{95}$$

therefore,

$$\boxed{\phi_0 = \sin^{-1}\left[\frac{y_P}{\sqrt{H\ (2a - H)}}\right],\ 0 \leq \phi_0 \leq \frac{\pi}{2}} \tag{96}$$

Using Equations (93), (95), and (96) the value of A_s is obtained. Notice that the above development was done under the restriction, $0 \leq \phi_0 \leq \frac{\pi}{2}$, in which case the entire lune of intersection, A_s, is in the first and fourth quadrants. If the intersection of the two caps occurs in the second quadrant (as in Case I of Figure 12), then ϕ_0 is in the second quadrant and the entire lune of intersection lies in the second and third quadrants. Instead of recomputing this case, note that (see Figure 13) if the lune of intersection, A_s, lies in the second and third quadrants one could rotate the x-y plane about the z-axis by 180°, resulting in the problem that has just been analyzed. Therefore, Equations (93), (94), and (96) give the correct value of the angular area A_s whether ϕ_0 actually lies in the first or second quadrant. Notice, however, that if $0 \leq \phi_0 \leq \frac{\pi}{2}$ then $x_P > 0$ and $\cos \phi_0 > 0$; but if $\frac{\pi}{2} \leq \phi_0 \leq \pi$ then $x_P < 0$ and $\cos \phi_0 < 0$. Thus, $\cos \phi_0$ can be used to discriminate between the two cases just mentioned.

A completely parallel development is used in order to compute A_p. The major difference is that all calculations are done in the (x'y'z') coordinate system. The resulting equations are:

$$\boxed{A_p = 2 \sin^{-1}\left[\sin \phi_0' \cos \theta_G'\right] - 2\phi_0'\left(1 - \frac{H'}{a}\right)} \tag{97}$$

$$\cos \phi_0' = \frac{x_P \cos \theta_C - (a - H) \sin \theta_C}{\sqrt{H'\ (2a - H')}} \tag{98}$$

$$\boxed{\sin \phi_0' = \frac{y_P}{\sqrt{H'\ (2a - H')}}} \tag{99}$$

$$\boxed{\phi_0' = \sin^{-1}\left[\frac{y_p}{\sqrt{H'\ (2a - H')}}\right] \quad 0 \leq \phi_0 \leq \frac{\pi}{2}} \tag{100}$$

where the primed quantities are related to the planet and θ_G' is given by Equation (78).

Finally, note that many quantities are expressed in terms of a, the radius of the great sphere, and H or H' the depth of the solar or planetary cap. By use of Equations (60) and (61) we have

$$\frac{H}{a} = \frac{\theta_S}{2\pi} \tag{101}$$

$$\frac{H'}{a} = \frac{\theta_P}{2\pi} \tag{102}$$

Thus all quantities may be expressed in terms of θ_S and θ_P which are already known. This is most easily accomplished by setting $a = 1$ (since the radius of the sphere is arbitrary) and letting $H = \frac{\theta_S}{2\pi}$ and $H' = \frac{\theta_P}{2\pi}$.

The computation of A_{EX}, the exposed angular area of the solar cap is shown for each of the five cases of Figure 12 in Table II. Note that the discriminants used to determine which case is to be evaluated are y_P^2, $\cos \phi_0$, and $\cos \phi_0'$.

Finally the penumbral illumination factor is given by Equation (57):

$$P = \frac{A_{EX}}{\theta_S}\ .$$

Table II

Computation of A_{EX}, the Exposed Solar Cap

Case I.	$y_P^2 > 0$	$x_P < 0$	$\cos \phi_0 < 0$	$\cos \phi_0' < 0$	$A_{EX} = A_S - A_P$
Case II.	$y_P^2 > 0$	$x_P > 0$	$\cos \phi_0 > 0$	$\cos \phi_0' < 0$	$A_{EX} = \theta_S - A_S - A_P$
Case III.	$y_P^2 > 0$	$x_P > 0$	$\cos \phi_0 > 0$	$\cos \phi_0' > 0$	$A_{EX} = \theta_S - \theta_P + A_S - A_P$
Case IV.	$y_P^2 > 0$	$x_P > 0$	$\cos \phi_0 > 0$	$\cos \phi_0' < 0$	$A_{EX} = \theta_S - A_S - A_P$
Case V.	$y_P^2 < 0$				$A_{EX} = \theta_S - \theta_P$

NUMERICAL INTEGRATION

The equations of motion for a space vehicle are second-order differential equations which describe the accelerations arising from the forces acting on the vehicle. Accounting for the primary gravitational field of the reference body and four types of perturbative accelerations, the equations of motion (from Equation (2)),

$$\ddot{\vec{R}} = -\frac{\vec{R}}{R^3} + \vec{P}_1 + \vec{P}_2 + \vec{P}_3 + \vec{P}_4 \qquad (2)$$

If the perturbations are considered to be zero, the right hand side of Equation (2) reduces to one term and the vehicle will follow a Keplerian orbit which may be described in closed form in terms of its true or eccentric anomaly. Usually, however, part or all of the perturbations are included and Equation (2) must be numerically integrated.

There are two basic methods by which the integration of Equation (2) may be formulated, Encke's method and Cowell's method. If Equation (2) were to be numerically integrated in a straight-forward manner, the integration would be known as Cowell's method. The simplicity of this method is offset by the large accelerations which must be integrated. As a consequence of the acceleration magnitudes, small time increments have to be used in the integration, and machine round-off error accumulates rapidly. Independent evaluations at many companies and universities have shown that Cowell's method requires more machine time than other perturbational schemes. See Baker[10, pp. 228-242] for a further discussion of Cowell's advantages and disadvantages. Despite its drawbacks, Cowell's method is still widely used and is especially suited if the accelerations due to perturbations are as large or larger than the term due to the central force field (e.g., during reentry). The program contains both methods and the option is left to the user.

Historically, Encke's method is older than Cowell's although the former is more sophisticated. Cowell's method requires a modern

high-speed computer to be practical, whereas Encke's was developed for hand computation. In Encke's method, it is assumed that the perturbative accelerations, $\vec{P}_i$, are small compared to the reference body acceleration. Consequently, when drag accelerations are small, the solution of Equation (1) is a good approximation to the true orbit. Under these conditions, it is only necessary to integrate the difference between the accelerations on the two-body orbit and the total accelerations acting on the vehicle. The equations of motion then become second-order differential equations describing the acceleration differences. Let

$$\vec{\xi} = \vec{R} - \vec{R}_{TB} \tag{103}$$

where $\vec{R}_{TB}$ is the position of the vehicle in terms of the two-body orbit. Then,

$$\ddot{\vec{\xi}} = -\mu\left[\frac{\vec{R}}{R^3} - \frac{\vec{R}_{TB}}{R_{TB}^3}\right] + \sum_{i=1}^{4} \vec{P}_i \tag{104}$$

Equation (104) is integrated to obtain $\vec{\xi}$ and $\dot{\vec{\xi}}$. These quantities are then added to $\vec{R}_{TB}$ and $\dot{\vec{R}}_{TB}$, respectively, to obtain the instantaneous position $(\vec{R})$ and velocity $(\dot{\vec{R}})$ of the vehicle. The quantity $\vec{\xi}$ is commonly referred to as the "Encke" term.

Encke's Method

Rewriting Equation (104) we have,

$$\ddot{\vec{\xi}} = \frac{\mu}{R_{TB}^3}\left[\vec{R}_{TB} + \vec{\xi} - \vec{\xi} - \vec{R}\left(\frac{R_{TB}^3}{R^3}\right)\right] + \sum_i \vec{P}_i$$

$$= \frac{\mu}{R_{TB}^3}\left[\left(1 - \frac{R_{TB}^3}{R^3}\right)\vec{R} - \vec{\xi}\right] + \sum_i \vec{P}_i$$

The above equation could be integrated directly; however, the term $\left(1 - \frac{R_{TB}^3}{R^3}\right)$ is not well suited for the numerical calculation since R_{TB}^3/R^3 is very close to 1. Hence we rewrite this term by setting

$$q = \frac{R^2}{R_{TB}^2} - 1 = \frac{\vec{R} \cdot \vec{R} + (\vec{R} \cdot \vec{R}_{TB} - \vec{R} \cdot \vec{R}_{TB}) - \vec{R}_{TB} \cdot \vec{R}_{TB}}{R_{TB}^2}$$

$$= \frac{\vec{R} \cdot (\vec{R}_{TB} + \vec{R}) - \vec{R}_{TB} (\vec{R}_{TB} + \vec{R})}{R_{TB}^2} = \frac{\vec{\xi} \cdot (2\vec{R}_{TB} + \vec{\xi})}{R_{TB}^2}$$

Then, $(1 + q)^{3/2} = R^3/R_{TB}^3$ and

$$\frac{R^3}{R_{TB}^3} - 1 = [(1+q)^{3/2} - 1] \cdot \frac{[(1+q)^{3/2} + 1]}{[(1+q)^{3/2} + 1]} = \frac{(1+q)^3 - 1}{1 + (1+q)^{3/2}} .$$

Expanding the numerator

$$\frac{R^3}{R_{TB}^3} - 1 = \frac{3q + 3q^2 + q^3}{1 + (1+q)^{3/2}} .$$

In summary, Encke's method computes the deviations from the nominal orbit by integrating

$$\ddot{\vec{\xi}} = \frac{\mu}{R^3} \left[\left\{ \frac{3q + 3q^2 + q^3}{1 + (1+q)^{3/2}} \right\} \vec{R}_{TB} - \vec{\xi} \right] + \sum_i \vec{P}_i \qquad (105)$$

where

$$q = \frac{\vec{\xi} \cdot (2\vec{R}_{TB} + \vec{\xi})}{R_{TB}^2} \qquad (106)$$

Determination of Keplerian Orbit Vectors

Encke's method requires the calculation of the position and velocity vectors, $\vec{R}_{TB}$ and $\dot{\vec{R}}_{TB}$, respectively, of the nominal Keplerian orbit. The position and velocity at time t may be written in terms of the position and velocity at an earlier time t_0 as follows:

$$\vec{R}_{TB}(t) = f\, \vec{R}_{TB}(t_0) + g\, \dot{\vec{R}}_{TB}(t_0) \qquad (107)$$

and

$$\dot{\vec{R}}_{TB}(t) = \dot{f}\, \vec{R}_{TB}(t_0) + \dot{g}\, \dot{\vec{R}}_{TB}(t_0) \qquad (108)$$

where f and g are explicit functions of the differential eccentric anomaly of the Keplerian orbit. The program uses Herrick's method to determine f, $\dot{f}$, g, and $\dot{g}$, and then computes $\vec{R}_{TB}(t)$ and $\dot{\vec{R}}_{TB}(t)$

from Equations (107) and (108). The equations for computing f, $\dot{f}$, g, and $\dot{g}$ are given below; their derivations may be found in Battin[4] or Baker[10].

$$f = 1 - C/r_0 \tag{109}$$

$$r_0 = |\vec{R}_{TB}(t_0)| \tag{110}$$

$$g = \frac{M - U}{\sqrt{\mu}}$$

$$\dot{f} = \frac{-\sqrt{\mu}\, S}{A\, r_0} \tag{111}$$

$$\dot{g} = 1 - C/A \tag{112}$$

where

$$M = \sqrt{\mu}\,(t-t_0) = r_0 X + d_0 C + c_0 U \tag{113}$$

$$C = X^2 \left[\frac{1}{2!} - \frac{X^2}{4!a} + \frac{X^4}{6!a^2} - \frac{X^6}{8!a^3} + \ldots\right] \tag{114}$$

$$U = X^3 \left[\frac{1}{3!} - \frac{X^2}{5!a} + \frac{X^4}{7!a^2} - \frac{X^6}{9!a^3} + \ldots\right] \tag{115}$$

$$S = X - \frac{U}{a} \tag{116}$$

$$d_0 = \frac{\vec{R}_{TB}(t_0) \cdot \dot{\vec{R}}_{TB}(t_0)}{\sqrt{\mu}} \tag{117}$$

$$A = r_0 + d_0 S + c_0 C \tag{118}$$

$$c_0 = \frac{r_0\, v_0^2}{\mu} - 1 \tag{119}$$

$$\frac{1}{a} = \frac{2}{r_0} - \frac{v_0^2}{\mu} \tag{120}$$

where

a is the semi-major axis of the Keplerian orbit,

μ is the universal gravitational constant,

and

$$v_0 = |\dot{\vec{R}}_{TB}(t_0)|.$$

Solution of Equations (109) through (112) requires the determination of X. Equation (113) is solved for X by writing

$$F(X) = M - r_0 X - d_0 C - c_0 U = 0$$

and

$$F'(X) = - r_0 - d_0 C' - c_0 U' = 0.$$

Selecting an initial estimate of X to be X_0, the root of $F(X) = 0$ may be determined by a Newton-Raphson iterative process, i.e.,

$$X_{i+1} = X_i - F(X_i)/F'(X_i)$$

From Equations (114) and (115)

$$C' = X - U/a$$

$$U' = C.$$

Since Equations (114) and (115) are series expansions in powers of $\frac{X^2}{a}$, a method must be found to limit the size of this term. For an ellipse,

$$X = (E - E_0)\sqrt{a}$$

where E, and E_0 are the eccentric anomalies at times t, and t_0 respectively. Hence, by updating the epoch t_0 at frequent intervals, the difference $E - E_0$ is kept small. By similar reasoning, frequent updating will keep $\frac{X^2}{a}$ small for hyperbolic orbits.

Cowell's Method

As described before, the general equations of motion of a space vehicle are:

$$\ddot{\vec{R}} = - \frac{\mu \vec{R}}{R^3} + \sum_{i=1}^{4} \vec{P}_i \qquad (121)$$

In Cowell's method, these equations are integrated, using numerical techniques, to obtain the instantaneous position and velocity of the vehicle.

The program performs the integration using the same techniques as it does for the Encke method. The Runge-Kutta starting procedure provides the initial data, and the Nordseick method is used as the long-term integration procedure.

Integration Technique

Equation (2) in Cowell's method or Equation (105) in Encke's method must be numerically integrated by the program. This process is divided into two stages, a starting procedure and a long-term procedure. The long-term numerical integration procedure requires knowledge of previous data points. Thus, the starting procedure is needed to provide the initial data points for the long-term procedure.

The procedure chosen by Sperry-Rand for long-term integration was based on their experience with methods used in the ITEM and MINIVAR programs, and the results of comparative testing. The justification of their choice is presented below as it appears in the original document on the SPACE program[1].

"The long-term numerical integration procedure presently in use in the ITEM and MINIVAR programs is an Adams sixth-order predictor method (without corrector) for second-order differential equations. It was desired, however, to test a broader class of procedures before deciding on one for use as the long-term numerical integration procedure to be used in the program. Accordingly, a program was written to test predictor, predictor-corrector, and iterated predictor-corrector, i.e., repeated application of correctors, techniques of various orders of approximation and with or without modifiers.

"The following results were obtained:

(a) Modifiers were found to leave the error unchanged. There is, therefore, no reason to use them.

(b) As time interval increases, there is more tendency for the solution to become unstable. Error increases with a large power of the time interval.

(c) As the degree of the approximating polynomial increases, a decrease in stability is noted. Error decreases about 3:1

for unit increase in degree of the approximating polynomial.

(d) Predictor-only methods (degree and time interval held fixed) are about 30:1 less accurate than predictor-corrector methods, i.e., one application of the corrector removes 97% of the error in the predictor. A second iteration of the corrector does not reduce the error, but does improve stability at the expense of a 2:1 increase in running time. The increase in running time is intolerable; therefore, a predictor-corrector method will be used with no iteration of the corrector.

(e) Either a fifth or sixth degree approximating polynomial yields a good compromise between accuracy and stability.

"The final choice of a long-term integrating procedure involves considerations other than only accuracy and stability:

(a) The ease of transforming the output of the starting procedure to the form of input starting data needed by the long-term procedure.

(b) Whether the long-term procedure can easily accomodate a change in the time interval.

(c) Whether the long-term procedure can easily interpolate to find conditions at an intermediate time at which data are desired.

"There are at least three forms in which the Adams long-term predictor-corrector formulas can be written. The only difference is in mathematical form; therefore, the accuracy and stability are the same for all three.

"The first form is the conventional one in terms of the successive backward differences; the second is in terms of the successive values of the function. The third is due to Nordsieck and uses the successive higher derivatives of the approximating polynomial. Each of the three forms has certain advantages and certain disadvantages which will be discussed now.

"The backward difference form is fairly easy to start but interpolation is somewhat difficult, and it is virtually impossible to change intervals except by use of the starting procedure. The successive value form of the method is trivial to start up, but inter-

polation involves the Lagrangian interpolation formulas, and changing intervals is, again, almost impossible. The inability to change intervals immediately after starting causes, as in the present ITEM program, a situation where the starting solution is called 28 times, but used only 7 times.

"The Nordsieck method is fairly difficult to start, but very amenable to arbitrary changes of time intervals and to interpolation to intermediate points. Five points are all that are needed to start after a change in time interval (of about 4:1). Due to its versatility, the Nordsieck method of degree 5 (called m = 6 by Nordsieck) without iteration and without choice of interval is used in the program."

Starting Procedure (Runge-Kutta-Gill, RKG, Method)

The program uses the Gill modification of Runge-Kutta[13] for the starting procedure. Runge-Kutta methods are widely used and the differences between Gill's method and others are minor. Therefore, only the formulas as given by Gill and not the derivations are presented. The method was chosen because it introduces some simplicity and error reduction over similar methods.

Given the differential equation

$$\frac{dy}{dx} = f(x, y)$$

and the initial values x_0 and $y(x_0)$, $y(x_0+h)$ is calculated by

$$y(x_0+h) = y(x_0) + \frac{1}{6} k_0 + \frac{1}{3} \left[1 - \sqrt{\frac{1}{2}}\right] k_1 + \frac{1}{3} \left[1 + \sqrt{\frac{1}{2}}\right] k_2 + \frac{1}{6} k_3 \qquad (122)$$

where

$$\begin{aligned}
k_0 &= h\, f(x_0, y_0) & y_0 &= y(x_0) \\
k_1 &= h\, f\left(x_0 + \frac{h}{2}, y_1\right) & y_1 &= y_0 + \frac{1}{2} k_0 \\
k_2 &= h\, f\left(x_0 + \frac{h}{2}, y_2\right) & y_2 &= y_0 + \left[-\frac{1}{2} + \sqrt{\frac{1}{2}}\right] k_0 + \left[1 - \sqrt{\frac{1}{2}}\right] k_1 \\
k_3 &= h\, f(x_0 + h, y_3) & y_3 &= y_0 + \left[-\sqrt{\frac{1}{2}}\right] k_1 + \left[1 + \sqrt{\frac{1}{2}}\right] k_2
\end{aligned} \qquad (123)$$

The above procedure could be used directly to compute $y(x_0 + h)$, $y(x_0 + 2h)$, ... , etc. However, Gill has introduced a "bridging" technique between one entry and the next. This modification increases the accuracy with little increase in complexity. The new procedure[13] may be summarized as:

Given x_0, y_0, $y'(x_i) = f(x_i, y(x_i))$

calculate for $i = 0, 1, 2, 3$

$$K_i = a_i(y'(x_i) - b_i q_i)$$

$$x_{i+1} = x_i + \tau_i h$$

$$y_{i+1} = y(x_{i+1}) = y_i + h K_i$$

$$q_{i+1} = q_i + 3 K_i - c_i y'(x_i)$$

where

$a_0 = \frac{1}{2}$	$b_0 = 2$	$c_0 = \frac{1}{2}$	$\tau_0 = \frac{1}{2}$
$a_1 = 1 - \sqrt{\frac{1}{2}}$	$b_1 = 1$	$c_1 = 1 - \sqrt{\frac{1}{2}}$	$\tau_1 = 0$
$a_2 = 1 + \sqrt{\frac{1}{2}}$	$b_2 = 1$	$c_2 = 1 + \sqrt{\frac{1}{2}}$	$\tau_2 = \frac{1}{2}$
$a_3 = \frac{1}{6}$	$b_3 = 2$	$c_3 = \frac{1}{2}$	$\tau_3 = 0$

For the first entry into the procedure, $q_0 = 0$, and the procedure is the same as given in Equations (122) and (123). For subsequent entries, q_0 is set equal to the previous q_4.

It should be noted that the program must apply the method to the three second-order differential equations given by Equation (105) (Encke's method), or by Equation (121) (Cowell's method). The program treats the problem as one of six first order differential equations given by:

$$\dot{y}_i = f_i(t, y_1, y_2, \ldots, y_6) \quad i = 1, 2, \ldots, 6 \tag{124}$$

where

$$y_1(t) = x(t) \qquad y_4(t) = \dot{x}(t)$$

$$y_2(t) = y(t) \qquad y_5(t) = \dot{y}(t)$$

$$y_3(t) = z(t) \qquad y_6(t) = \dot{z}(t)$$

where (x, y, z) and $(\dot{x}, \dot{y}, \dot{z})$ are the geocentric position and velocity vectors (in Cowell's method) or the perturbations from the nominal orbit (in Encke's method).

The procedure is programmed as follows:

1. $q_i \leftarrow 0 \quad i = 1, 2, \ldots, 6$
2. $\vec{y} = (y_1, y_2, \ldots, y_6) = (\vec{R}(t_0), \dot{\vec{R}}(t_0))$
3. For $k = 1, 2, 3, 4$
   - A. $\dot{\vec{y}} = (\dot{y}_1, \dot{y}_2, \ldots, \dot{y}_6) \quad (\dot{\vec{R}}, \ddot{\vec{R}})$
   - B. For $i = 1, 2, \ldots, 6$
     1. $K \leftarrow a_k (\dot{y}_i - b_k \cdot q_i)$
     2. $y_i \leftarrow y_i + K \cdot h$
     3. $q_i \leftarrow q_i + 3 \cdot K - c_k \cdot \dot{y}_i$
   - C. $\vec{R} \leftarrow (y_1, y_2, y_3)$
     $\dot{\vec{R}} \leftarrow (y_4, y_5, y_6)$
     $t \leftarrow t + \tau_k \cdot h$
     call DERIV, i.e., cal. $\ddot{\vec{R}} = F(\vec{R}, \dot{\vec{R}}, t)$

Hence the program exits with $\vec{R}(t_0 + h)$, $\dot{\vec{R}}(t_0 + h)$, and $\ddot{\vec{R}}(t_0 + h)$. Also, steps 1 and 2 are only executed upon the first entry into the procedure. For second or later entries, the initial value of q_i is the value computed during the last entry for $K = 4$. Clearly, $\vec{y}$ already contains $(\vec{R}(t), \dot{\vec{R}}(t))$ and need not be reset.

Transition from Starting Procedure to Long-Term Integration

The starting procedure yields the solutions of the six differential equations and their rates of change at six successive times. It is necessary to transform these data into the form required by the Nordsieck long-term numerical integration procedure.

For each first order differential equation, the Nordsieck method requires the following five higher derivatives evaluated at $t = t_0$:

$$\left.\begin{aligned} a(t_0) &= \frac{h\,\ddot{y}(t_0)}{2!} \\ b(t_0) &= \frac{h^2 y^{(III)}(t_0)}{3!} \\ c(t_0) &= \frac{h^3\, y^{(IV)}(t_0)}{4!} \\ d(t_0) &= \frac{h^4\, y^{(V)}(t_0)}{5!} \\ e(t_0) &= \frac{h^5 y^{(VI)}(t_0)}{6!} \end{aligned}\right\} \tag{125}$$

The RKG starting method provides data for $y(t)$ and $\dot{y}(t)$ at the six time intervals up to and including t_0, i.e., RKG provides:

$y(t_0)$	$\dot{y}(t_0)$
$y(t_0 - h)$	$\dot{y}(t_0 - h)$
$y(t_0 - 2h)$	$\dot{y}(t_0 - 2h)$
$y(t_0 - 3h)$	$\dot{y}(t_0 - 3h)$
$y(t_0 - 4h)$	$\dot{y}(t_0 - 4h)$
$y(t_0 - 5h)$	$\dot{y}(t_0 - 5h)$

The required values for $a(t_0)$, $b(t_0)$, $c(t_0)$, $d(t_0)$, and $e(t_0)$ will be found by using Lagrange's Interpolation formula to fit a power series of degree five to the $\dot{y}(t)$ data provided by the RKG method. The power series will then be successively differentiated to obtain the required data. Let

$$x = \frac{t - t_0}{h}$$

and let primes denote derivatives with respect to x. Therefore,

$$\left.\begin{aligned}
\dot{y}'(t) &= h\,\ddot{y}(t) \\
\dot{y}''(t) &= h^2\,\dddot{y}(t) \\
\dot{y}'''(t) &= h^3\,y^{(IV)}(t) \\
\dot{y}''''(t) &= h^4\,y^{(V)}(t) \\
\dot{y}'''''(t) &= h^5\,y^{(VI)}(t) \\
\dot{y}''''''(t) &= h^6\,y^{(VII)}(t)
\end{aligned}\right\} \tag{126}$$

From Lagrange's Interpolation Formula,

$$\dot{y}(x) = \sum_{i=0}^{5} F_i(x)\,\dot{y}_i \tag{127}$$

where

$$\left.\begin{aligned}
F_0(x) &= \frac{(x+1)(x+2)(x+3)(x+4)(x+5)}{120} \\
F_1(x) &= \frac{-x(x+2)(x+3)(x+4)(x+5)}{24} \\
F_2(x) &= \frac{x(x+1)(x+3)(x+4)(x+5)}{12} \\
F_3(x) &= \frac{-x(x+1)(x+2)(x+4)(x+5)}{12} \\
F_4(x) &= \frac{x(x+1)(x+2)(x+3)(x+5)}{24} \\
F_5(x) &= \frac{-x(x+1)(x+2)(x+3)(x+4)}{120}
\end{aligned}\right\} \tag{128}$$

and $\dot{y}_i$ are the values determined by the RKG method. Multiplying out the factors in Equation (128) yields

$$
\left.
\begin{aligned}
F_0(x) &= \frac{x^5 + 15x^4 + 85x^3 + 225x^2 + 274x + 120}{120} \\
F_1(x) &= \frac{-(x^5 + 14x^4 + 71x^3 + 154x^2 + 120x)}{24} \\
F_2(x) &= \frac{x^5 + 13x^4 + 59x^3 + 107x^2 + 60x}{12} \\
F_3(x) &= \frac{-(x^5 + 12x^4 + 49x^3 + 78x^2 + 40x)}{12} \\
F_4(x) &= \frac{x^5 + 11x^4 + 41x^3 + 6x^2 + 30x}{24} \\
F_5(x) &= \frac{-(x^5 + 10x^4 + 35x^3 + 50x^2 + 24x)}{120}
\end{aligned}
\right\} \qquad (129)
$$

From Equations (125) and (126)

$$
\left.
\begin{aligned}
a(t_0) &= \frac{\dot{y}'(0)}{2!} \\
b(t_0) &= \frac{\dot{y}''(0)}{3!} \\
c(t_0) &= \frac{\dot{y}'''(0)}{4!} \\
d(t_0) &= \frac{\dot{y}''''(0)}{5!} \\
e(t_0) &= \frac{\dot{y}'''''(0)}{6!}
\end{aligned}
\right\} \qquad (130)
$$

Successively differentiating Equation (127) with respect to x, (using Equation (129)), setting $x = 0$, and substituting into Equation (130) yields the following in matrix notation;

$$
\begin{bmatrix} 2a(t_0) \\ 3b(t_0) \\ 4c(t_0) \\ 5\,d(t_0) \\ 6\,e(t_0) \end{bmatrix} = \frac{1}{120} \cdot \begin{bmatrix} -24 & 150 & -400 & 600 & -600 & 274 \\ -50 & 305 & -780 & 1070 & -770 & 225 \\ -35 & 205 & -490 & 590 & -355 & 85 \\ -10 & 55 & -120 & 130 & -70 & 15 \\ -1 & 5 & -10 & 10 & -5 & 1 \end{bmatrix} \cdot \begin{bmatrix} \dot{y}(t_0 - 5h) \\ \dot{y}(t_0 - 4h) \\ \dot{y}(t_0 - 3h) \\ \dot{y}(t_0 - 2h) \\ \dot{y}(t_0 - h) \\ \dot{y}(t_0) \end{bmatrix}
$$

or

$$\begin{bmatrix} a(t_0) \\ b(t_0) \\ c(t_0) \\ d(t_0) \\ e(t_0) \end{bmatrix} =$$

$$\frac{1}{1440} \cdot \begin{bmatrix} -144 & 900 & -2400 & 3600 & -3600 & 1644 \\ -200 & 1220 & -3120 & 4280 & -3080 & 900 \\ -105 & 615 & -1470 & 1770 & -1065 & 255 \\ -24 & 132 & -288 & 312 & -168 & 36 \\ -2 & 10 & -20 & 20 & -10 & 2 \end{bmatrix} \cdot \begin{bmatrix} \dot{y}(t_0 - 5h) \\ \dot{y}(t_0 - 4h) \\ \dot{y}(t_0 - 3h) \\ \dot{y}(t_0 - 2h) \\ \dot{y}(t_0 - h) \\ \dot{y}(t_0) \end{bmatrix} \qquad (131)$$

Equation (131) is used to compute the sets of coefficients $[a(t_0), b(t_0), x(t_0), d(t_0), e(t_0)]^T$ for the six differential equations given by Equation (124).

Long-Term Integration (Nordsieck Method)

The Nordsieck method is used to continue the solution of Equation (124)

$$\frac{dy_i}{dt} = f_i(t, y_1, \ldots, y_6) \quad i = 1, 2, \ldots, 6 \qquad (132)$$

once begun by the RKG method.

Considering the single equation

$$\frac{dy}{dt} = f(t, y)$$

and approximating its solution by a polynomial of degree five

$$y^P(t_0+h) = y(t_0) + h[\dot{y}(t_0) + \frac{h}{2!}\ddot{y}(t_0) + \frac{h^2}{3!}y^{(III)}(t_0) + \frac{h^3}{4!}y^{(IV)}(t_0) + \frac{h^4}{5!}y^{(V)}(t_0) + \frac{h^5}{6!}y^{(VI)}(t_0)] \qquad (133)$$

where

h is the integration step size,

t_0 is the value of t at the last integration.

Substituting from Equation (125)

$$y^P(t_0+h) = y(t_0) + h[f(t_0, y) + a(t_0) + b(t_0) + c(t_0) + d(t_0) + e(t_0)] \quad (134)$$

Differentiating Equation (133) with respect to $t = t_0 + h$ and using Equation (125)

$$f^P = f(t_0, y) + 2a(t_0) + 3b(t_0) + 4c(t_0) + 5e(t_0) \quad (135)$$

Having obtained a predicted value of $f(t_0 + h, y(t_0 + h))$ a value of $f(t_0 + h) = f(t_0 + h, y^P)$ is computed and combined with f^P to give the Nordsieck corrector,

$$K_1\, h[f(t_0 + h) - f^P]$$

where

$$K_1 = \frac{19087}{60480} = 0.315591931$$

The values of $a(t_0 + h)$, $b(t_0 + h)$, $c(t_0 + h)$, $d(t_0 + h)$ and $e(t_0 + h)$ are then computed in terms of their values at $t = t_0$ by

$$\begin{aligned}
a(t_0 + h) &= a(t_0) + 3b(t_0) + 6c(t_0) + 10d(t_0) + 15e(t_0) \\
&\quad + K_2[f(t_0 + h) - f^P] \\
b(t_0 + h) &= b(t_0) + 4c(t_0) + 10d(t_0) + 20e(t_0) \\
&\quad + K_3[f(t_0 + h) - f^P] \\
c(t_0 + h) &= c(t_0) + 5d(t_0) + 15e(t_0) + K_4[f(t_0 + h) - f^P] \\
d(t_0 + h) &= d(t_0) + 6e(t_0) + K_5[f(t_0 + h) - f^P] \\
e(t_0 + h) &= e(t_0) + K_6[f(t_0 + h) - f^P]
\end{aligned} \quad (136)$$

where

$$K_2 = \frac{137}{120} = 1.141666667$$

$$K_3 = \frac{5}{8} = 0.625$$

$$K_4 = \frac{17}{96} = 0.1770833333$$

$$K_5 = \frac{1}{40} = 0.025$$

$$K_6 = \frac{1}{720} = 0.00138888889$$

The Nordsieck method may now be summarized as follows. For each entry, y^P is computed by Equation (134), f^P by Equation (135), and $f(t_0 + h) = f(t_0 + h, y^P)$ by the functional relationship implied by Equation (132). Then $y(t_0 + h)$ is found by

$$y(t_0 + h) = y^P + K_1\, h(f(t_0 + h) - f^P).$$

Finally the coefficients $a(t)$ through $e(t)$ are updated by Equation (136).

The integration interval, h, is readily changed; the change being accomplished by using new values of $a(t)$, $b(t)$, $c(t)$, $d(t)$, and $e(t)$. These new values are obtained from the following equations:

$$B = \frac{h_n}{h_0}$$

$$a_n(t) = Ba_0(t)$$

$$b_n(t) = B^2 b_0(t)$$

$$c_n(t) = B^3 c_0(t)$$

$$d_n(t) = B^4 d_0(t)$$

$$e_n(t) = B^5 e_0(t)$$

where the subscripts n and 0 stand for new and old, respectively.

COORDINATE SYSTEMS AND TRANSFORMATIONS

The equations of motion of a vehicle are given by Equation (2). It is necessary to express the vectors used in this equation in an inertial coordinate frame, i.e., a coordinate system in which inertial forces due to the system's acceleration are absent or at least negligible. A coordinate system rigidly attached to the Earth is inappropriate, since such a system experiences noticeable accelerations due to the daily rotation of the Earth.

The inertial frame chosen for this program is a so-called "mean equinox of base date" system which is determined by the vernal equinox of 0.0 hours 1 January of the year subsequent to the epoch time (initial input time) used in a given run. This particular base date system has been chosen as a basis for calculation because the planetary, lunar, and solar coordinates are written on tapes in that coordinate system. Rather than transform the tape information, the vehicle initial conditions and the oblateness accelerations are transformed into the base date system.

The definition of the base date system and various auxiliary Earth referenced systems is given below along with the transformations between them.

Terminology

First, consider the celestial sphere (Figure 14) which is a sphere of infinite radius with the Earth at its center upon which the positions of stars, planets, the Sun, and the Moon are projected. It is sometimes convenient to pick the center of the sphere to be at an observer or the center of the Sun, but for the purpose of our discussion its center will always be taken to be at the geocenter. The stars may be taken to be fixed on the sphere (their small proper motions being neglected) while the Sun, planets, and the Moon appear to move and describe certain paths along its inner surface. The apparent path of the Sun during the course of a year on the celestial

sphere is a great circle called the ecliptic. The north celestial pole is the point where the extension of the Earth's north pole intersects the celestial sphere and the south celestial pole is defined similarly. The great circle where the extension of the Earth's equator intersects the celestial sphere is called the celestial equator. The point on the celestial equator where the apparent path of the sun crosses into the northern half of the celestial sphere at the beginning of spring is called the vernal equinox. This is one of two points where the ecliptic and equator intersect. In the following discussion the word celestial will usually be dropped and we will just speak of the north pole or the equator.

The equator and ecliptic are constantly in motion due to the effects of nutation and precession. It should be pointed out that this is astronomical precession which is distinct from the force free precession due to the flattening at the poles. The former is caused by the net torque on the equatorial "bulges" due to the gravitational attraction of the sun and moon. The torque is quite small so that the precession is extremely slow - the period being 26,000 years compared to the rotational period of one day. The total applied torque is not constant in time, because the torques of the Sun and Moon have slightly different directions to the ecliptic and vary as the three bodies move around each other. As a result, there are irregularities in the precession, commonly designated as astronomical nutation. The astronomical nutation is not to be confused with the "true nutation" which is present even in the force-free precession of the Earth's rotation axis. In the subsequent discussion the astronomical precession and nutation will simply be referred to as precession and nutation.

Precession may be separated into luni-solar precession, and planetary precession. The luni-solar precession causes the north pole to move around the ecliptic pole. The ecliptic pole is the point of intersection of the extension of the normal to the ecliptic plane at the geocenter, and the celestial sphere. Nutation is an

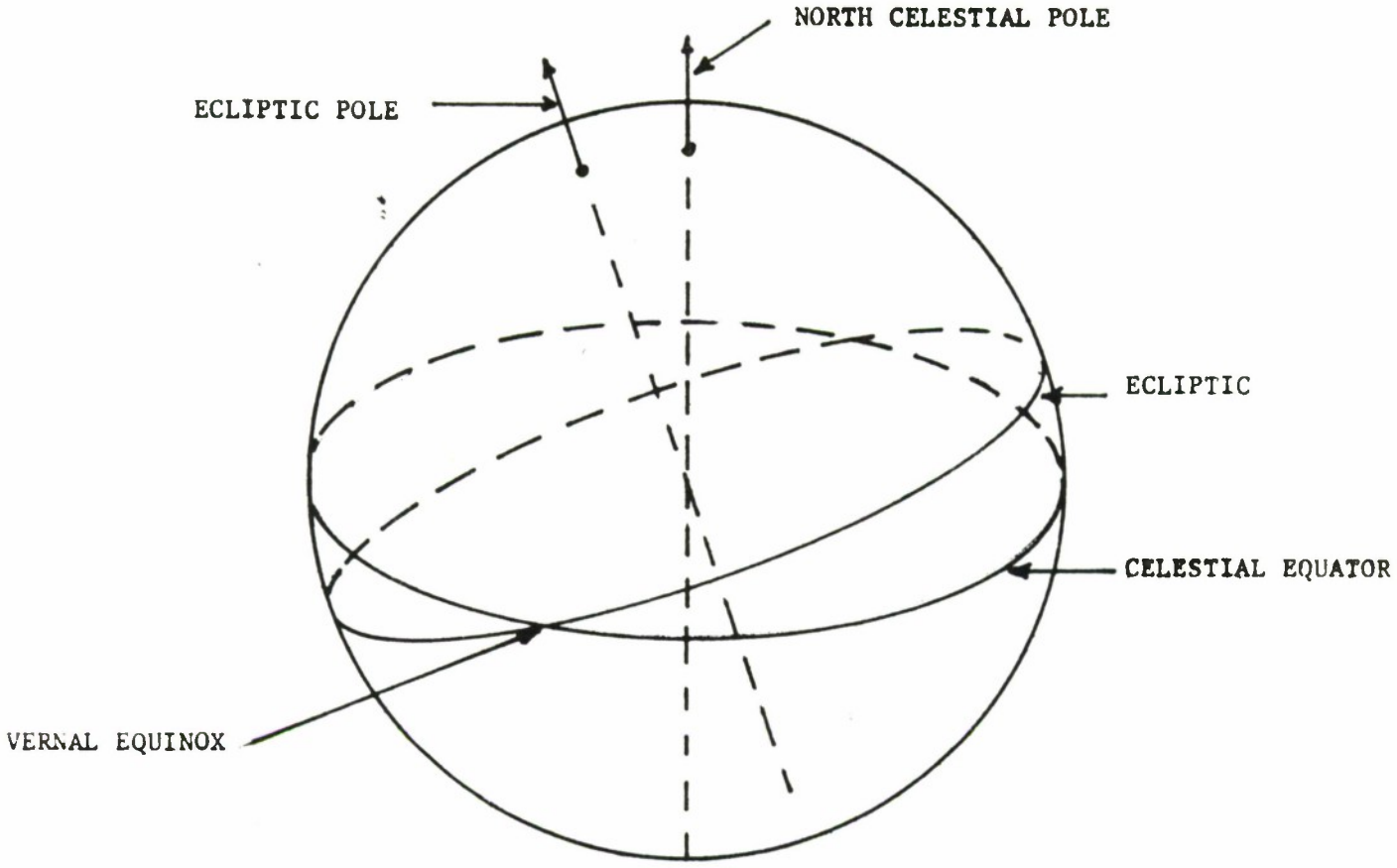

Figure 14. Celestial Sphere

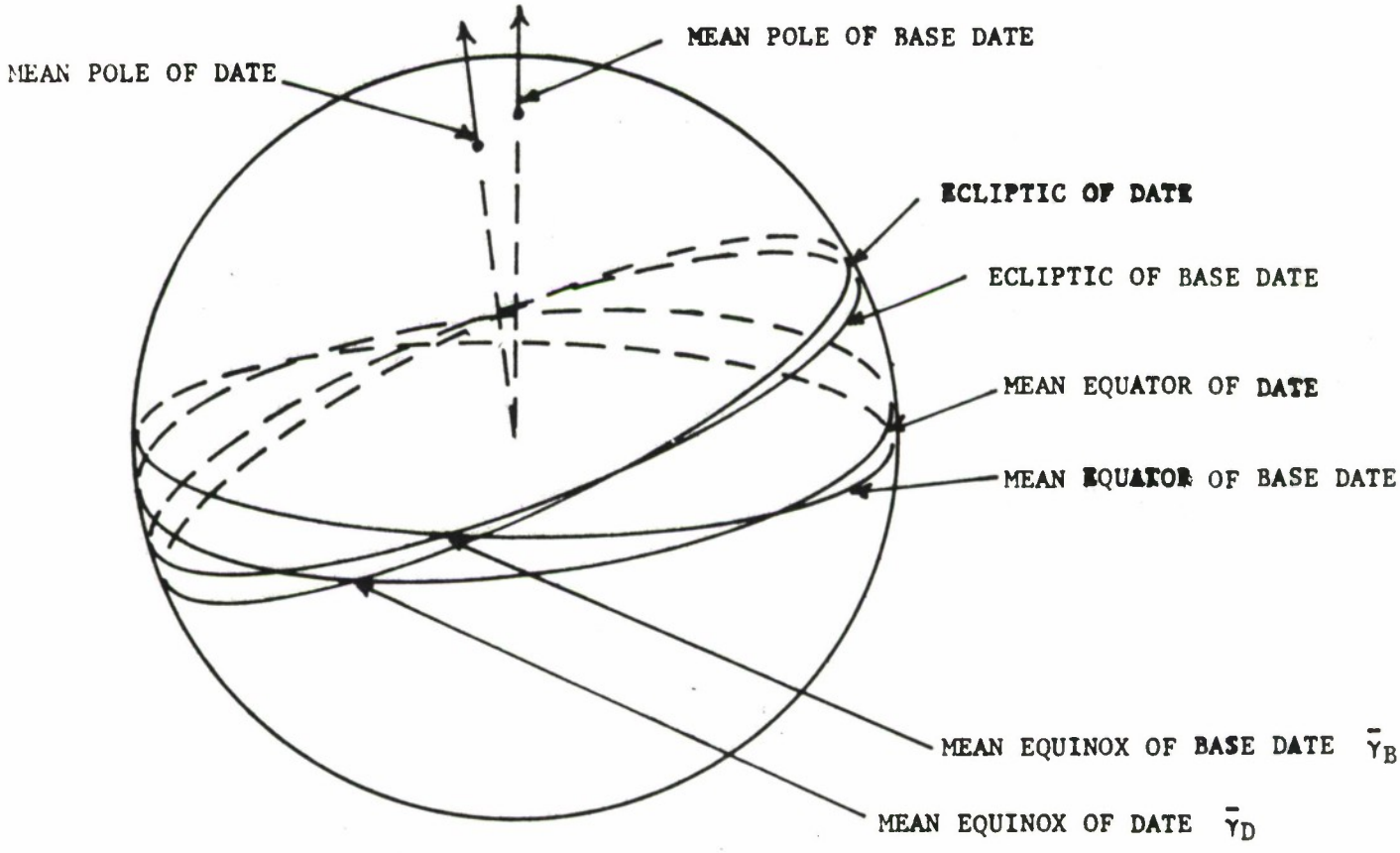

Figure 15. Precession

irregular motion of the pole with a period of about 18.6 years. These two effects combine to model the motion of the true equator. The actual equator at any time is called the true equator of date. The word date here refers to any arbitrary time. The mean equator of date is defined by the location of the equator when the effects of nutation are removed (i.e., where the true equator of date would be if there were no nutation).

The gravitational action of the planets on the Earth causes the plane of the Earth's orbit to slowly precess. This motion appears from the earth as a slow precession of the ecliptic, and is called planetary precession. This effect causes the obliquity (the angle between the equator and the ecliptic) to decrease at the rate of about 47" a century. Therefore, to be precise we refer to the ecliptic of a specified date.

The effect of precession is illustrated in Figure 15. The mean pole, mean equator, and ecliptic at time t_0 are labeled base date and at a later time, t, are labeled date. Luni-solar precession causes the mean equator to move between base date and date, while planetary precession moves the ecliptic. Figure 16 illustrates how nutation causes the true equator of date to differ from the mean equator of date.

In this discussion we will use several coordinate systems which will be defined in terms of the true equator and ecliptic and mean equator and ecliptic at a given time. The true vernal equinox (or true equinox) is defined by the point of intersection of the true equator and ecliptic. The mean vernal equinox (or mean equinox) is defined by the point of intersection of the mean equator and the ecliptic. The true equinox and the mean equinox are points on the celestial sphere that experience a slow motion and hence we must specify a time to indicate their exact positions.

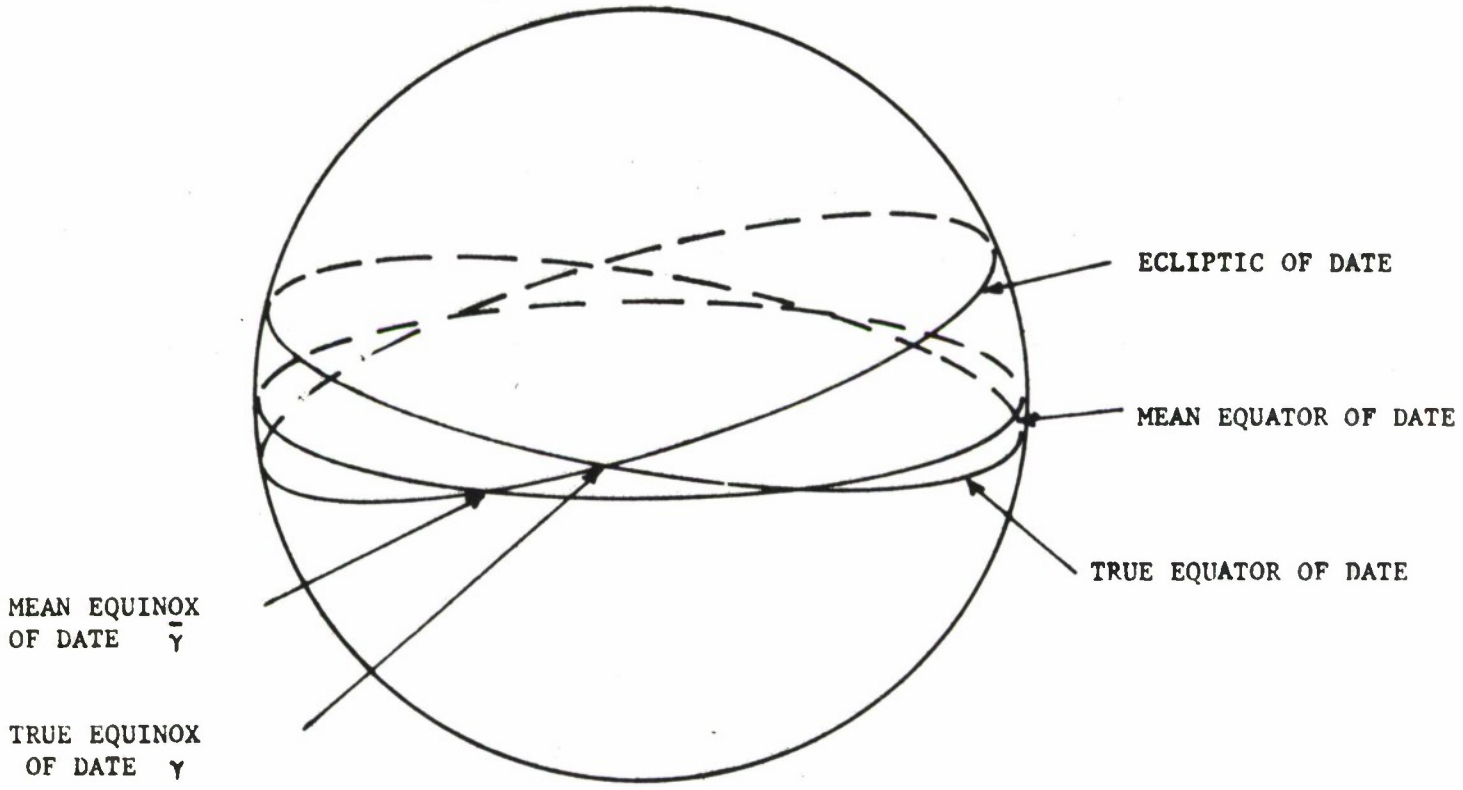

Figure 16. Nutation

Coordinate Systems

The five coordinate systems used by the program for generating trajectories are:

(1) The mean equinox of base date system. This coordinate system is the inertial system employed by the program and employs unit basis vectors $\bar{x}$, $\bar{y}$, and $\bar{z}$ defined as follows:

$\bar{x}$ is a unit vector directed towards the mean vernal equinox of base date.

$\bar{z}$ is a unit vector normal to the mean equatorial plane of base date, positive in the northern hemisphere.

$\bar{y}$ is a unit vector orthogonal to $\bar{x}$ and $\bar{z}$.

(2) The mean equinox of date system. This system employs unit basis vectors $\bar{x}_M$, $\bar{y}_M$, and $\bar{z}_M$ defined as follows:

$\bar{x}_M$ is a unit vector directed toward the mean vernal equinox of date.

$\bar{z}_M$ is a unit vector normal to the mean equatorial plane of date.

$\bar{y}_M$ is a unit vector orthogonal to $\bar{x}_M$ and $\bar{z}_M$.

(3) The true equinox of date system. This system employs unit basis vectors $\bar{x}_T$, $\bar{y}_T$, and $\bar{z}_T$ defined as follows:

$\bar{x}_T$ is a unit vector directed toward the true vernal equinox of date.

$\bar{z}_T$ is a unit vector normal to the true equatorial plane of date.

$\bar{y}_T$ is a unit vector orthogonal to $\bar{x}_T$ and $\bar{z}_T$.

(4) The Greenwich coordinate system. This system employs unit basis vectors $\bar{x}_G$, $\bar{y}_G$, and $\bar{z}_G$ defined as follows:

$\bar{x}_G$ is a unit vector directed toward the intersection of the Greenwich meridian with the true equator of date.

$\bar{z}_G$ is a unit vector normal to the true equator of date.

$\bar{y}_G$ is a unit vector orthogonal to $\bar{x}_G$ and $\bar{z}_G$.

(5) The topocentric coordinate system. This system employs three orthogonal basis vectors $\bar{x}_S$, $\bar{y}_S$ and $\bar{z}_S$, directed toward the east, north, and local vertical, respectively, at a point on the Earth's surface (considered as an ellipsoid). It is only used for observation calculations and its details are discussed under OBSERVATIONS.

The differences between the above coordinate systems are due to dynamical effects of the Earth's motion or to the geometry of the Earth. It is possible to express a 3 × 1 vector of position or velocity written in the basis of one coordinate system in terms of another coordinate basis by applying 3 × 3 orthogonal matrix transformations. Table III below lists the transformations used by the program. $\vec{R}$ is a 3 × 1 vector whose subscript indicates the basis in which the vector is expressed.

Table III.

Transformation Matrices.

MATRIX	EFFECT	FROM	TO	EQUATION
[G]	Earth Geometry	$\bar{x}_S\ \bar{y}_S\ \bar{z}_S$	$\bar{x}_G\ \bar{y}_G\ \bar{z}_G$	$\vec{R}_G = [G]\ \vec{R}_S$
[γ]	Right Ascension of Greenwich from True Equinox of Date (Daily Rotation)	$\bar{x}_G\ \bar{y}_G\ \bar{z}_G$	$\bar{x}_T\ \bar{y}_T\ \bar{z}_T$	$\vec{R}_T = [\gamma]\ \vec{R}_G$
[N]	Nutation	$\bar{x}_T\ \bar{y}_T\ \bar{z}_T$	$\bar{x}_M\ \bar{y}_M\ \bar{z}_M$	$\vec{R}_M = [N]\ \vec{R}_T$
[P]	Precession	$x_M\ y_M\ z_M$	$\bar{x}\ \bar{y}\ \bar{z}$	$\vec{R} = [P]\ \vec{R}_M$

The derivations of [γ], [N], and [P] are given below. It should be recognized that these three matrices are functions of time.

Sidereal Time

When computing the inertial coordinates of a point or station on the surface of the rotating Earth at a particular time, a relationship must be found between the Greenwich meridian (the great circle that passes through the true north pole and Greenwich) and the vernal equinox at that instant. The angle measured in the equatorial plane

from the Greenwich meridian to the true vernal equinox is called the apparent Greenwich sidereal time.

The right ascension of the mean equinox measured from the true equinox is called the equation of the equinoxes or nutation in right ascension and is usually denoted by $\delta\alpha$. The relationship between the apparent sidereal time and the mean sidereal time is:

Mean sidereal time = Apparent sidereal time - $\delta\alpha$.

$\delta\alpha$ is always measured along the true equator from the true equinox eastward. The apparent and mean Greenwich sidereal times are tabulated in the American Ephemeris and Nautical Almanac[4] for 0^h of each day of the year along with the equation of the equinoxes, $\delta\alpha$. Each entry is given in hours, minutes and seconds of time to $0^s.001$, where

$$1^h = 15°, \quad 1^m = 15', \quad \text{and} \quad 1^s = 15''.$$

Apparent Greenwich sidereal time, θ_G, since it is measured from the true equinox, is affected by nutation and hence changes at an irregular rate (see Figure 17). Since mean sidereal time, $\bar{\theta}_G$, is measured from the mean equinox, which is affected only by precession, it increases at almost a constant rate with only a small acceleration and may be calculated at 0^h of any day by the formula

$$\bar{\theta}_G = 6^h\ 38^m\ 45^s.836 + 8{,}640{,}184^s.542T + 0^s.0929T^2 \qquad (137)$$

where T is the number of Julian centuries (36,525 days) from noon 0 January, 1900 (Julian day 2,415,020.).

An equivalent formula in degrees is

$$\bar{\theta}_G(d) = 100°.0755426 + 0°.985647346\ d + 2°.9015 \times 10^{-13}\ d^2 \qquad (138)$$

where d is the integer number of days past 0^h 1 January, 1950. Equations (137) and (138) may be reformulated as a function of the time past any conveniently chosen epoch resulting in an equation of the same form with different coefficients.

Evaluating the above formula for $\bar{\theta}_G(d + 1)$ and $\bar{\theta}_G(d)$, we

can find the angle through which the Greenwich meridian rotates in a day with respect to the moving mean equinox.

$$\bar{\theta}_G(d + 1) - \bar{\theta}_G(d) + 360^\circ = 360^\circ.985647346 + 5^\circ \times 10^{-13}\, d, \tag{139}$$

in which the additive term $2^\circ.9015 \times 10^{-13}$ has been neglected. Dividing Equation (139) by the number of seconds in a day (86,400) and neglecting the final term whose contribution is insignificant over a period of only a few years (< 25 yrs.), we have ω_s, the rotational rate of the Earth with respect to the moving mean equinox,

$$\omega_s = 0^\circ.0041780\ 74622\ \text{sec.}^{-1} \tag{140}$$

Therefore, to find the mean Greenwich sidereal time at time $d + \tau$ we use

$$\bar{\theta}_G(d + \tau) = \bar{\theta}_G(d) + \omega_s\, \tau \tag{141}$$

where d represents the integer number of days past 0^h 1 January, 1950, and τ the number of seconds that have elapsed since 0^h of the day.

The apparent Greenwich sidereal time θ_G can be found at time t by

$$\theta_G(t) = \bar{\theta}_G(t) + \delta\alpha. \tag{142}$$

Now, ω_s will be referred to as the sidereal rotational rate of the Earth. The word sidereal is used since the rate is with respect to the mean equinox, which is the reference point used for sidereal time.

Transformations

The effects of nutation and precession are fairly small and over a period of a few days the errors introduced by neglecting these effects is on the order of ten meters at most. Therefore, for short trajectory determination runs the program has the option of not including them by setting the [P] and [N] matrices equal to the identity matrix, [I]. The [γ] matrix which includes the effects of daily rotation must be included, however.

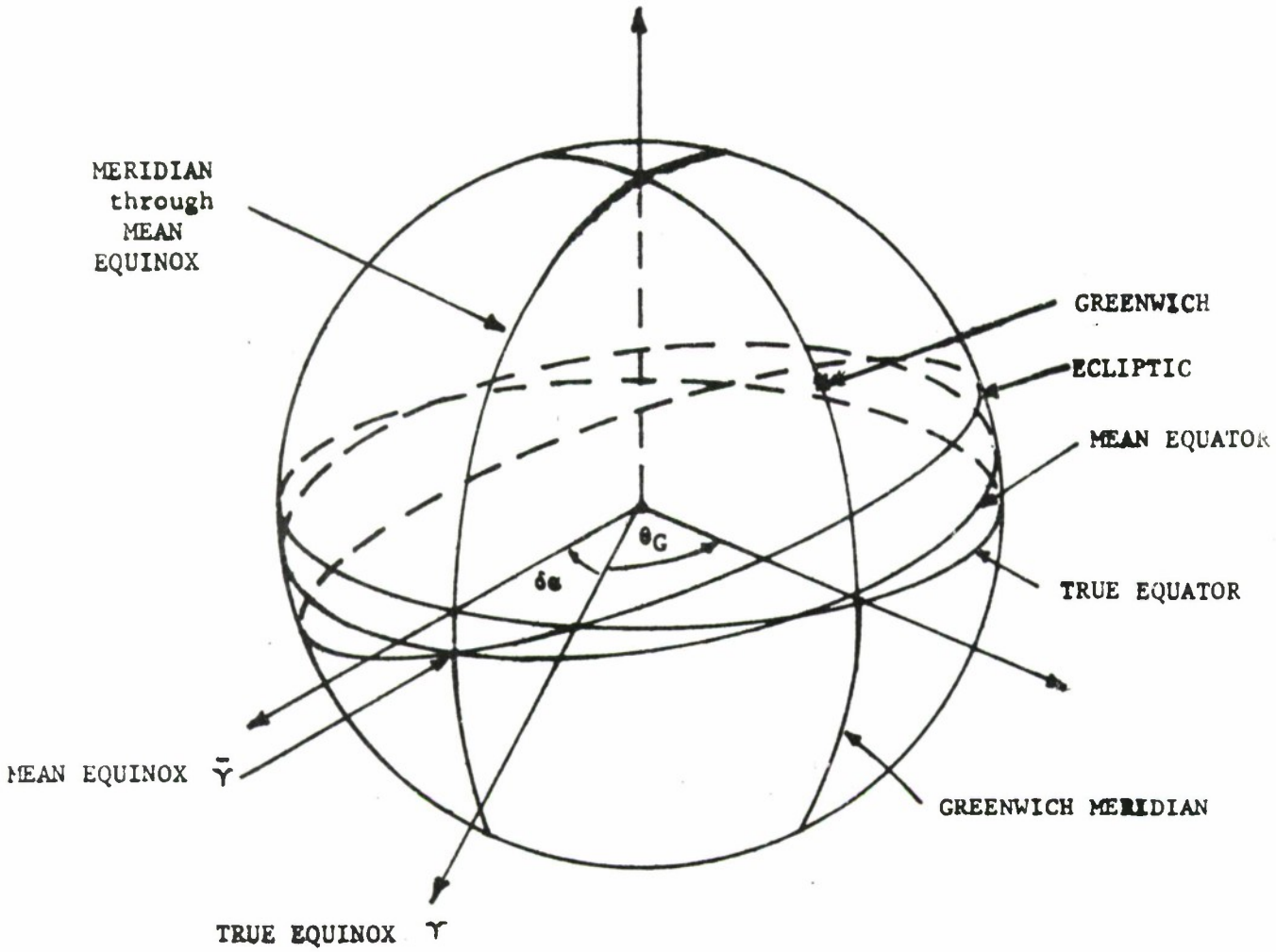

Figure 17. Sidereal Time

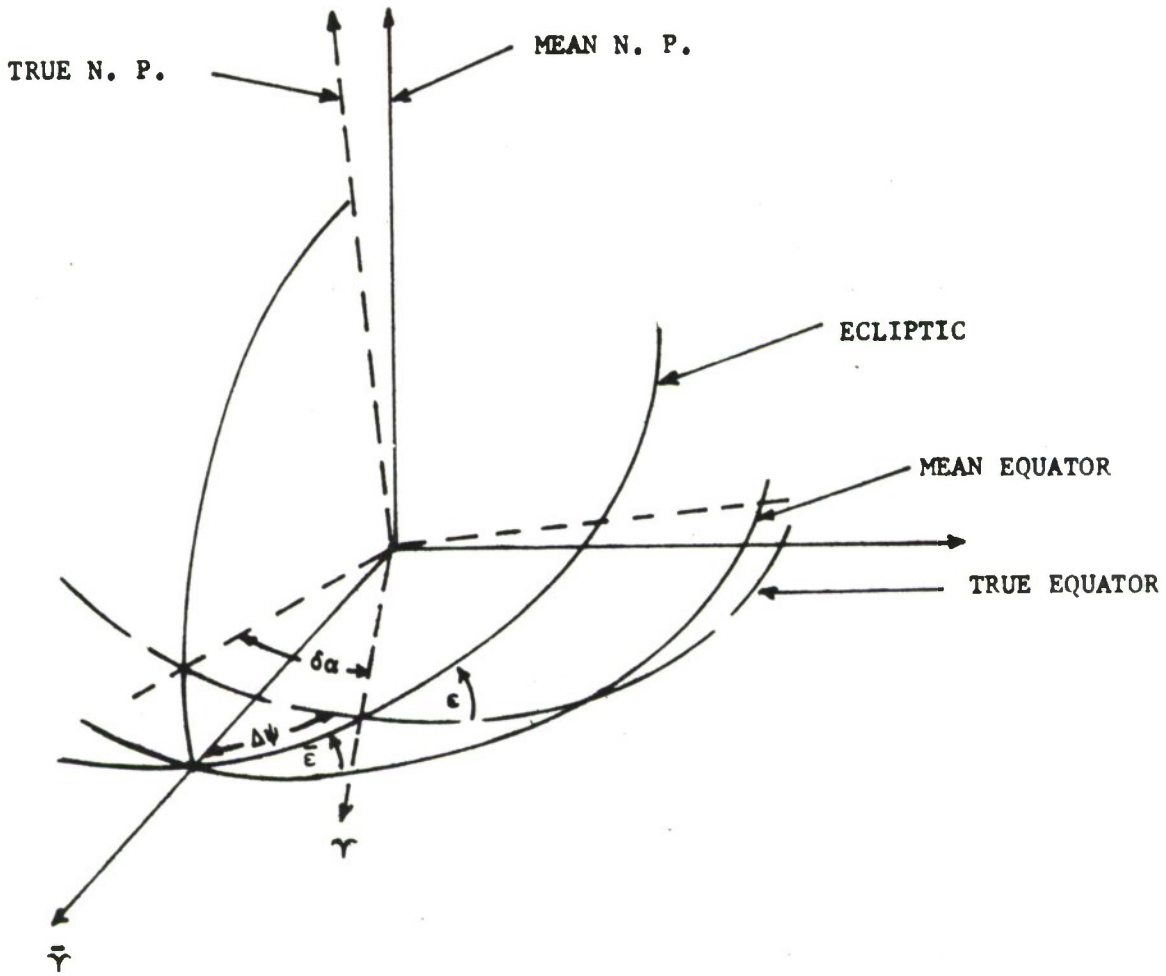

Figure 18. Formation of Nutation Matrix

Referring to Figure 17 the transformation from the Greenwich coordinate system to the true equinox of date system consists of a rotation along the true equator through the angle $\theta_G(t)$ where $\theta_G(t)$ is given by Equation (142). Thus the $[\gamma]$ matrix is given by:

$$[\gamma] = \begin{bmatrix} \cos\theta_G(t) & -\sin\theta_G(t) & 0 \\ \sin\theta_G(t) & \cos\theta_G(t) & 0 \\ 0 & 0 & 1 \end{bmatrix} \tag{143}$$

If the effects of nutation and precession are to be neglected then $\bar{\theta}_G(t)$ replaces $\theta_G(t)$ in Equation (143), and the reference system of the computation may be considered as the system defined by the mean equinox of date (i.e., the effects of nutation and precession are neglected).

Next, an expression for the nutation matrix [N] is found.

In Figure 18, γ is the true equinox of date and $\bar{\gamma}$ is the mean equinox of date. The right ascension of the mean vernal equinox referred to the true equinox is $\delta\alpha$, the equation of the equinoxes. Notice that $\delta\alpha$ is less than zero as it is drawn in Figure 18, since right ascension is measured positively toward the east. The nutation in longitude, $\Delta\psi$, is the longitude of the mean equinox measured from the true equinox. Celestial longitudes are measured along the ecliptic, and since the positive direction is east, $\Delta\psi$ is also negative in Figure 18. The mean obliquity, $\bar{\varepsilon}$, is the inclination of the ecliptic to the mean equator, and ε, the true obliquity, is the inclination of the ecliptic to the true equator. The nutation in obliquity is $\delta\varepsilon$, where

$$\delta\varepsilon = \varepsilon - \bar{\varepsilon}.$$

From inspection of Figure 18, and by using Napier's rules for right spherical triangles,

$$\sin(90^\circ - \varepsilon) = \tan\delta\alpha \tan(90^\circ - \Delta\psi)$$

or

$$\tan \delta\alpha = \tan \Delta\psi \cos \varepsilon$$

Using the series expansion for the tangent function we have

$$\delta\alpha + \frac{(\delta\alpha)^3}{3} + \frac{2\ (\delta\alpha)^5}{15} + \ldots = \cos \varepsilon \left(\Delta\psi + \frac{(\Delta\psi)^3}{3} + \frac{2\ (\Delta\psi)^5}{15} + \ldots\right).$$

Now, $|\delta\alpha|$, and $|\delta\psi|$ are less than $1. \times 10^{-4}$ radians. Therefore, the approximation

$$\delta\alpha = \Delta\psi \cos \varepsilon$$

should never produce an error greater than 1×10^{-12} radians or 2×10^{-7} seconds of arc.

The nutation matrix [N], is now derived which transforms coordinates referred to the true equinox of date into coordinates referred to the mean equinox of date. This transformation consists of three rotation matrices. Using Figure 18, we note that the first, [A], is a rotation about the x-axis through the angle ε. The second, [B], is a rotation about the z'-axis through $\Delta\psi$, and the third, [C], is a rotation about the x"-axis through $-\bar{\varepsilon}$.

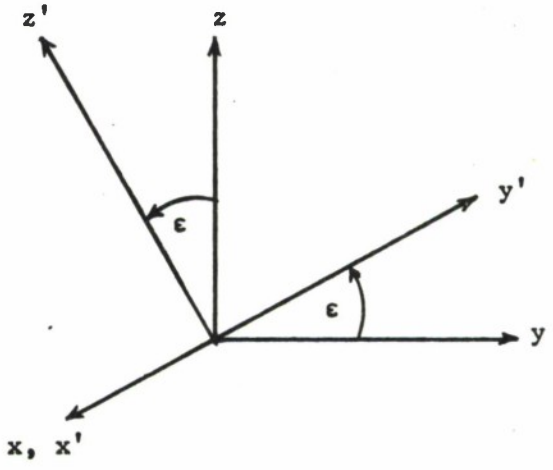

$$[A] = \begin{bmatrix} 1 & 0 & 0 \\ 0 & \cos \varepsilon & \sin \varepsilon \\ 0 & -\sin \varepsilon & \cos \varepsilon \end{bmatrix}$$

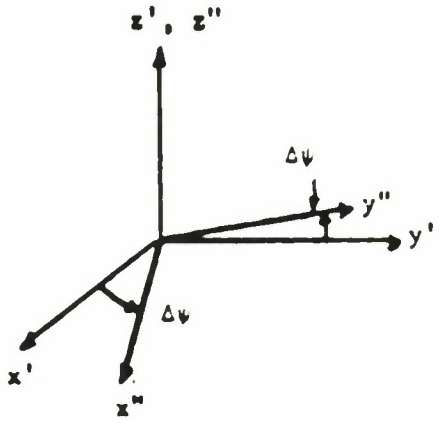

$$[B] = \begin{bmatrix} \cos \Delta\psi & \sin \Delta\psi & 0 \\ -\sin \Delta\psi & \cos \Delta\psi & 0 \\ 0 & 0 & 1 \end{bmatrix}$$

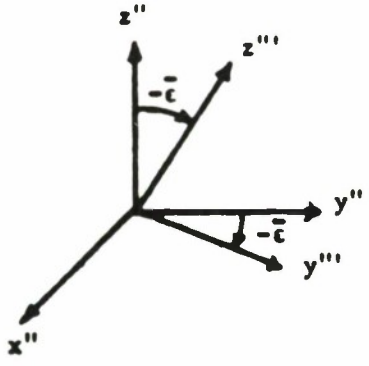

$$[C] = \begin{bmatrix} 1 & 0 & 0 \\ 0 & \cos\bar{\varepsilon} & -\sin\bar{\varepsilon} \\ 0 & \sin\bar{\varepsilon} & \cos\bar{\varepsilon} \end{bmatrix}$$

$[N] = [C][B][A] =$

$$\begin{bmatrix} \cos\Delta\psi & \sin\Delta\psi\cos\varepsilon & \sin\Delta\psi\sin\varepsilon \\ -\cos\bar{\varepsilon}\sin\Delta\psi & \cos\bar{\varepsilon}\cos\Delta\psi\cos\varepsilon + \sin\bar{\varepsilon}\sin\varepsilon & \cos\bar{\varepsilon}\cos\Delta\psi\sin\varepsilon - \sin\bar{\varepsilon}\cos\varepsilon \\ -\sin\bar{\varepsilon}\sin\Delta\psi & \sin\bar{\varepsilon}\cos\Delta\psi\cos\varepsilon - \cos\bar{\varepsilon}\sin\varepsilon & \sin\bar{\varepsilon}\cos\Delta\psi\sin\varepsilon + \cos\bar{\varepsilon}\cos\varepsilon \end{bmatrix} \tag{144}$$

Since $|\delta\psi| < 10^{-4}$ and $|\varepsilon - \bar{\varepsilon}| < 10^{-4}$ the nutation matrix is often approximated by the following matrix:

$$[N'] = \begin{bmatrix} 1 & \Delta\psi\cos\varepsilon & \Delta\psi\sin\varepsilon \\ -\Delta\psi\cos\varepsilon & 1 & \delta\varepsilon \\ -\Delta\psi\sin\varepsilon & -\delta\varepsilon & 1 \end{bmatrix}$$

The error in the elements in [N'] should be less than one unit in the eighth significant figure[14, p.43].

Reference [14] gives formulas for $\Delta\psi$ and $\delta\varepsilon$ which depend on the mean longitude of the Sun, the mean longitude of the perigee of the Sun, the mean longitude of the Moon, the mean longitude of the ascending node of the Moon, and the mean longitude of the lunar perigee. There are 69 terms in the expression for $\Delta\psi$ and 40 terms in $\delta\varepsilon$. Truncated expressions for $\Delta\psi$ and $\delta\varepsilon$ are given in Reference [1].

Finally, an expression for [P], the precession matrix is derived below. Figure 19 illustrates the effect of precession over the period of time $t - t_0$. In this figure, $90° - \zeta_0$ is the right ascension of the ascending node of the mean equator at time t on the mean equator at t_0 measured from the mean equinox of t_0; $90° + z$ is the right ascension of the node measured from the mean equinox of t; and θ is the inclination of the mean equator at time t to the

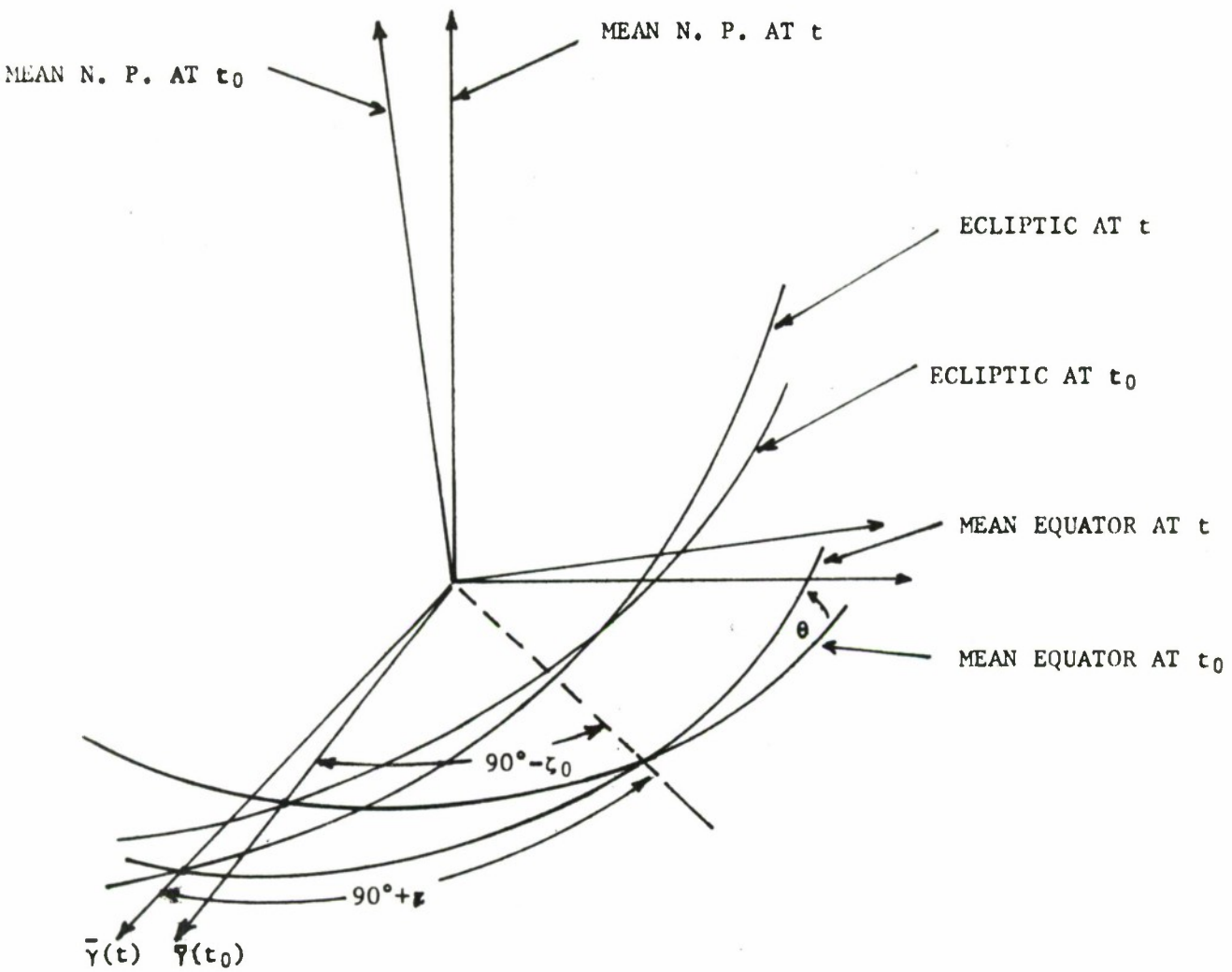

Figure 19. Formation of Precession Matrix

mean equator of t_0.

The precession matrix, [P], is now derived which transforms coordinates referred to $\bar{\gamma}(t)$ to coordinates referred to $\bar{\gamma}(t_0)$.

[P] is a result of three rotation matrices. From Figure 19 we see that the first, [A'], is a rotation of $(90° + z)$ about the z-axis. The second, [B'], is a rotation about x through $-\theta$ and the third, [C'], is a rotation about z through $(\zeta_0 - 90°)$.

$[P] = [A'] \; [B'] \; [C']$, where

$$[A'] = \begin{bmatrix} \cos(90° + z) & \sin(90° + z) & 0 \\ -\sin(90° + z) & \cos(90° + z) & 0 \\ 0 & 0 & 1 \end{bmatrix} = \begin{bmatrix} -\sin z & \cos z & 0 \\ -\cos z & -\sin z & 0 \\ 0 & 0 & 1 \end{bmatrix},$$

$$[B'] = \begin{bmatrix} 1 & 0 & 0 \\ 0 & \cos(-\theta) & \sin(-\theta) \\ 0 & -\sin(-\theta) & \cos(-\theta) \end{bmatrix} = \begin{bmatrix} 1 & 0 & 0 \\ 0 & \cos\theta & -\sin\theta \\ 0 & \sin\theta & \cos\theta \end{bmatrix}$$

$$[C'] = \begin{bmatrix} \cos(\zeta_0 - 90°) & \sin(\zeta_0 - 90°) & 0 \\ -\sin(\zeta_0 - 90°) & \cos(\zeta_0 - 90°) & 0 \\ 0 & 0 & 1 \end{bmatrix} = \begin{bmatrix} \sin\zeta_0 & -\cos\zeta_0 & 0 \\ \cos\zeta_0 & \sin\zeta_0 & 0 \\ 0 & 0 & 1 \end{bmatrix}$$

Hence,

$$[P] = \begin{bmatrix} -\sin z \sin\zeta_0 + \cos z \cos\theta \cos\zeta_0 & \cos z \sin\zeta_0 + \sin z \cos\theta \cos\zeta_0 & \sin\theta \cos\zeta_0 \\ -\sin z \cos\zeta_0 - \cos z \cos\theta \sin\zeta_0 & \cos z \cos\zeta_0 - \sin z \cos\theta \sin\zeta_0 & -\sin\theta \sin\zeta_0 \\ -\cos z \sin\theta & -\sin z \sin\theta & \cos\theta \end{bmatrix} \quad (145)$$

Reference [14] gives the following numerical expression for ζ_0, a, and θ for the case when coordinates are precessed to a <u>later</u> epoch.

Initial epoch, $t_0 = 1900.0 + \tau_0$

Final epoch, $t = 1900.0 + \tau_0 + \tau$

$$\zeta_0 = (2304.''250 + 1.''396\,\tau_0)\,\tau + 0.''302\,\tau^2 + 0.''018\,\tau^3$$

$$z = \zeta_0 + 0.''791\,\tau^2$$

$$\theta = (2004.''682 - 0.''853\,\tau_0)\,\tau - 0.''426\,\tau^2 - 0.''042\,\tau^3$$

where τ_0 and τ are in units of tropical centuries.

When the initial epoch is $1900.0 + \tau_0 + \tau$ and the final epoch is $1900.0 + \tau_0$ (i.e., we are precessing a vector to an earlier epoch) one whould replace

ζ_0 by $-z$

z by $-\zeta_0$

θ by $-\theta$

in the above matrices [A'], [B'], [C'], and [P].

Combining the results of Equations (143), (144), and (145) with the relations in Table III, all necessary coordinate transformations may be performed by the program.

OBSERVATIONS

The SPACE-A program has a provision for a total of 25 observation types of which a number of ground-based observations are specified and described here. The specified observations include:

azimuth,	A
elevation,	E
round-trip range,	2ρ
one-way range rate,	$\dot{\rho}$
hour angle,	H
declination,	D
ℓ-direction cosine,	ℓ
m-direction cosine,	m
X-angle,	X
Y-angle,	Y
range equivalent time,	Δt
range-rate equivalent time,	$\Delta t'$

The position and velocity of a vehicle is available at all times from the trajectory generation portion of the program. The station position and velocity is computed from input data concerning its geodetic coordinates. Therefore, one may consider the relative geometry

of the vehicle and station to obtain the observations.

The program has the option to include the effects of refraction upon ground-based observations. A simple model of the Earth's atmospheric effects upon observations is employed in which the index of refraction varies only with altitude. Neglecting the effects of refraction causes the predicted elevation angle to be less than the observed elevation. Errors are also made in the computation of range and range-rate related observations.

The method used to include the effects of refraction is to compute range and range rate from the relative geometry of the station and the actual vehicle position and velocity and then to apply corrections based on the refraction model in order to obtain the range and range rate related observations. In the case of angle related measurements a slightly different approach is taken. A vector pointing from the station to the computed vehicle position is constructed. Then the refraction model is used to obtain a new vector pointing from the station to the observed vehicle position. All angle observations are then computed directly or indirectly using this new vector.

Coordinates Used in Observation Calculations

The input coordinates of the station (the station is assumed to be on an ellipsoidal Earth) are initially given as geodetic longitude, (λ_G), geodetic latitude (ϕ_G), and height. Given this information the position and velocity of the station in the true system of date coordinate system is given by:

$$\left.\begin{aligned} x_T &= [c + h] \cos \phi_G \cos (\lambda_G + \gamma) \\ y_T &= [c + h] \cos \phi_G \sin (\lambda_G + \gamma) \\ z_T &= [c(1-e^2) + h] \sin \phi_G \\ \dot{x}_T &= - \omega_e y_T \\ \dot{y}_T &= \omega_e x_T \\ \dot{z}_T &= 0 \end{aligned}\right\} \qquad (146)$$

$$c = \frac{R_e}{\sqrt{1 - e^2 \sin^2 \phi_G}} \tag{147}$$

$$e^2 = 2f - f^2 \tag{148}$$

where

x_T, y_T, z_T are the true system of date coordinates of the station,

λ_G, ϕ_G, h are the geodetic coordinates of the station,

γ is the right ascension of the Greenwich meridian in the true system of date,

R_e is the equatorial radius of the Earth,

and f is the flattening constant of the Earth $\left(\frac{1}{298.30}\right)$

Using the precession matrix, [P] and the nutation matrix, [N], we can express the station coordinates in the inertial (base date) coordinate system. From the position and velocity vectors of the station and the vehicle one can obtain the vectors of position and velocity of the vehicle with respect to the station expressed in the inertial system. Thus

$$\vec{\rho} = \vec{\rho}_s - \vec{R} \tag{149}$$

$$\dot{\vec{\rho}} = \dot{\vec{\rho}}_s - \dot{\vec{R}} \tag{150}$$

where $\vec{\rho}, \dot{\vec{\rho}}$ are vectors of the vehicle with respect to the station,

$\vec{\rho}_s, \dot{\vec{\rho}}_s$ are the vectors of the station, and

$\vec{R}, \dot{\vec{R}}$ are the vectors of the vehicle.

Note that all of these vectors are expressed in the inertial coordinate system.

For observation calculations it is convenient to define a station oriented coordinate system which has a basis consisting of three unit orthogonal vectors pointed toward the east, north and local vertical. Using station oriented coordinates the unit vectors are:

$$\vec{x}_S = [1\ 0\ 0]^T, \quad \text{east vector}$$
$$\vec{y}_S = [0\ 1\ 0]^T, \quad \text{north vector}$$
$$\vec{z}_S = [0\ 0\ 1]^T, \quad \text{up vector}$$

Expressed in terms of the inertial base date system these vectors are:

$$\vec{e} = [T]\,\vec{x}_S \quad \text{east vector} \tag{151}$$
$$\vec{n} = [T]\,\vec{y}_S \quad \text{north vector} \tag{152}$$
$$\vec{u} = [T]\,\vec{z}_S \quad \text{up vector} \tag{153}$$

and
$$[T] = [P][N][\gamma][G][\alpha] \tag{154}$$

where all vectors are 3 × 1 vectors.

$[\alpha]$ is a 3 × 3 rotation matrix to account for misalignments between the station oriented coordinates and the true topocentric east, north, and vertical coordinates,

$[G]$ is a 3 × 3 matrix transforming coordinates expressed in the topocentric system into coordinates of the Greenwich system,

$[P]$, $[N]$, and $[\gamma]$ are the 3 × 3 matrices of precession, nutation, and right ascension of the Greenwich meridian which transform the coordinates into the inertial base date system.

$$[G] = \begin{bmatrix} -\sin\lambda_G & -\sin\phi_G\cos\lambda_G & \cos\phi_G\cos\lambda_G \\ \cos\lambda_G & -\sin\phi_G\sin\lambda_G & \cos\phi_G\sin\lambda_G \\ 0 & \cos\phi_G & \sin\phi_G \end{bmatrix} \tag{155}$$

where λ_G and ϕ_G are, respectively, geodetic longitude and geodetic latitude of the station.

The final result of the above transformations is that the station oriented basis vectors ($\vec{e}$, $\vec{n}$, and $\vec{u}$) are expressed in the inertial base date coordinate system.

Computation of Observation Types

In the following discussion all computations are made using vectors expressed in the inertial (base date) coordinate system.

Azimuth and elevation measurements are illustrated in Figure 20.

Azimuth, A, is measured easterly from station north from $0 \leq A \leq 2\pi$. Elevation, E, is measured from the stations horizontal plane upward with a range $-\frac{\pi}{2} \leq E \leq \frac{\pi}{2}$. If $\vec{\rho}$ is the station to vehicle vector the azimuth and elevation are given by:

$$A = \tan^{-1}\left[\frac{\vec{\rho} \cdot \vec{e}}{\vec{\rho} \cdot \vec{n}}\right] \tag{156}$$

$$E = \tan^{-1}\left[\frac{\vec{\rho} \cdot \vec{u}}{\sqrt{(\vec{\rho} \cdot \vec{e})^2 + (\vec{\rho} \cdot \vec{n})^2}}\right] \tag{157}$$

If refraction is to be included in the computations, the vector, $\vec{\rho}$, is replaced by the vector $\vec{\rho}'$, where $\vec{\rho}'$ is the vector from the station to the observed vehicle position as described below.

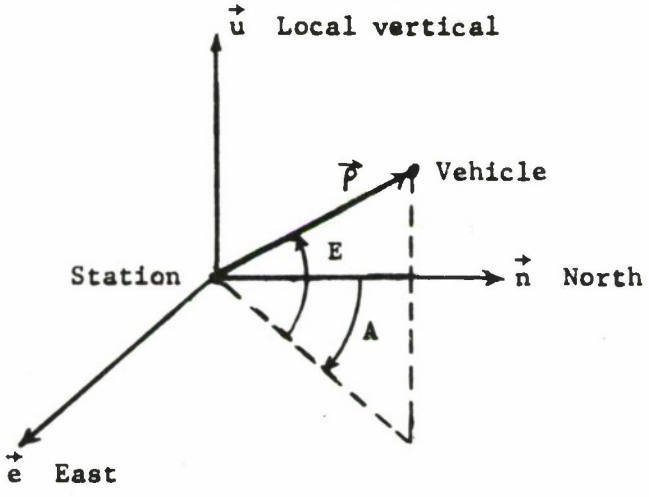

Figure 20. Azimuth and Elevation

The round-trip range, 2ρ, is twice the distance from the station to the vehicle and its value is given by:

$$2\rho = 2|\vec{\rho}| + 2\Delta\rho \tag{158}$$

If the effects of refraction are not included in the calculation $2\Delta\rho = 0$. If the refraction effects are included $\Delta\rho$ is a correction

term the value of which is given by Equation (202).

The one-way range-rate, $\dot{\rho}$, is equal to the magnitude of the time derivative of the vector from the station to the vehicle and its value is given by:

$$\dot{\rho} = \frac{\dot{\vec{\rho}} \cdot \vec{\rho}}{|\vec{\rho}|} + \Delta\dot{\rho} \tag{159}$$

If the effects of refraction are not included $\Delta\dot{\rho} = 0$. If the effects of refraction are included $\Delta\dot{\rho}$ is a correction term the value of which is given by Equation (206).

The hour angle, H, is the angle between the station meridian and the projection on the true equator of the station to vehicle vector measured in the true equatorial plane. It is measured westward from $-\pi \leq H \leq \pi$. The declination, D, is the angle made with the true equatorial plane by the station to vehicle vector. Declination is measured positive in the northern hemisphere and has a range $-\frac{\pi}{2} \leq D \leq \frac{\pi}{2}$. Hour angle and declination are illustrated in Figure 21 which shows the station at the center of a celestial sphere and the projected true equator on the celestial sphere. The hour angle and declination may be derived using spherical trigonometric relations in terms of geodetic latitude, azimuth and elevation (ϕ, A, E). The values are given by:

$$H = \tan^{-1}\left[\frac{\sin A}{\cos A \sin \phi_G - \cos \phi_G \tan E}\right] \tag{160}$$

$$D = \sin^{-1}\left[\sin \phi_G \sin E + \cos \phi_G \cos E \cos A\right] \tag{161}$$

The values of A and E used above are given by Equations (156) and (157).

The ℓ-direction cosine, ℓ, and m-direction cosine, m, are shown in Figure 22. The ℓ-direction cosine is the cosine of the angle between the station to vehicle vector $\vec{\rho}$, and the station east vector, $\vec{e}$. The m-direction cosine is the cosine of the angle between the station to vehicle vector $\vec{\rho}$, and the station's north vector, $\vec{n}$. The

values of ℓ and m are given by:

$$\ell = \frac{\vec{\rho} \cdot \vec{e}}{|\vec{\rho}|} \tag{162}$$

$$m = \frac{\vec{\rho} \cdot \vec{n}}{|\vec{\rho}|} \tag{163}$$

If refraction effects are included $\vec{\rho}'$ replaces $\vec{\rho}$ in the above equations.

The X-angle and Y-angle measurements are illustrated in Figure 23. The Y-angle is the angle between the station to vehicle vector, $\vec{\rho}$, and the perpendicular projection of this vector on the station's east-vertical plane. It is positively measured toward the north, negatively toward the south with limits $-\frac{\pi}{2} \leq Y \leq \frac{\pi}{2}$. The X-angle is measured between the vertical vector, $\vec{u}$, and the perpendicular projection of the station to vehicle vector onto the station's east-vertical plane. It is measured from the positive vertical eastward with limit $-\pi \leq X \leq \pi$. The value of X and Y are given by:

$$X = \tan^{-1}\left[\frac{\vec{\rho} \cdot \vec{e}}{\vec{\rho} \cdot \vec{n}}\right] \tag{164}$$

$$Y = \tan^{-1}\left[\frac{\vec{\rho} \cdot \vec{n}}{\sqrt{(\vec{\rho} \cdot \vec{e})^2 + (\vec{\rho} \cdot \vec{u})^2}}\right] \tag{165}$$

If refraction effects are included $\vec{\rho}'$ replaces $\vec{\rho}$ in the above equations.

The range time equivalent, Δt, and the range-rate time equivalents $\Delta t'$, are included since the raw data from typical tracking systems are the time between a transmitted and received signal for range, and the time to count a given number of Doppler cycles for range-rate. In most systems, these quantities are first converted to range and range-rate units. However, it may be found useful in some cases to use the raw data equivalents. The values of Δt and $\Delta t'$ are given by:

$$\Delta t = \frac{2|\vec{\rho}|}{c} \tag{166}$$

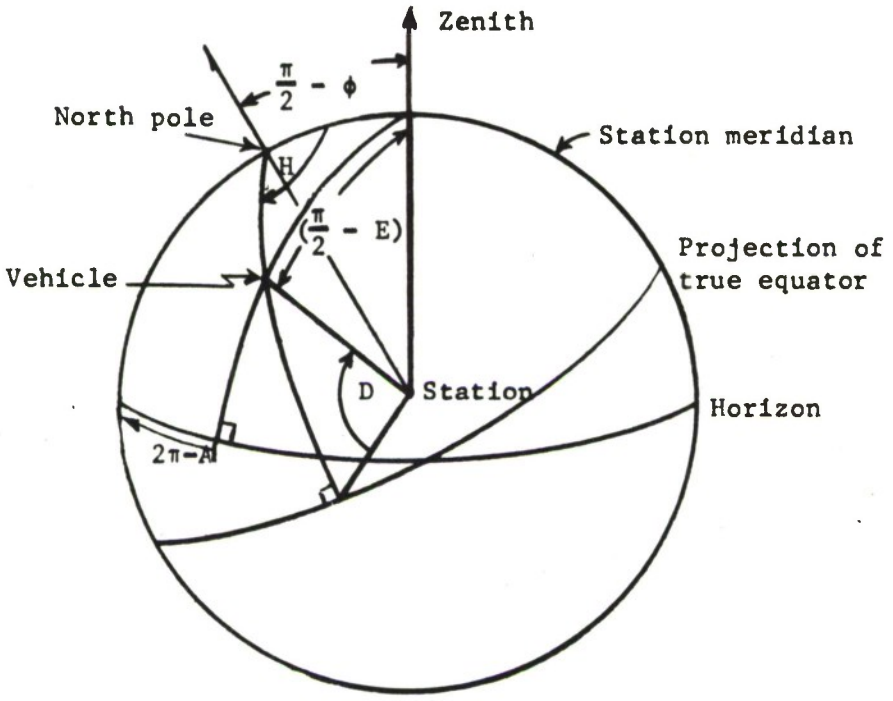

Figure 21. Geometry Illustrating Hour Angle and Declination

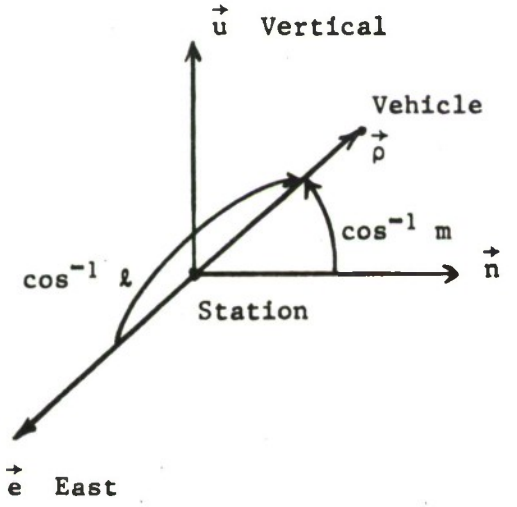

Figure 22. ℓ-cosine and m-cosine

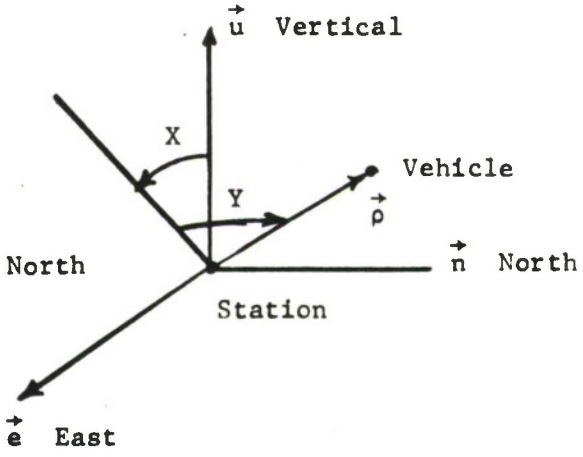

Figure 23. X-Angle and Y-Angle

$$\Delta t' = \frac{|\vec{\rho}_2| - |\vec{\rho}_1|}{c} \tag{167}$$

where

c is the velocity of light,

$|\vec{\rho}_1|$ and $|\vec{\rho}_2|$ are the ranges at the beginning and end of the measurements, respectively.

Specific provision is made in the program for computing doppler shift frequency measurements. The equations for these observations are not included, since the method of computation can change depending on the specific hardware in use for a particular mission.

Effects of Refraction

Because of variations in the refractive index of the atmosphere the propagation path of a tracking beam is subject to refractive bending.

Two models for the variations of refractive index are included in the program: one is a model for the troposphere, the other is a model for ionosphere. A numerical method due to Weisbrod and Anderson[13] is employed in which the effects of refractive bending are determined by numerically integrating over the total propagation path, the index of refraction at each point being determined by the assumed model. The vector from the station to the current calculated position of the vehicle, $\vec{\rho}$, is available from the program. Using numerical methods a correction to the elevation angle is found and a new vector, $\vec{\rho}'$, from the station toward the observed position of the vehicle is determined.

In addition to angle corrections due to refractive bending, the effects on range measurements due to signal retardation, and the effects on range-rate measurements due to refractive bending are also found.

Index of Refraction Models

In order to simplify computational problems, atmospheric models

representative of average conditions are employed in which the following assumptions are made:

(1) The gradient of the index of refraction varies only with altitude.

(2) The index of refraction profile is approximated by a number of linear segments in which the length of each segment is very small compared to the Earth's radius.

(3) The troposphere extends to 40 kilometers.

(4) The region between the end of the troposphere and the beginning of the ionosphere is assumed to have zero refractivity (and therefore no bending or signal retardation occurs).

(5) The ionosphere lies between a height h_0 (input data) and 2,000 kilometers.

(6) The index of refraction is zero beyond 2,000 kilometers.

In the tropospheric model, refractivity (N) is assumed to decay exponentially, with the ground index of refraction and the scale height as parameters. The equation for the tropospheric model is as follows:

$$N = N_0 e^{-h/H} = (n - 1)10^6 \tag{168}$$

where

N_0 is the refractivity at sea level, an input quantity for each station (usually 313),

h is the height above the Earth,

H is the scale height, an input quantity for each station (usually 7 kilometers),

n is the index of refraction.

For the tropospheric model, the refractive errors are considered to be independent of signal frequency since the index of refraction is virtually independent of frequency up to 30,000 MHz,

In the ionospheric model, the index of refraction is dependent upon more parameters than those considered for the tropospheric model. The ionosphere consists of several belts of charged particles. The F layer is very much larger than any other layer, and contains a greater number of charged particles than the other layers. The F

layer is the one closest to the Earth's surface. It is subdivided into the F1 and F2 layers. In the ionospheric model, the index of refraction is primarily dependent upon the height, h_0, of the base of the ionosphere's F2 layer, the maximum electron density of the F2 layer, and the height of the maximum electron density of the F2 layer.

Both index of refraction and the height, h_0, are dependent upon diurnal, solar activity, seasonal, and geographical variations as well as other miscellaneous sporadic variations. Unlike the tropospheric model, the refractive errors in the ionospheric model are frequency dependent.

In constructing the model, the range of the signal frequency has been limited to frequencies above 100 MHz, since this range of spectrum both represents the situation of greatest interest and enables equation simplification.

The relationship between the index of refraction (n) the angular frequency of the incident signal (ω), and the electron density in the ionosphere[15] is given by

$$n = \left[1 - \frac{\rho_e \, e^2}{\varepsilon_0 \, m \, \omega^2}\right]^{1/2} \tag{169}$$

where

ρ_e is the electron density per cubic meter,

e is the electron charge (1.6×10^{-19} Couloumbs),

m is the electron mass (9.08×10^{-31} kilograms)

ε_0 is the permittivity of free space (8.854×10^{-12} farads/meter).

Using the first two terms of the binomial expansion as an approximation, the equation for the index of refraction reduces to:

$$n = 1 - 40.3 \frac{\rho_e}{f^2} 10^{-12} \tag{170}$$

where $f = \frac{\omega \, 10^6}{2\pi}$. Note that f has the dimensions of MHz. This equation is true for frequencies above the critical frequency, f_c,

which is defined as:

$$f_c = 8.97\ \rho_0^{1/2} \times 10^{-6}\ \text{(MHz)} \tag{171}$$

where ρ_0 is the maximum electron density per cubic meter.

From the definition of N in Equation (168), Equation (170) can be written as

$$N = -4.03\ \frac{\rho_e}{f^2} \times 10^{-5} \tag{172}$$

The model selected for electron density versus height consists of a parabolic variation below the height of maximum electron density matched to a hyperbolic secant profile above the maximum. The relationships are as follows:

$$\left.\begin{aligned} \rho_e &= \rho_0\ [1 - (1 - \sigma)^2] \quad \text{for} \quad 0 \leq \sigma \leq 1 \\ \rho_e &= \operatorname{sech}\left[\frac{\pi}{4}\ (\sigma - 1)\right] \quad \text{for} \quad \sigma \geq 1 \end{aligned}\right\} \tag{173}$$

where

$$\sigma = \frac{h - h_0}{h_m - h_0}$$

h is the height above the Earth,

h_0 is the height of the base of the F2 layer (input quantity),

h_m is the height of the maximum electron density in the F2 layer (input quantity).

Figure 24 is a plot of the ionosphere model normalized with respect to σ and $1/2\ (\rho_e/\rho_0)$. The h, h_m, ρ_0 parameters refer to the ionosphere's F layer. Using this model, the refractive effects of the D and E layers are not singled out, because they are quite small in comparison with those due to the F layer and are approximately accounted for by allowing the electron density at the bottom edge of the F layer to be zero.

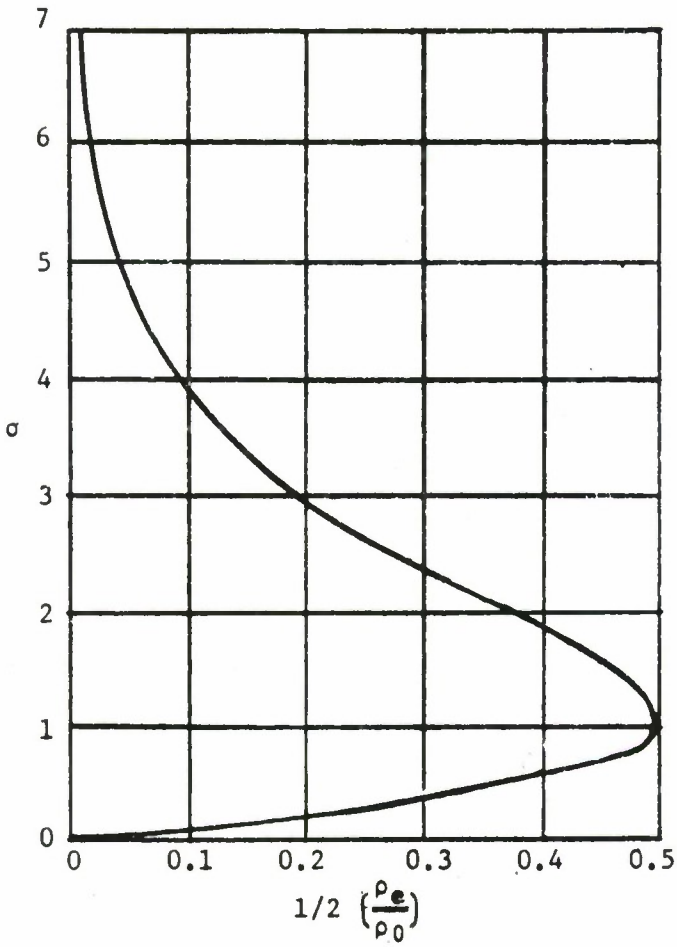

Figure 24. Normalized 3-Parameter Model of Atmosphere

Computation of Ray Bending

The major effect of ray bending due to refraction is that the observed elevation angle, E, of a vehicle in view of a station is greater that the actual or computed value of elevation, E_c. This effect is clearly seen in Figure 25. The difference between the computed and observed elevation is the angle δ.

In Figure 25 three vectors of importance are shown:

$\vec{\rho}$, the vector from the station to the vehicle,

$\vec{\rho}'$, a vector from the station toward the observed vehicle position (i.e., tangent to the ray path at the station), and

$\Delta\vec{\rho}$, a vector constructed perpendicular to $\vec{\rho}$.

The value of azimuth, A, and computed elevation, E_c, are obtained from Equations (156) and (157) using the value of $\vec{\rho}$, since these values do not incorporate refraction effects. From the geometry of Figure 25, one can find the components of $\Delta\vec{\rho}$ in the east, north, and vertical station-oriented coordinate system. Thus:

$$\Delta\vec{\rho} = |\vec{\rho}| \tan \delta [T] \begin{bmatrix} \sin E_c \sin A \\ \sin E_c \cos A \\ -\cos E_c \end{bmatrix} \tag{174}$$

where $|\vec{\rho}|$ is the magnitude of the vector $\vec{\rho}$, and $[T]$ is the 3×3 matrix of Equation (154) used to transform the coordinates of $\Delta\vec{\rho}$ from the station oriented coordinate system into the inertial system.

From the figure it is also obvious that

$$\vec{\rho}' + \Delta\vec{\rho} = \vec{\rho} \tag{175}$$

or

$$\vec{\rho}' = \vec{\rho} - |\vec{\rho}| \tan \delta [T] \begin{bmatrix} \sin E_c \sin A \\ \sin E_c \cos A \\ -\cos E_c \end{bmatrix} \tag{176}$$

In the program the vector $\vec{\rho}'$ is actually normalized to a unit vector. The length of $\vec{\rho}'$ is not important, however, since it is used

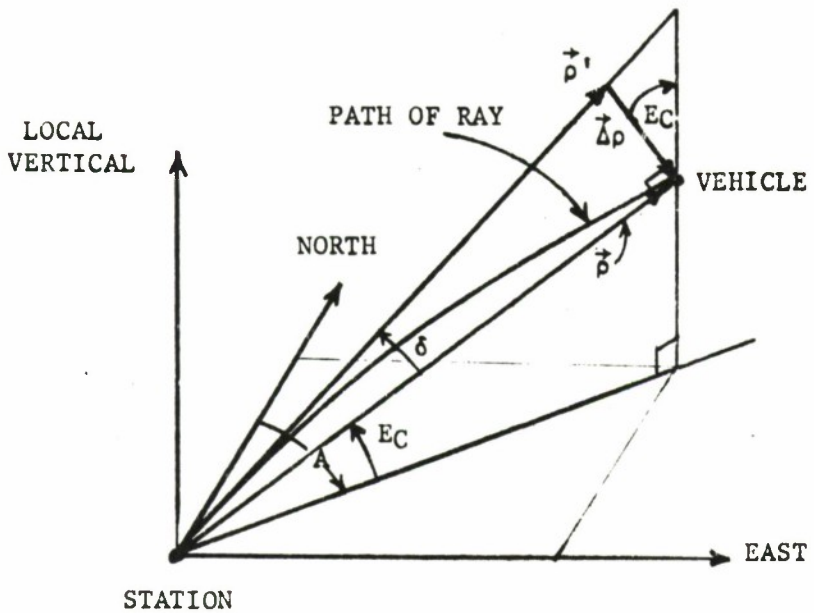

Figure 25. Geometry of Ray Path Used to Obtain $\vec{\rho}'$

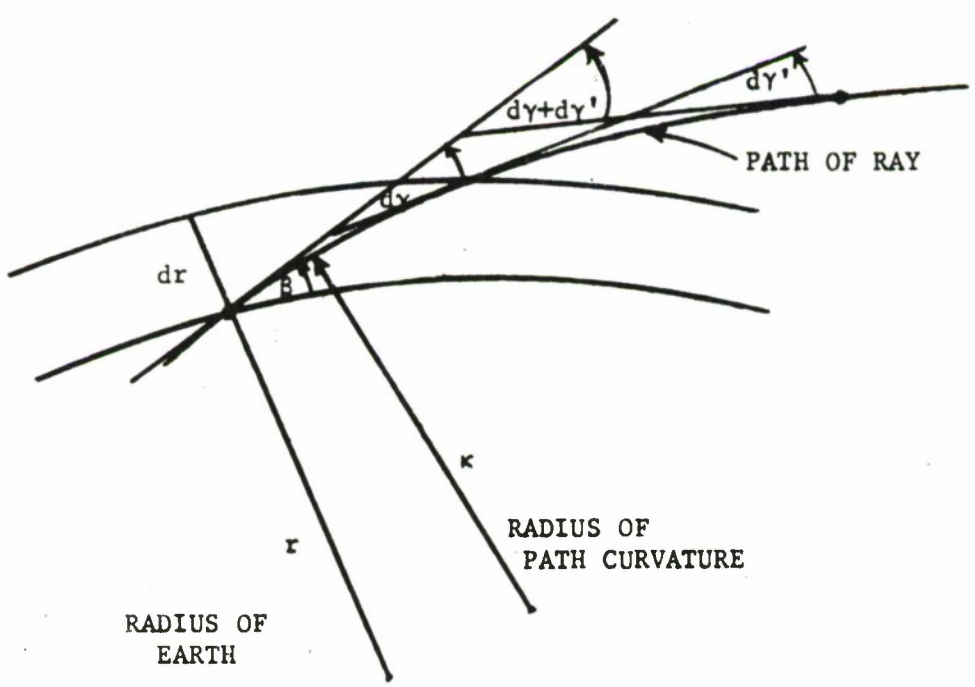

Figure 26. Geometry of Ray Path Used to Obtain $d\gamma$

only to calculate observed angle-related measurements such as azimuth, elevation, ℓ-cosine, m-cosine, X-angle, Y-angle, and indirectly, hour angle and declination as described above.

In Equation (176) all quantities are easily computed with the exception of δ, the "error" in the elevation angle. The method of computing δ used by the program is that due to Weisbrod and Anderson[15]. Only an outline of their analysis is presented here.

First, consider the ray of Figure 26 entering an infinitesimal layer of thickness dr at an angle β. At a boundary between two infinitesimal layers Snell's law holds. Thus:

$$n \cos \beta = \text{constant} \tag{177}$$

where n is the index of refraction. Differentiating Equation (177) with respect to path length, s, yields Equation (178) below. Since n varies only with altitude or distance along an earth radius, r, one obtains:

$$\frac{dn}{ds} \cos \beta - n \frac{d\beta}{ds} \sin \beta = 0 \tag{178}$$

$$\frac{dn}{dr} \frac{dr}{ds} \cos \beta - n \frac{d\beta}{ds} \sin \beta = 0 \tag{179}$$

but

$$\frac{dr}{ds} = \sin \beta, \tag{180}$$

and from the definition of curvature one gets:

$$\frac{d\beta}{ds} = \frac{1}{\kappa} \tag{181}$$

where κ is the radius of curvature of the ray. Thus, after substitution, Equation (179) becomes:

$$\frac{1}{\kappa} = \frac{1}{n} \frac{dn}{dr} \cos \beta \, . \tag{182}$$

From Figure 26, an infinitesimal length ds of the ray path is given by:

$$ds = \kappa \, d\gamma = \frac{dr}{\sin \beta} \tag{183}$$

thus,

$$d\gamma = \frac{1}{\kappa \sin \beta} \frac{dr}{} . \tag{184}$$

Combining Equations (184) and (182) results in an expression for $d\gamma$:

$$d\gamma = \frac{1}{n} \frac{dn}{dr} \cot \beta \, dr \tag{185}$$

Also, from Figure 26, it is seen that the $d\gamma$'s of all elementary layers are directly additive. Therefore, the angle γ_{jk} due to the total bending between layers bounded by the heights r_j and r_k is simply the integral of Equation (185):

$$\gamma_{jk} = \int_{r_j}^{r_k} \frac{1}{n} \frac{dn}{dr} \cot \beta \, dr \tag{186}$$

If a ray departs from a given layer (where $r = r_k$ and $n = n_k$) at an angle of β_k, from Snell's law for spherical stratification, one has:

$$n_k r_k \cos \beta_k = \text{constant} \tag{187}$$

If the angle γ_{jk} due to refractive bending is computed for only a very small layer of atmosphere between the heights $r = r_j$ and $r = r_k$, the following assumptions are justified:

(1) $\frac{dn}{dr} = \text{constant}$,

(2) the index of refraction n is close to unity, and

(3) $\Delta h = r_k - r_j \ll r_j$ (Δh is an infinitesimal layer of height).

Using these assumptions along with Equations (186) and (187), Weisbrod and Anderson[15] derive an expression for γ_{jk} in terms of the angle β and the refractivity N (see equation (168) for its definition); for the details the reader is referred to their paper. Their expression for γ_{jk} through a small layer of atmosphere is:

$$\gamma_{jk} = \frac{N_j - N_k}{500 \, (\tan \beta_j + \tan \beta_k)} \quad \text{(milliradians)} \tag{188}$$

The total bending through the atmosphere is the sum of the

individual contributions. Thus,

$$\gamma = \sum_{i=1}^{n} \frac{N_{i-1} - N_i}{500 \, (\tan \beta_{i-1} + \tan \beta_i)} \text{ (milliradians)} \tag{189}$$

From Equation (187), the value of $\cos \beta_i$ is given as:

$$\cos \beta_i = \frac{n_{i-1} \, r_{i-1} \, \cos \beta_{i-1}}{n_i \, r_i} = \frac{n_{i-1} \cos \beta_{i-1}}{n_i} \left[1 - \frac{\Delta h}{R_e + h_i} \right] \tag{190}$$

and it follows:

$$\tan \beta_i = \frac{\sqrt{1 - \cos^2 \beta_i}}{\cos \beta_i} \tag{191}$$

Equations (189), (190), and (191) determine the value of γ where β_i is the value of the angle of incidence of the ray at a height h_i $N_i = N(h_i)$ is the refractivity at height h_i obtained from the atmospheric model, and Δh is the increment of height used in Equations (189) and (190). Note that $h_i = h_{i-1} + \Delta h$ and that h_n is the computed height of the vehicle obtainable from the program. At the station $h = h_0$, which is the height of the station, and β_0 is set equal to the computed elevation, E_c.

Once γ has been found, consideration of the geometry in Figure 27 leads to the evaluation of δ, the "error" in the elevation angle. Thus, we note from Figure 27:

$$\epsilon = \gamma - (\alpha - \beta) \tag{192}$$

Using Snell's law for spherical stratification and the application of the law of sines to triangle SOQ results in:

$$\cos \beta = \frac{n_0 \, r_0}{nr} \cos \beta_0 \tag{193}$$

$$r_0 = \beta_0 = r \cos \alpha \tag{194}$$

Combining Equations (193) and (194) yields:

$$\cos \beta = \frac{n_0}{n} \cos \alpha = \cos (\alpha - (\alpha - \beta)) \tag{195}$$

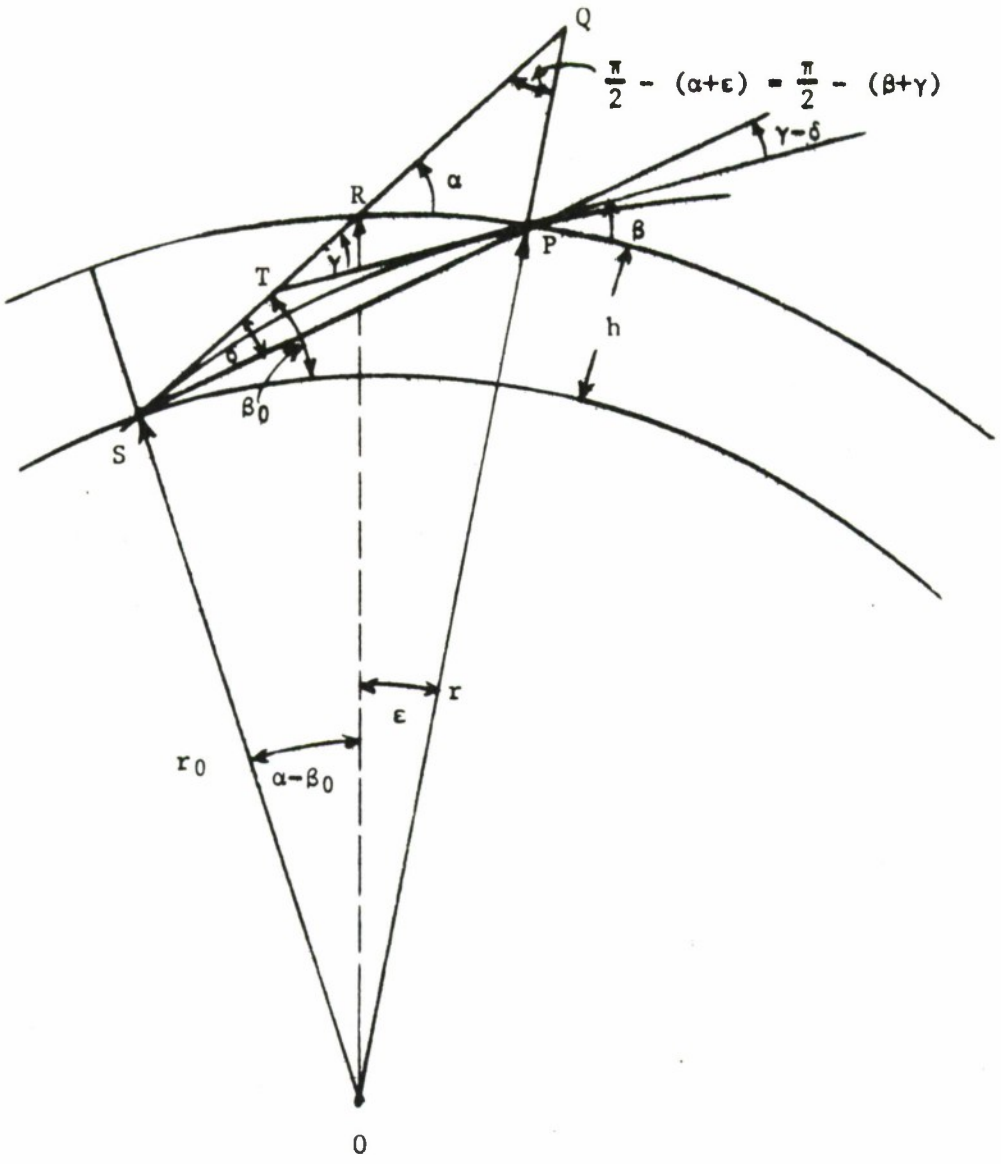

Figure 27. Geometry of Ray Path Used to Obtain δ

Since $\alpha - \beta$ is a small angle, a small angle approximation and an approximation for $\frac{n_0}{n}$ is used[15] in Equation (195) to obtain an expression for $\alpha - \beta$ in terms of refractivity at the station (N_0) and at the vehicle (N):

$$\alpha - \beta = (N_0 - N)\ 10^{-6} \cot \beta \tag{196}$$

Using Equations (192) and (196), the value of ε is determined.

Applying the law of sines to triangle SOP results in:

$$r_0 \cos (\beta_0 - \delta) = r \cos ((\alpha + \varepsilon) - \delta) \tag{197}$$

Combining Equations (194) and (197) gives an expression for δ:

$$\tan \delta = \frac{\sin \varepsilon \tan \alpha + (1 - \cos \varepsilon)}{\sin \varepsilon + \cos \varepsilon \tan \alpha - \tan \beta_0} \tag{197}$$

Finally, using small angle approximations for δ and ε:

$$\boxed{\delta = \frac{\varepsilon \tan \alpha + \frac{\varepsilon^2}{2}}{\varepsilon + \tan \alpha - \tan \beta_0}} \tag{199}$$

This value of δ can now be used in Equation (176) to find the vector $\vec{\rho}'$, which determines all angle related observations including the effects of refraction. Due to the approximations used in the analysis, below elevations of about 5° the errors in the propagation corrections amount to a few percent. Because of this fact, propagation corrections due to refraction should be computed only when the elevation of the vehicle exceeds 5°.

Refraction Effects on Range and Range Rate

Because of signal retardation caused by the refractive gradient of the atmosphere, the round-trip range computation of Equation (158) includes a correction term, $\Delta\rho$. The signal retardation caused by an infinitesimal layer of thickness dr is given by:

$$d\tau = \left(\frac{1}{v} - \frac{1}{c}\right) \csc \beta \, dr$$

$$= \left(\frac{c}{v} - 1\right) \frac{\csc \beta}{c} \, dr$$

$$= N \times 10^{-6} \frac{\csc \beta}{c} \, dr \qquad (200)$$

The effect on range between layers bounded by heights $r = r_j$ and $r = r_k$ is given by:

$$\Delta\rho_{jk} = \int_{r_j}^{r_k} c \, d\tau = \int_{r_j}^{r_k} N \times 10^{-6} \csc \beta \, dr \qquad (201)$$

Using methods similar to the computation of refractive bending, Weisbrod and Anderson[15] arrive at the expression for the refractive round-trip range correction, $2\Delta\rho$, due to the passage of the ray through the entire atmosphere:

$$2\Delta\rho = 2 \times 10^{-6} \sum_{i=1}^{m} \frac{|N_{i-1} + N_i|(h_i - h_{i-1})}{\sin \beta_{i-1} + \sin \beta_i}$$

$$+ 10^{-6} \left[1 + \frac{f_2^2}{f_1^2}\right] \sum_{i=m+1}^{i=n} \frac{|N_{i-1} - N_i|(h_i - h_{i-1})}{\sin \beta_{i-1} + \sin \beta_i} \qquad (202)$$

where

N_i is the refractivity in the i^{th} layer,

h_i is the height of the i^{th} layer,

β_i is obtained from equation (190),

f_1 is the transmitted (or up) frequency,

f_2 is the received (or down) frequency.

The indices in the first summation refer to layers in the troposphere, and those in the second refer to layers in the ionosphere. The values of $N_i = N(h_i)$ are obtained from the models of refractive index.

Due to refractive bending, the range-rate measurement of Equation (159) also includes a correction term, $\Delta\dot{\rho}$. This correction term arises because the program initially computes the component of

vehicle velocity along the vector $\vec{\rho}$, i.e., along the straight line $\overline{SP}$ of Figure 27. The measured range-rate is the component of vehicle velocity along the tangent to the ray path at the vehicle, i.e., along the straight line $\overline{TP}$ of Figure 27.

The velocity of the vehicle and the station is available from the program. If one denotes the component of vehicle velocity along the line $\overline{SP}$ by v_x, and the component of vehicle velocity perpendicular to $\overline{SP}$ by v_y, then the range rate computation without the correction for refraction (i.e., $\Delta\dot{\rho} = 0$) is:

$$\dot{\rho}_c = \frac{\dot{\vec{\rho}} \cdot \vec{\rho}}{|\vec{\rho}|} = v_x \tag{203}$$

The measured component of velocity along the tangent to the ray path at the vehicle as seen from Figure 27 is

$$\dot{\rho}_m = v_x \cos(\gamma - \delta) + v_y \sin(\gamma - \delta) \tag{204}$$

The correction to range-rate, $\Delta\dot{\rho}$, is given by:

$$\Delta\dot{\rho} = \dot{\rho}_m - \dot{\rho}_c \tag{205}$$

A factor should also be included to account for the round-trip frequency dependent effects in the ionosphere. After making a small angle approximation the final equation used for $\Delta\dot{\rho}$, the one-way correction to range-rate, is:

$$\boxed{\Delta\dot{\rho} = \frac{1}{2}\left[1 + \frac{f_2^2}{f_1^2}\right] v_y (\gamma - \delta)} \tag{206}$$

where

v_y is the component of vehicle-station velocity perpendicular to the vector $\vec{\rho}$, and lying in the plane which includes the center of the Earth,

f_1 is the transmitted frequency,

f_2 is the received frequency.

SECTION III.

USER'S GUIDE

INTRODUCTION

The information in this section is intended as a guide for those desiring to use SPACE-A. SPACE-A generates a vehicle ephemeris and associated observations from ground stations and has four modes of operation. They are:

(1) Computation of vehicle ephemeris only;

(2) Generation of observations from ground stations;

(3) Same as (2) with the writing of the observations onto tape in a format suitable for processing by SPACE-B;

(4) Same as (2) with the following included as standard outputs:

  (a) the acquisition time,

  (b) total time in sight, and

  (c) the option of the printing time of polar and meridian crossings.

DESCRIPTION OF INPUT DATA

All input data is read at the beginning of each run. The format and arrangement of the data is designed to make the data preparation as convenient as possible. It is seldom necessary to read all the data; in fact, most runs require a minimum of cards. Many variables have standard values which are preset by the program and should be satisfactory for most cases.

The input data is divided into three parts. The first consists of a single card, called the basic input card, which must be included in each run. The second and third parts are designated group I and group II inputs, respectively. Each group is divided into several sections, each of which must be preceded by a card containing the section number, in integer format, in columns four and five. Any

section may be omitted from the input deck. Parts of sections, however, must not be omitted. See Figure 28 for the setup of a sample input deck.

The basic input card, which precedes each case, contains four variables. The first pertains to the standard values which may be set in place of the group II data and will be explained later. The second, MDE, indicates the function to be performed (i.e., trajectory computation, observables, etc.). The third indicates the desired precision and determines the set of standard values used for integration. The last specified Encke or Cowell integration.

The group I inputs consists of several sections. Any of these sections may be omitted from the input deck if the variables contained in the section are not needed for the run or in the case of stacked cases, the values from the last case are to be used again. The description of each variable given in the data summary (see Table IV) is sufficient to understand most of the inputs. Therefore, only a brief discussion of the variables given in Table IV is presented here.

In the group I input data, if the variable KLM2 of Section 2 is 0 or 1, the initial conditions are assumed to be referred to the base date system or true system of date, respectively.

Sections 7 and 9 deal with observations from observing systems on vehicles and with powered flight and have been omitted since they are not presently used. The variables in Section 8 control the output and are discussed in DESCRIPTION OF OUTPUT INFORMATION.

The end of the group I input data is indicated by a card containing a 10 in columns four and five. This card must always be included in the data deck. After reading this card the program advances to the group II inputs.

Before the program reads the group II input data, the value of the first variable contained on the basic input card, KSTDRD, is tested. If this variable is negative, standard values of the vari-

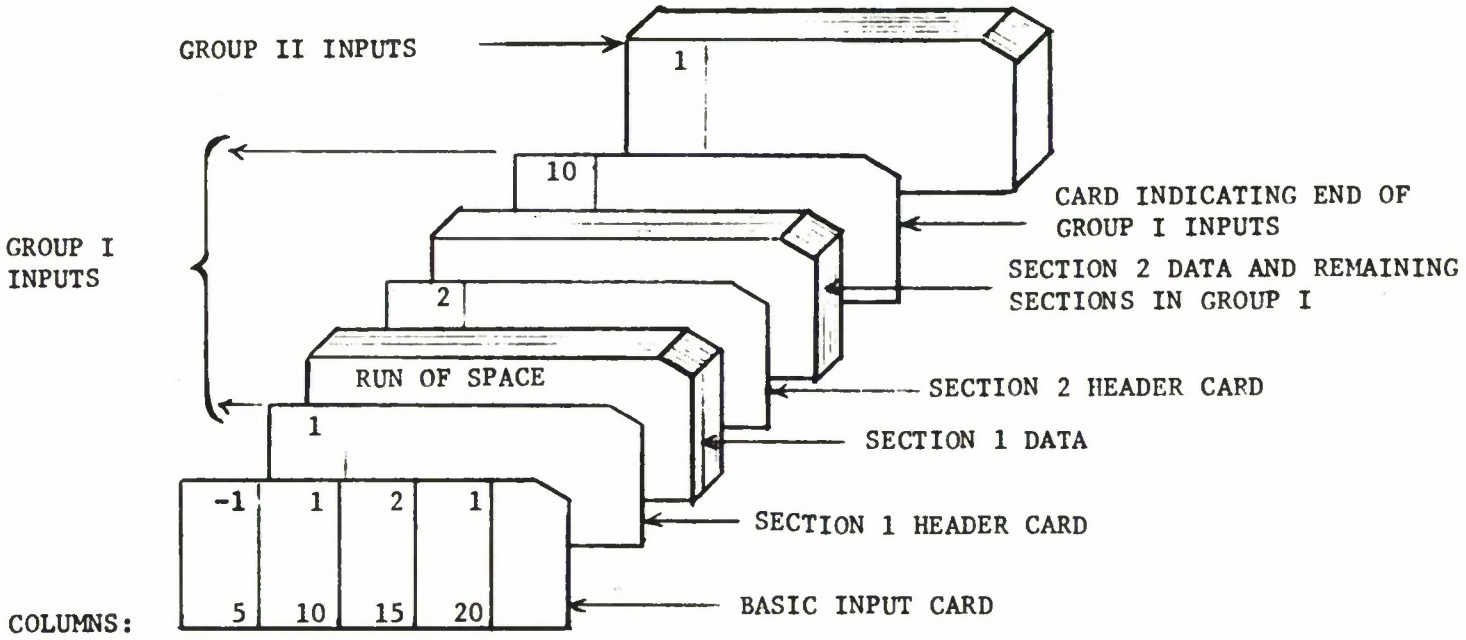

Figure 28. Sample Input Deck

ables in the group II input data are computed from stored information and the program then begins to read the group II inputs to augment or replace any of the standard values. Table V gives a list of the standard values used by the program. If KSTDRD is not negative, none of the standard values is set and all values should be read in unless values from a preceding stacked case are used. The end of group II inputs is indicated by reading a card with a 20 in integer format in columns four and five.

Table IV.

Summary of Input Data

Basic Input Card

COLUMN	NAME	FORMAT		DESCRIPTION
2-5	KSTDRD	I5	< 0	Will want at least some standard inputs from group II
6-10	MDE	I5	≥ 0	No standard. All values will be read in.
			= 1	Trajectory computation.
			= 2	Observable computations without simulated data.
			= 3	Observable computations with simulated data.
			= 4	Prediction mode
11-15	PRECIS	F5.0	= 1	Low precision level.
			= 2	Intermediate precision level.
			= 3	High precision level
16-20	CEPID	F5.0	= 0,1	Encke integration
			= - 1	Cowell integration

Group I Inputs

SECTION	CARD	COLUMNS	NAME	FORMAT	DESCRIPTION
1	1	2-72	ITITLE(1-12)	12A6	Title
	2	2-5	NYEARP	I5	Year of initial conditions
		6-10	DAYS	F5.0	Day of initial conditions.
		11-15	HRS	F5.0	Hour of initial day.
		16-20	HMIN	F5.0	Minute of initial hour.
		21-40	SEC	E20.16	Seconds of initial minute.
	3	1-24	TMAX	E24.16	Time of run in hours.
2	1	2-5	KLM	I5	Indicator for units of position and velocity vector. = 1 KM,KM/SEC = 2 ER,ER/HR = 3 FT,FT/SEC = 4 MI,MI/HR = 5 NM,NM/HR = 6 NM,FT/SEC = 7 AU,AU/HR
		6-10	KLM1	I5	Indicator for coordinate system of input vectors. = 1 Cartesian coord. WE = 0 = 2 Cartesian coord. Compute WE = 3 Geodetic long, lat, alt, V_e, V_n, V_h; WE = 0 = 4 Geodetic long, lat, alt, V_e, V_n, V_h; Compute WE

Group I Inputs

(continued)

SECTION	CARD	COLUMNS	NAME	FORMAT	DESCRIPTION
					= 5 Geodetic long, lat, alt, $\|V\|$, γ, az; WE = 0
					= 6 Geodetic long, lat, alt, $\|V\|$, γ, az; compute WE
					= 7 Geocentric ra, decl, alt, V_{ra}, V_d, V_h; WE = 0
					= 8 Geocentric ra, decl, alt, V_{ra}, V_d, V_h; compute WE
					= 9 Geocentric ra, decl, alt, $\|V\|$, β, az; WE = 0
					= 10 geocentric ra, decl, alt, $\|V\|$, β, az; compute WE
		11-15	KLM2	I5	Indicator for nutation and precession of input vector.
					= 0 no
					= 1 yes
		16-20	KSNAP	I5	Indicator for nutation and precession of vectors during run.
					= 0 no
					= 1 yes
		21-25	KLM3	I5	Indicator for libration of input vectors.
					= 0 no
					= 1 yes

Group I Inputs

(continued)

SECTION	CARD	COLUMNS	NAME	FORMAT	DESCRIPTION
		26-30	KLIBR	I5	Indicator for libration of vectors during run = 0 no = 1 yes
		31-35	MRREF	I5	Indicator for initial reference body = 1 Earth = 2 Sun = 3 Moon = 4 Mars = 5 Venus = 6 Jupiter = 7 Saturn
	2	1-24	RCIN(1)	E24.16	Initial position vector
		25-48	(2)	E24.16	See KLM and KLM1 for units and type.
		49-72	(3)	E24.16	
	3	1-24	RCIN(1)	E24.16	Initial velocity vector.
		25-48	(2)	E24.16	See KLM and KLM1 for units and type.
		49-72	(3)	E24.16	
3	1	2-5	PASFX	F5.0	Total number of passes.
4	1	2-5	KS2BY	I5	Indicator for two-body integration = 0 no = 1 yes
		6-10	KSPLT	I5	Indicator for inclusion of planetary perturbations = 0 no = 1 yes

Group I Inputs

(continued)

SECTION	CARD	COLUMNS	NAME	FORMAT	DESCRIPTION
		11-15	KSOBL	I5	Indicator for inclusion of oblateness perturbation. = 0 no = 1 yes
		16-20	KSDRG	I5	Indicator for inclusion of Earth drag perturbation. = 0 no = 1 yes
		21-25	KSRAP	I5	Indicator for inclusion of radiation pressure perturbation. = 0 no = 1 yes
		26-30	KSDRGM	I5	Indicator for inclusion of Mars drag perturbation. = 0 no = 1 yes
		31-35	KSDRGV	I5	Indicator for inclusion of Venus drag perturbation. = 0 no = 1 yes
		36-40	KSMNOB	I5	Indicator for inclusion of Moon oblateness perturbation. = 0 no = 1 yes
		41-45	KRF	I5	Indicator for inclusion of refraction effects. = 0 no = 1 yes

Group I Inputs

(continued)

SECTION	CARD	COLUMNS	NAME	FORMAT	DESCRIPTION
		46-50	KECLPS	I5	Indicator for inclusion of eclipse information print. = 0 no = 1 yes
5	1	2-5	MAXSTA	I5	Total number of stations used in run.
	2	2-5	K	I5	Station number.
		10-15	STANM(L)	A6	Station name.
		20-30	TYPE(L)	4XI11	A(1)+1.E2*A(2) +1.E4*A(3)+1.E6*A(4) +1.E8*K where A = observation types used by station K in ascending order. L = packed station number
	3	1-24	STALT(K)	E24.16	Latitude of station K.
		25-48	STALN(K)	E24.16	Longitude of station K.
		49-72	STAHT(K)	E24.16	Altitude of station K.
	4	1-36	RRATE(1,L)	E36.16	Repetition rates (hrs). For each observation Type
		37-72	RRATE(2,L)	E36.16	
	5	1-36	RRATE(3,L)	E36.16	
		37-72	RRATE(4,L)	E36.16	
	6	1-18	TDELAY(1,L)	E18.8	Times in hrs before which each observation is not to be computed.
		19-36	TDELAY(2,L)	E18.8	
		37-54	TDELAY(3,L)	E18.8	
		55-72	TDELAY(4,L)	E18.8	

Group I Inputs

(continued)

SECTION	CARD	COLUMNS	NAME	FORMAT	DESCRIPTION
	7	1-18	FUP(K)	E18.8	Station transmit freq. (MHz).
		19-36	FDOWN(K)	E18.8	Station receive freq. (MHz).
	8	1-24	STAOR(NCDST+1)	E24.16	ΔEE station rotation angle.
		25-48	STAOR(NCDST+2)	E24.16	ΔEV station rotation angle.
		49-72	STAOR(NCDST+3)	E24.16	ΔEN station rotation angle.
	9	1-24	STAOR(NCDST+4)	E24.16	ΔU } station location errors caused by geodetic net error.
		25-48	STAOR(NCDST+5)	E24.16	ΔV }
		49-72	STAOR(NCDST+6)	E24.16	ΔW }
	10	1-24	STAOR(NCDST+7)	E24.16	NO; refractivity at sea level.
		25-48	STAOR(NCDST+8)	E24.16	H; troposphere scale fact.
		49-72	STAOR(NCDST+9)	E24.16	PO; max. electron density.
	11	1-24	STAOR(NCDST+10)	E24.16	HO; loser limit of ionosphere.
		25-48	STAOR(NCDST+11)	E24.16	HM; Ht of PO (KM)
		49-72	STAOR(NCDST+12)	E24.16	- open -
	12	1-24	STAOR(NCDST+13)	E24.16	ΔT for timing.
		25-48	STAOR(NCDST+14)	E24.16	Bias added for obser.A(1)
		49-72	STAOR(NCDST+15)	E24.16	Bias added for obser.A(2).

Group I Inputs

(continued)

SECTION	CARD	COLUMNS	NAME	FORMAT	DESCRIPTION
	13	1-24	STAOR(NCDST+16)	E24.16	Bias added for obser.A(3)
		25-48	STAOR(NCDST+17)	E24.16	Bias added for obser.A(4)
		REPEAT CARDS 2-13 FOR EACH STATION			
6	1	1-18	DAREAS	E18.8	Effective surface area of vehicle pertaining to drag (ft^2).
		19-36	PAREAS	E18.8	Effective surface area pertaining to radiation pressure (ft^2).
		37-54	SPADD(6)	E18.8	Mass of vehicle (lb-masses)
7		OPEN			
8	1	2-5	IUNIT	I5	Indicator for output units (see KLM)
		6-55	IPSEC(I),I=1.10	1015	Indicator for suppression of each of 10 print sections.
	2	1-18	DTPI	E18.8	Print portion (hrs) and suppress portion (hrs), of total print period.
		19-36	DTSUP	E18.8	
		37-54	PRATE	E18.8	Interval within DTPI at which to print.
9		OPEN			
10		END OF GROUP I INPUTS			

Group II Inputs

SECTION	CARD	COLUMNS	NAME	FORMAT	DESCRIPTION
1	1-7	1-72	(DT3(I,J), I=1,3) J=1,7	3E24.12	Integration intervals for each of 7 working bodies for near, medium and far reference.
2	1	1-72	R1(1-3)	3E24.12	R1 and R2 are distances in E.R. for each of 7 working bodies for switching from near to medium and medium to far integration intervals.
	2	1-72	R1(4-6)	3E24.12	
	3	1-72	R1(7),R2(1-2)	3E24.12	
	4	1-72	R2(3-5)	3E24.12	
	5	1-48	R2(6-7)	3E24.12	
3	1	1-24	RT1	E24.12	Values used as tolerances in rectification criteria.
		25-48	RT2	E24.12	
4	1	1-18	DH1	E18.8	Troposphere integration step size (KM).
		19-36	DH2	E18.8	Ionosphere integration step size (KM).
		37-54	H2	E18.8	Upper limit troposphere (KM).
		55-72	H4	E18.8	Upper limit ionosphere (KM).
5	1	2-5	KOBLAT	I5	Number of oblateness coefficient terms.
	2	2-5	N	I5	N index.
		6-10	M	I5	M index.
	3	1-24	SORC1	E24.12	Value of C coefficient.

Group II Inputs

(continued)

SECTION	CARD	COLUMNS	NAME	FORMAT	DESCRIPTION
		25-48	SORC2	E24.12	Value of S coefficient.
	REPEAT CARDS 2-3 UNTIL KOBLAT VALUES HAVE BEEN READ IN.				
6	1	2-5	MBMAX	I5	Number of working bodies.
		6-10	KWBMU(I) I=1,MBMAX	I5	Indices of working bodies.
	2	1-72	TPMAT8(1) I=1,MBMAX	3E24.12	Gravitational constants of working bodies.
	REPEAT CARD 2 FOR EACH VALUE OVER 3N NEEDED.				
7	1	1-24	DYN(48)	E24.12	Solar flux in 10^{-22} w/m^2-Hz at 10.7 cm.
		25-48	DYN(49)	E24.12	Open
8	1	1-72	DYN(51-53)	3E24.12	Coefficients for lunar oblateness (kg · km^2).
9	1	1-24	COMB(1)	E24.12	Velocity of light.
10	1	1-72	PRNT3(1-3)	3E24.12	Print intervals (hrs) for near medium and far reference.
11	1	1-24	EMIN	E24.12	Minimum value of elevation angle (radians).
12	1	1-18	RTO	E18.8	Ratio of Nordsieck integration interval to that in Runge-Kutta.

Group II Inputs

(continued)

SECTION	CARD	COLUMNS	NAME	FORMAT	DESCRIPTION
13	1	1-24	DSPL	E24.12	Special integration interval in A4 mode to obtain acquisition time (hrs).
14	1	1-72	RATEC(1-3,1)	3E24.12	Rotation vector used in Mars drag computations.
	2	1-72	RATEC(1-3,2)	3E24.12	Rotation vector used in Venus drag computations.
15	1-10	1-72	XMACH(I) I=1,40	4E18.8	Mach number table.
	11-20	1-72	CDT(I) I=1,40	4E18.8	Drag coefficient table
16	OPEN				
17	OPEN				
18	OPEN				
19	OPEN				
20	END OF GROUP II INPUTS				

Table V.

Standard Values for Group II Inputs

Section 1.

DT3 ARRAY (3 × 7 array of integration intervals)

DT3(1,I); I=1,3,4,5,6,7 $.1953125 \times 10^{-2}$

DT3(2,I); I=1,3,4,5,6,7 $.15625 \times 10^{-1}$

DT3(3,I); I=1,3,4,5,6,7 .125

DT3(1,2) = 4.

DT3(2,2) = 6.

DT3(3,2) = 10.

Note: The above values are always used for Encke integration and for Cowell when low precision is specified. When Cowell and intermediate precision is specified, each value in the DT3 array is divided by 2; when Cowell and high precision is specified each value is divided by 4. The precision desired is controlled by the variable CEPID on the Basic Input Card.

Section 2.

R1 ARRAY (1 × 7 array of reference body change criteria)

R1(I) = 4 · RADII(I)

R2(I) = 10 · RADII(I)

where RADII(I) is the radius of the I^{th} working body (Earth, Sun, Moon, Venus, Mars, Jupiter, Saturn).

Section 3.

RT1 = $1. \times 10^{-6}$

RT2 = $1. \times 10^{-6}$

If low precision is specified

RT1 = 1×10^{-4}

RT2 = 1×10^{-4}

Table V.

(continued)

Section 4.

DH1 = 1.

DH2 = 10.

H2 = 40.

H4 = 2,000.

Section 5.

KOBLAT = 3

$C_{20} = -1082.3 \times 10^{-6}$ $S_{20} = 0$

$C_{30} = 2.3 \times 10^{-6}$ $S_{30} = 0$

$C_{40} = 1.8 \times 10^{-6}$ $S_{40} = 0$

Section 6.

KBMAX = 7

KWBMU(I) = I; I = 1,2,3,4,5,6,7

TPMAT8(1) = 19.909416

(2) = 6629965.8

(3) = .24478289

(4) = 16.1983009

(5) = 2.14364682

(6) = 6338.16258

(7) = 1897.36734

Section 7.

DYN(48) = 200.

Section 8.

DYN(51) = .88746 $\times 10^{29}$ kg · km^2

DYN(52) = .88764 $\times 10^{29}$ kg · km^2

DYN(53) = .88807 $\times 10^{29}$ kg · km^2

Table V.

(continued)

Section 9.

COMB(1) = 169210.58004

Section 10.

PRNT3(1) = .25

PRNT3(2) = .5

PRNT3(3) = 1.

Section 11.

EMIN = (5. degrees; expressed in radians)

Section 12.

RTO = 3

Section 13.

DSPL = $1. \times 10^{-3}$

Section 14.

RATEV(1,1) = 0.0

RATEV(2,1) = 0.0

RATEV(3,1) = 0.255175469

RATEV(1,2) = 0.0

RATEV(2,2) = 0.0

RATEV(3,2) = 0.0

Table V.

(concluded)

Section 15.

MACH TABLE ARRAY (XMACH(I), I = 1,40)

- .5	1.5	25.	96.
0.0	1.85	30.	97.
.5	2.0	50.	98.
.75	2.7	70.	99.
.85	3.4	90.	100.
.9	4.2	91.	101.
1.04	5.6	92.	102.
1.1	6.75	93.	103.
1.2	8.5	94.	104.
1.3	15.	95.	105.

DRAG COEFFICIENT TABLE (CDT(I) I = 1,40)

.8	1.4	1.14	1.14
.8	1.38	1.14	1.14
.82	1.36	1.14	1.14
.92	1.285	1.14	1.14
.99	1.23	1.14	1.14
1.04	1.19	1.14	1.14
1.18	1.16	1.14	1.14
1.21	1.155	1.14	1.14
1.26	1.15	1.14	1.14
1.3	1.45	1.14	1.14

DESCRIPTION OF OUTPUT INFORMATION

The input quantities which determine the form of the output of the program are given in Section 8 of the Group I inputs in Table IV. The choice of output units are determined by IUNIT. The choices of units with corresponding values of IUNIT are given below.

Value of IUNIT	OUTPUT UNITS
1	KM,KM/SEC
2	ER,ER/HR
3	FT,FT/SEC
4	MI,MI/HR
5	NM,NM/HR
6	MM,FT/SEC
7	AU,AU/HR

Time may be divided into periods of print and suppression of print by setting the input variables DTPI and DTSUP. A period of printing (DTPI) is executed followed by a period of suppression (DTSUP) and the cycle is then repeated.

The variable PRATE, is used to determine the print interval within DTPI. Since conditions occur where the print routine is entered more than once with the same time, printing is normally only executed upon the first entry. However, by using a negative PRATE, printing will occur each time the print subroutine is entered during the print interval determined by DTPI.

The user has the option of choosing the information he would like printed by setting IPSEC(I) = 1, where I is the output section number given in Table VI, that contains certain information. By reading a zero for IPSEC(I), the printing of the I^{th} section is surpressed. There are ten sections of output information as shown in Table VI. See Figure 29 for a sample listing with various sections labeled.

Table VI.

Ten Sections of Output Information

Section 1.

Program time in hours since launch;

Current program date in hours, minutes, seconds, day and year;

Planetary body which is the current reference.

Section 2.

Station number;

Observation types which station handles.

Section 3.

Components and magnitudes of position and velocity vectors in units specified by the user.

Section 4.

Components and magnitudes of perturbations in position, velocity and acceleration in units specified by the user.

Section 5.

Components and magnitudes of vectors between vehicle and each planetary body in specified units.

Section 6.

Components and magnitudes of vectors between the Earth and each of the other planetary bodies in specified units.

Section 7.

Components and magnitudes of vectors between the Sun and each of the planetary bodies in specified units.

Table VI.

(concluded)

Section 8.

Right ascension;

Declination;

Greenwich hour angle;

Longitude and latitude of Earth subsatellite point;

Geocentric altitude, azimuth and elevation;

Geodetic azimuth and elevation.

Section 9.

True, eccentric and mean anomalies;

Semi-major axis;

Eccentricity;

Inclination;

Argument of perigee;

Perigee passage time;

Right ascension of ascending node;

Period;

Mean motion;

Perigee and apogee heights;

Unit vector to perigee;

Unit angular momentum vector.

Section 10.

Station name;

Program time in hours;

Station location;

Observation values.

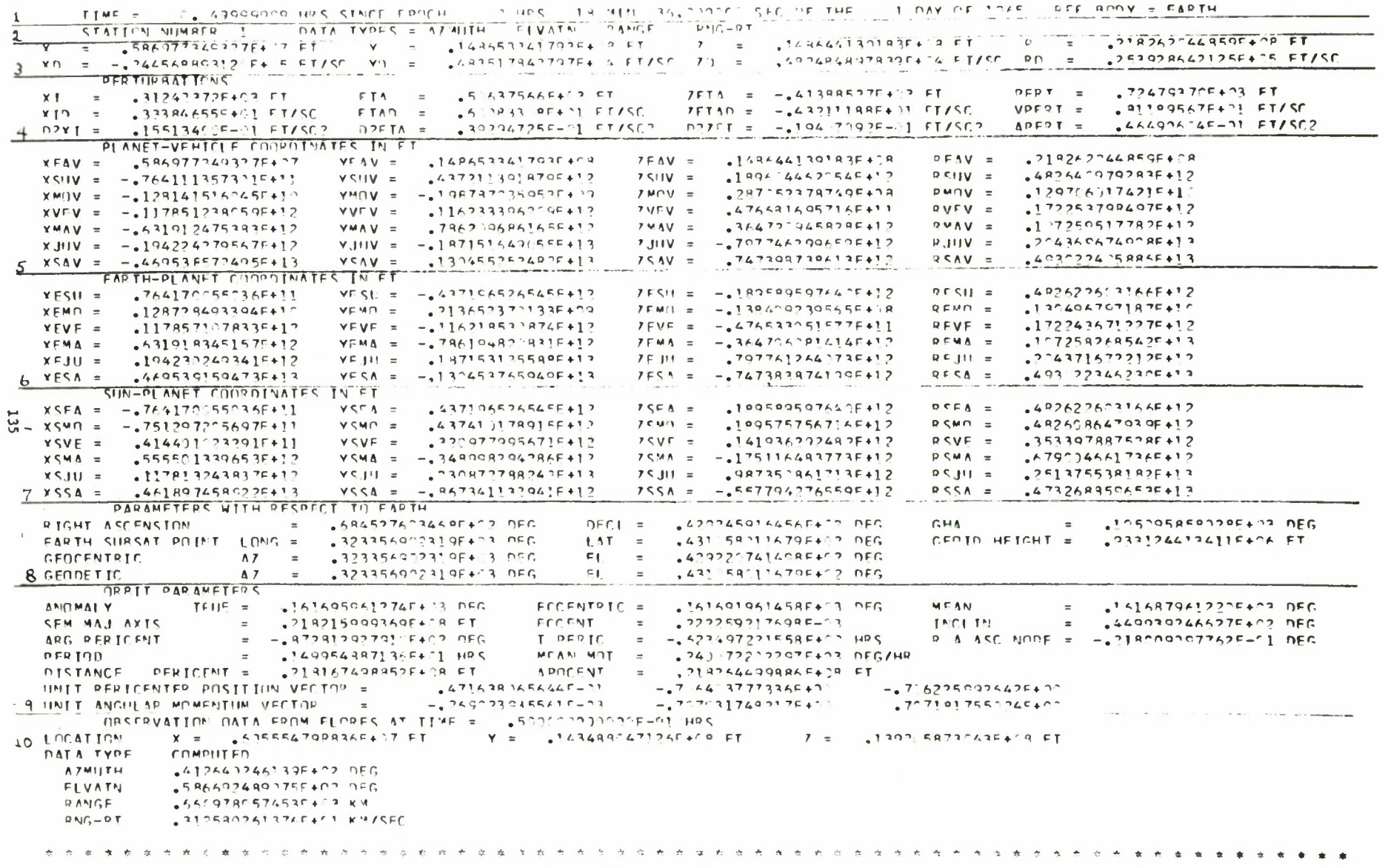

PROGRAM DECK SETUP

This section describes the deck setup for running the A-mode of SPACE on the 7030 computer. The program is executed under the control of MCP (Master Control Program). The binary cards containing the compiled routines are kept on a magnetic tape at the MITRE 7030 computer facility and only a few control cards and the data deck are needed by the user.

Those cards shown in Figure 30 that have a B or T punched in column 1 are control cards for the MCP. They are described in greater detail in the MITRE 7030 Facility Manual.

JOB Card

The job card is always the first card of an input deck. This card contains necessary information for accounting and no job can be run without it. The fields on the JOB card are variable in length and separated by commas.

Format

1	10
B	JOB,'JOBID','NAME','PROJECT','DEPT','MAXTIME','DEST'

Field Name	Description
B	Punched in column 1
JOB,	Punched in columns 10-13
'JOBID'	1 to 7 character job identification
'NAME'	Name of programmer (up to 13 characters)
'PROJECT'	Project number (3 to 9 characters)
'DEPT'	Department number (3 characters)
'MAXTIME'	Maximum running time in minutes (up to 3 characters)
'DEST'	Destination of output (up to 6 characters)

Example:

```
|1          |10
|B          |JOB,SPACE,BOND J, 007, D84, 13, A141
```

TYPE Card

This card defines the type of job (GO), and the proper monitor system (FORTRAN) to the MCP to execute this program.

Format:

```
|1          |10
|B          |TYPE,GO,FORTRAN
```

ADDIO Card

This card contains the library number of the program tape that contains the binary decks of the SPACE program. Since modifications to the program may be made in the future, the user should periodically check the current tape number with Department D-84.

Format:

```
|1          |10
|BLIB1      |ADDIO,PLBXXXX
```

Field Name	Description
BLIB1	Punched in columns 1-5
ADDIO,PLBXXXX	Beginning in column 10, the XXXX indicate the field where the tape number is to be punched.

SUBTYPE,BIN Card

This card tells the MCP that the cards that follow are binary.

Format:

```
|1          |10
|T          |SUBTYPE,BIN
```

TMAIN Card

This card results in the construction of a dummy main program which calls the executive routine of SPACE (EXECA). EXECA is compiled

as a subroutine and the binary cards are contained on the library tape. This card is the equivalent to the Fortran routine.

```
      CALL      EXECA
       RETURN
       END
```

Format:

```
|1        |10
|T        |MAIN,EXECA
```

Processed FIOD Deck

Since the programmer cannot choose the input-output channels to be used (they are assigned by MCP at execution time), the FIOD deck specifies the I/O channel requirements of the program. The processed FIOD deck is the result of compiling the following subprogram:

```
|1        |10
|T        |SUBTYPE,FIOD
 B2       IOD,$READER
 B3       IOD,$PRINTER
 B9       IOD,TAPE,,,,,,SAVE
 B8       IOD,TAPE,,,,,,SAVE
 B        REEL,PLBDL680
          END
```

Logical units 2 and 3 are the system input and output units respectively. Logical unit 9 is used for the output of the observation tape generated when that option is exercised. Logical unit 8 is used for the input of the ephemeris tape containing the positions of the Moon and planets. The reel card specifies that the ephemeris tape, whose label is PLBL680, is to be mounted.

SUBTYPE,DATA Card

This card tells the MCP that the following cards contain the data for the program.

Format:

1	10
T	SUBTYPE,BIN

Input Data Deck

This is the data deck described in the Description of Input Data.

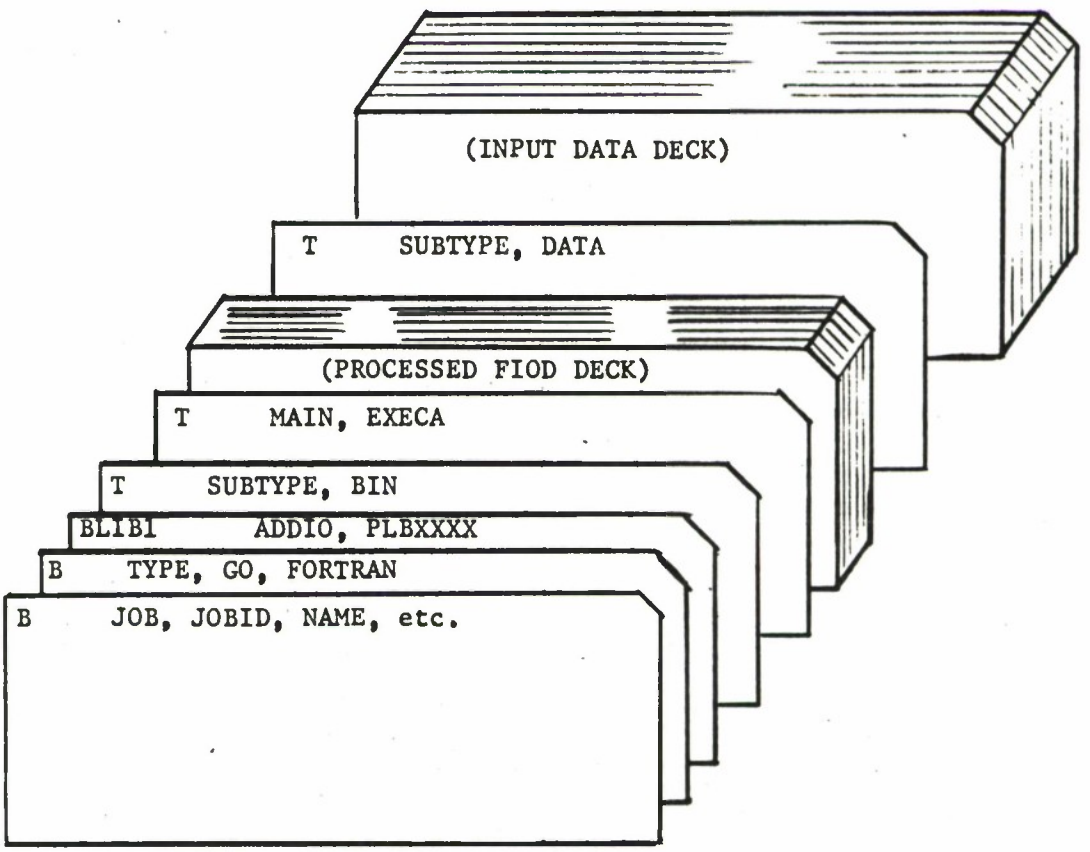

Figure 30. Deck Setup

SECTION IV.
PROGRAMMING

GENERAL FLOW OF PROGRAM

The general flow of the program is shown in Figure 31. The user does not need to specify the number of cases to be run, as the program returns to read the data for the next case until all data cards are exhausted.

The program structure and linkage of the program between basic routines is shown in Figure 32. It is to be noted, however, that the figure does not indicate every linkage but only the major ones. For instance, in some cases it is necessary for OBSERA (which usually only computes observations) to call the integration package.

The routines listed under the heading of General Routines, in Figure 32 are used by many of the major routines. The linkage of these routines is not included as this would defeat the purpose of the figure, which is to indicate the position of the major routines in the overall structure of the program.

DESCRIPTION OF SUBROUTINES

The following part of the document gives a brief description of the subroutines used by SPACE-A. Each subroutine description gives the purpose and a brief description of the subroutine, as well as the other subroutines which call and are called by the given subroutine. For understanding the details of each subroutine one ought to refer to the pertinent portions of Section II and Section III dealing with the function of that subroutine as well as referring to the computer listing.

It should be noted that, as of the writing of this document, certain subroutines have not been tested. These non-operational subroutines are: LUNOBL, MVDRAG, OBD, PFINIT, PFLGHT, STACUL. These subroutines deal with lunar oblateness gravitational perturbations,

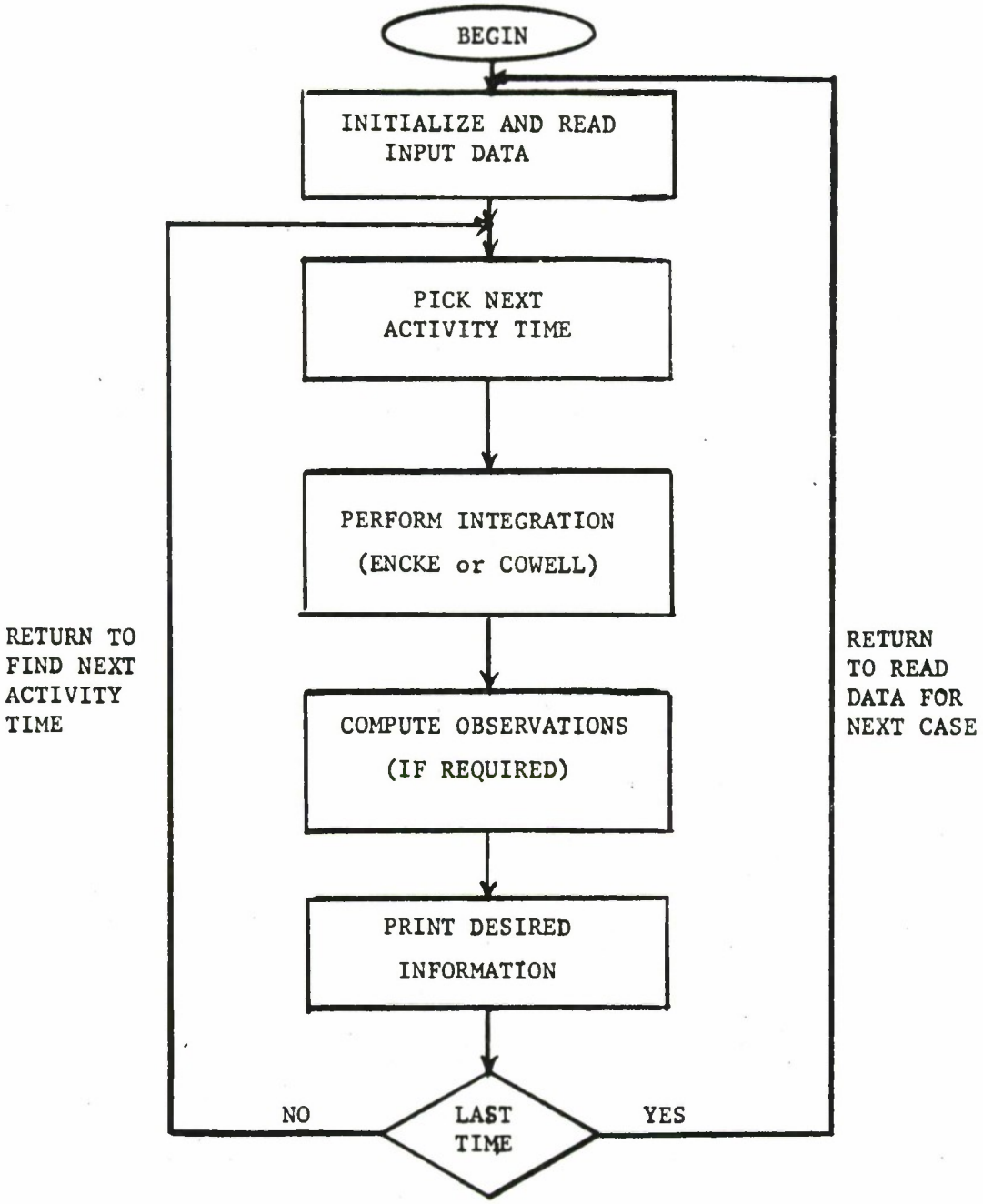

Figure 31. General Flow of Program

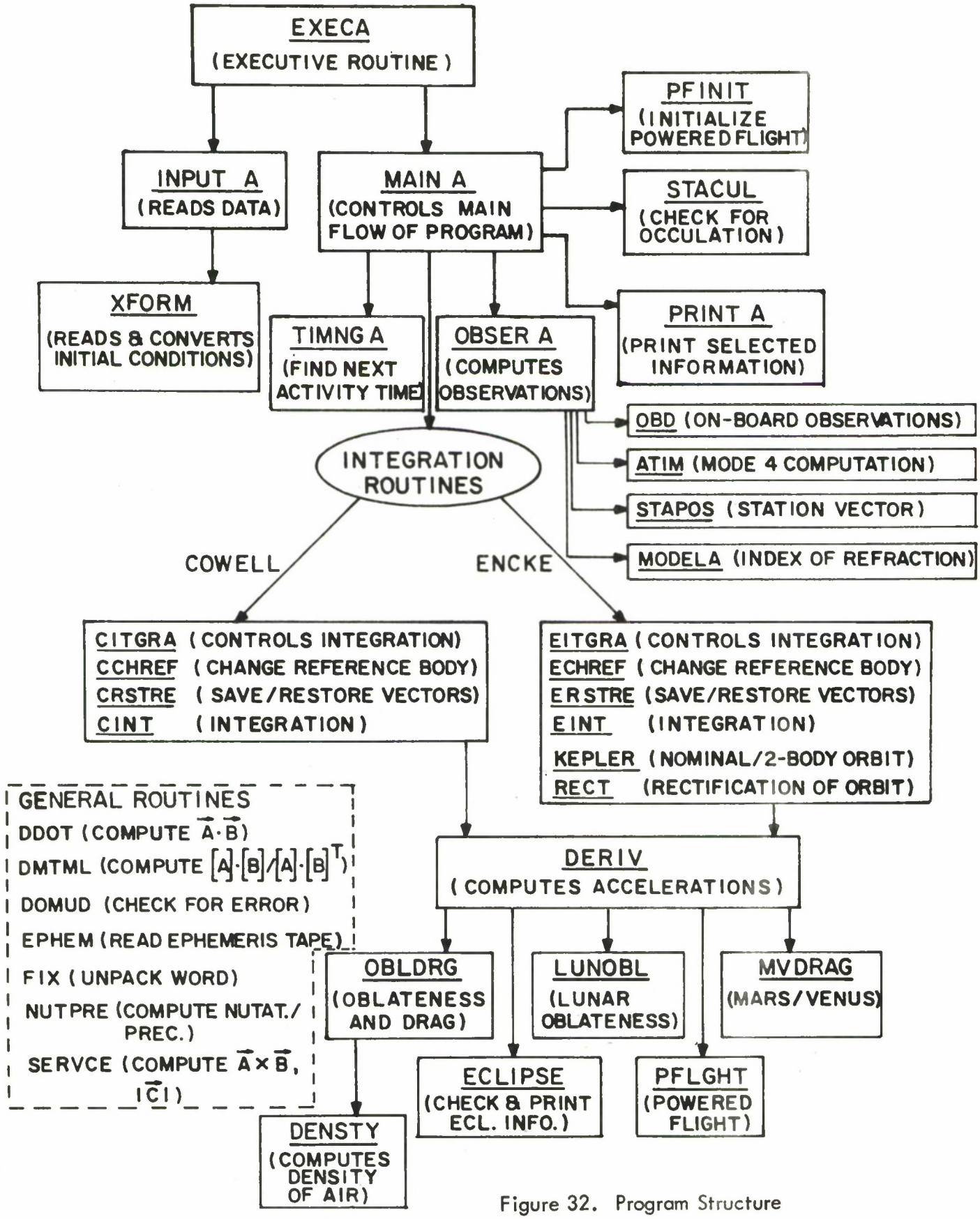

Figure 32. Program Structure

IA-872 D-84

Mars and Venus drag model, on-board observations, perturbations due to vehicle thrust, and observations dealing with occultation.

EXECA

Purpose:

This is the executive routine for SPACE-A.

Description:

The program alternates between calling INPUTA and MAINA until all cases have been exhausted.

Subroutines Called: INPUTA, MAINA

ATIM

Purpose:

This subroutine is used in the visibility computation mode (mode 4). It determines the time a vehicle comes within sight of a given ground station or the time of polar baseline crossing (the time that the vehicle crosses the east-west vertical plane through the zenith) and meridian crossing.

Description:

When the vehicle is in sight, the ℓ and m direction cosines are tested and used to interpolate for the times of polar and meridian crossings. When the acquisition time is to be determined, the integration routines CINT and EINT or the two-body routine KEPLER is employed to predict ahead until the vehicle comes into view.

Called By: OBSERA

Subroutines Called: CINT, CRSTRE, EINT, ERSTRE, KEPLER

CCHREF

Purpose:

This subroutine tests criteria for changing the reference body when the Cowell integrator is used. Even though a change of reference body in the Cowell method is not necessary, it is utilized in the program in the same manner as in the Encke integrator.

Description:

Criteria for changing the reference body based on regions of influence are tested.

Called By: CITGRA

Subroutines Called: DDOT, EPHEM, SERVCE

CINT (EINT)

Purpose:

This subroutine performs the integration when the Cowell formulation is employed.

Description:

The Gill modification of Runge-Kutta is used for short-term integration and as a starting procedure for the Nordsieck long-term integration.

Called By: ATIM, CITGRA, MAINA, OBSERA

Subroutines Called: CCHREF, CINT, CRSTRE

CITGRA

Purpose:

This subroutine serves as the sub-main program governing calls to the integration routines in the Cowell method.

Description:

If not in powered flight, the program checks for a change of reference bodies. The delta of integration is determined by the distance of the vehicle from the reference body and integration is performed up to the next activity time by calling the integration routine.

Called By: MAINA

Subroutines Called: CCHREF, CINT, CRSTRE

CRSTRE (ICR)

Purpose:

This subroutine saves or restores time, position, and velocity

and acceleration of the vehicle at any designated time for the Cowell integrator.

Description:

Depending on the value of the argument (IRC) the information is saved (IRC $\leq$ 1) or restored (IRC > 1).

Called By: ATIM, CITGRA, MAINA, OBSERA

DDOT(A,B)

Purpose:

This function computes the dot product of two vectors.

Description:

The program uses the formula

$$DDOT = A(1)* B(1) + A(2)* B(2) + A(3)* B(3)$$

Called By: CCHREF, DERIV, ECHREF, LUNOBL, MVDRAG, OBD, OBLDRG, OBSERA, PRINTA, RECT, STACUL

DENSTY(X1, X2, X3, DENP, DENEQ)

Purpose:

This subroutine evaluates the density of air in the upper atmosphere.

Description:

Tables of the logarithm of $\rho \cdot C_{av}$ obtained from the Harris-Priester data are stored in this routine. Interpolation is performed to calculate $\log(\rho \cdot C_{av})$ (DENEQ) at the equator as a function of the altitude of the vehicle (X1), solar flux (X2), and solar time (X3). Interpolation is also performed to calculate $\log(\rho \cdot C_{av})$(DENP) at the poles, as a function of the altitude and solar flux.

Called By: OBLDRG

DERIV

Purpose:

This subroutine evaluates the acceleration terms for the Encke

and Cowell integrators.

Description:

This subroutine computes the planetary perturbations and the solar radiation pressure perturbations as presented in the theory section of this manual. Earth oblateness perturbations and drag are computed by calling OBLDRG. Provisions are included for computing powered flight accelerations.

Called By: CINT, EINT

Subroutines Called: DDOT, DOMUD, ECLIPS, EPHEM, KEPLER, LUNOBL, MVDRAG, OBLDRG, PFLGHT, SERVCE

DMTML (A, B, C, I, J, K, L, M, N, IAC, JAB, KBC, IFLAG)

Purpose:

This subroutine multiplies two matrices of any size (up to 26 × 26), or two matrices in which the second is transposed.

Description:

The matrices A, B, and C are dimensioned I × J, K × L, and L × M respectively.

When IFLAG = 0, 1, multiplication is done by rows of A so that A can be overwritten if desired (i.e., the argument C in the calling sequence may actually be the same as A).

When IFLAG = 2, 3, multiplication is done by columns of B and the result is stored in B.

The following table summarizes the results of the program for various values of IFLAG.

IFLAG	COMPUTE	STORE RESULT IN
0	$A \cdot B^T$	C
1	$A \cdot B$	C
2	$A \cdot B^T$	B
3	$A \cdot B$	B

IAC is the number of rows of A and C to be used,

JAB is the number of columns of A and rows of B (or B^T) to be used,

IBC is the number of columns of B (or B^T) and C to be used.

Called By: LUNOBL, NUTPRE, OBLDRG, OBSERA, STACUL, STAPOS, XFORM

DOMUD (TEST)

Purpose:

This subroutine checks for errors.

Description:

The Overflow and Divide Check indicators are checked. If either is on, and the argument TEST is not equal to zero, TEST is assumed to be a BCD word and the message "ERROR IN 'TEST'" is printed.

Called By: DERIV, KEPLER, NUTPRE, OBLDRG, OBSERA, PRINTA, RECT, STAPOS, XFORM

ECHREF

Purpose:

This subroutine tests criteria for changing the reference body when the Encke integrator is used.

Description:

Criteria for changing the reference body based on regions of influence are tested.

Called By: EITGRA

Subroutines Called: DDOT, EPHEM, KEPLER, SERVCE

ECLIPS (J, K)

Purpose:

This subroutine checks for a change in the illumination of the vehicle and prints out an appropriate message when the vehicle changes between the three states: umbra, penumbra, or sunlight.

Description:

This first argument in the calling sequence indicates whether the reference body is the Earth (J=1), the Moon (J=2), or some other

body (J>2). The second argument indicates whether the vehicle is in the umbra (K=1), penumbra (K=2), or sunlight (K=3). Values of the second argument are saved from one entry to the next and hence a simple comparison is made for determining a change in vehicle status. If a change has occurred, a message is printed containing the reference body, the time of change and the entered state (umbra, penumbra, sunlight).

Called By: DERIV

EINT (IENT)

Purpose:

This subroutine performs the integration when the Encke method is employed.

Description:

The Gill modification of Runge-Kutta is used for short-term integration and as a starting procedure for the Nordsieck long-term integration.

Called By: DERIV

Subroutines Called: ATIM, EITGRA, OBSERA

EITGRA

Purpose:

This subroutine serves as the sub-main program governing calls to the integration routines in the Encke method.

Description:

If not in powered flight, the program checks for a change of reference bodies. The delta of integration is determined by the distance of the vehicle from the reference body and integration is performed up to the next activity time by calling the integration routine. Frequent checks are also made on the magnitude of the deviations from the nominal orbit. If the magnitudes increase beyond specified limits, a rectification of the orbit is accomplished by calling RECT.

Called By: MAINA

Subroutines Called: ECHREF, EINT, ERSTRE, KEPLER, RECT

EPHEM

Purpose:

This subroutine evaluates the position and velocity vectors of each of the seven bodies with respect to the reference body.

Description:

Tabular planetary positions are read from an ephemeris tape and Everett's interpolation formula is fitted to six points. It is evaluated to find the position vector and its derivative is evaluated to find the velocity.

Called By: CCHREF, DERIV, ECHREF, STACUL

Subroutines Called: SERVCE

ERSTRE (IRC)

Purpose:

This subroutine saves or restores time, position, velocity, and acceleration of the vehicle at any designated time for the Encke integrator.

Description:

Depending on the value of the argument (IRC) the information is saved (IRC $\leq$ 1) or restored (IRC > 1).

Called By: ATIM, EITGRA, MAINA, OBSERA

FIX (KTEMP, ITEMP, KNAME)

Purpose:

This subroutine unpacks a word into five separate words.

Description:

The argument KTEMP is assumed to contain a number of the form VVWWXXYYZZ. The word is unpacked and stored as follows:

KNAME = VV

ITEMP(1) = ZZ

ITEMP(2) = YY

ITEMP(3) = XX

ITEMP(4) = WW

Called By: OBSERA

INPUTA

Purpose:

This subroutine reeds all data necessary for one run.

Description:

The subroutine initializes necessary data and reads in sections desired.

Called By: EXECA

Subroutines Called: XFORM

KEPLER

Purpose:

This subroutine computes the two-body position and velocity vectors.

Description:

A Newton Raphson scheme is used to determine the differential eccentric anomaly. After convergence, the two-body position end velocity vectors are evalueted. The subroutine uses Herrick's method.

Called By: ATIM, DERIV, ECHREF, EITGRA, OBSERA, STACUL

Subroutines Called: SERVCE, DOMUD

LUNOBL(K)

Purpose:

This subroutine computes the acceleration due to lunar oblateness. Optionally, it can compute the libration and effect of the eerth's J_{20} term.

Description:

When K = 1, the libration matrix is computed and then precessed and nutated.

When K = 2, the Earth's J_{20} obleteness term is calculated.

When K = 3, both lunar and Earth oblateness (J_{20} term) are computed.

Called By: DERIV, OBD

Subroutines Called: DDOT, DMTML, NUTPRE, SERVCE

MAINA

Purpose:

This subroutine handles the main flow of the program.

Description:

The routine calls subroutines which determine the next activity time, govern the integration, compute the observations, and print the chosen information.

Called By: EXECA

Subroutines Called: CITGRA, CRSTRE, EITGRA, ERSTRE, OBSERA, PFINIT, PRINTA, RECT, SERVCE, STACUL, TIMNGA

MODELA(K)

Purpose:

This subroutine computes the index of refraction for the troposphere or ionosphere.

Description:

The index of refraction is computed with the tropospheric model when K = 1 and the ionospheric model when K = 2.

Called By: OBSERA

MVDRAG

Purpose:

This subroutine computes the perturbations due to drag in the atmospheres of Mars or Venus.

Description:

The coefficient of drag is determined by interpolation from given

tables as a function of altitude and the velocity of the vehicle.

Called By: DERIV

Subroutines Called: DDOT, SERVCE

NUTPRE(K)

Purpose:

This subroutine computes the expressions for determining the Greenwich hour angle, as well as the rotational matrices between coordinate systems.

Description:

When K = 1, the expressions used in the nutation matrix and the libration matrix are computed.

When K = 2, the rotation matrix through the Greenwich hour angle is computed.

When K = 3, the precession-nutation matrix is computed.

Called By: LUNOBL, OBLDRG, PRINTA, STAPOS, XFORM

Subroutines Called: DMTML, DOMUD

OBD

Purpose:

This subroutine computes observations from on-board instrumentation.

Description:

The subroutine uses present position of vehicle with respect to reference bodies, landmarks, or ground stations to determine observations.

Called By: OBSERA

Subroutines Called: DDOT, LUNOBL, SERVCE, STAPOS

OBLDRG

Purpose:

This subroutine computes the oblateness and air drag perturbations due to the Earth and its atmosphere.

Description:

Oblateness is computed in a flexible algorithm which can be used for zonal, tesseral, or sectorial harmonics of any order. The drag perturbation is computed from the Harris-Priester tables (at high altitudes) and the U. S. Standard Atmosphere (at low altitudes).

Called By: DERIV

Subroutines Called: DDOT, DENSTY, DMTML, DOMUD, NUTPRE, SERVCE

OBSERA

Purpose:

This subroutine computes the observables as seen from a given ground station.

Description:

Given present vehicle location and ground station location, both referenced to inertial space, the observed values are computed. When specified, refraction corrections are included. When in mode 4, the total time in sight at the station is also computed.

Called By: MAINA

Subroutines Called: ATIM, CINT, CRSTRE, DDOT, DMTML, DOMUD, EINT, ERSTRE, FIX, KEPLER, MODELA, OBD, SERVCE, STAPOS

PFINIT

Purpose:

This subroutine performs initialization procedures at the entry of a burn period.

Description:

The subroutine determines coefficients of six Chebyshev polynomials which are valid for the first burn period.

Called By: MAINA

PFLGHT

Purpose:

This routine computes the effect of a thrust perturbation in the Encke method.

Description:

The thrust acceleration vector at the initial burn time, the vehicle mass and mass rate are converted to a set of coefficients for 6 Chebyshev polynomials. These coefficients are determined in PFINIT. The subroutine, PFLGHT, uses these coefficients to describe the powered flight trajectory as a function of time. Effectively, the subroutine replaces KEPLER in Encke's method. Integration of the equations of motion continues exactly as if powered flight was not involved.

Called By: DERIV

Subroutines Called: SERVCE

PRINTA

Purpose:

This subroutine prints out current trajectory information and observations.

Description:

Depending on whether the time entered corresponds to a print time, the program checks each of the ten elements in the IPSEC array. If the value is > 0, the corresponding section is printed.

To determine whether it is a print time, the subroutine first checks to see whether the present time is within the print portion (DTPI) of a total print period (TAU). If not, no printing is done. If so, it next checks the value of the print interval within DTPI (PRATE). If it is negative, it always prints. If it is positive, and it is the first time into the present print period, it prints, otherwise no printing is done. When MDE = 1 or 4, printing occurs at each entry to the routine.

Called By: MAINA

Subroutines Called: DDOT, DOMUD, NUTPRE, SERVCE

RECT

Purpose:

This subroutine computes the parameters pertinent to a rectification in Encke's method.

Description:

The two-body position and velocity vectors are equated to the true position and veolcity vectors. In addition, these components are saved. Perturbations in position and velocity are set equal to zero, and elements used by the KEPLER subroutine are computed.

Called By: EITGRA, MAINA

Subroutines Called: DDOT, DOMUD

SERVCE (A, B, C, I)

Purpose:

This subroutine computes the cross product of two vectors as well as the magnitude, magnitude squared and magnitude cubed of a vector.

Description:

When I = 1, the cross product of A and B is computed and the result stored in C(1), C(2), and C(3), and then continues as when I = 2.

When I = 2, the magnitude cubed, magnitude, and magnitude squared is stored in C(4), C(5), and C(6), respectively.

Called By: CCHREF, DERIV, ECHREF, EPHEM, KEPLER, LUNOBL, MAINA, MVDRAG, OBD, OBLDRG, OBSERA, PFLGHT, PRINTA, STACUL

STACUL

Purpose:

This subroutine determines the time of occultation (YCOM(23)). One of two types of occultation may be considered, vehicle or star occultation.

Description:

A Newton-Raphson iteration is used on the two-body solution to determine the time of occultation. When considering star occultation, the occulting body is the reference body, except in the Earth-Moon system, in which either the Moon or the Earth can do the occulting. Vehicle occultation occurs only in Moon reference. Up to three different ground stations may be considered for occultation.

Called By: MAINA

Subroutines Called: DDOT, DMTML, EPHEM, KEPLER, SERVCE, STAPOS

STAPOS

Purpose:

This subroutine computes the station position and velocity vectors.

Description:

Given the geodetic latitude, longitude, and altitude of the station, the coordinates of the station in the Greenwich coordinate system are computed. A rotation through the Greenwich hour angle then brings the coordinates into the inertial system. The velocity of the station is computed from the rotational speed of the earth.

Called By: OBD, OBSERA, STACUL

Subroutines Called: DMTML, DOMUD, NUTPRE

TIMNGA

Purpose:

This subroutine determines the next activity time (i.e., the next time at which an observation is to be computed or a printout of the trajectory is to occur).

Description:

Logic is set up for establishing an array of times of interest from which the earliest time is selected. Flags are set when the time selected is the final time or when a time is repeated.

Called By: MAINA

XFORM

Purpose:

This routine accepts the input information concerning the vehicle's initial conditions, and transforms them into the proper units and coordinate system.

Description:

After the initial conditions and associated flags are read in (Section 2 of the group I inputs), the program converts them into the position and velocity vectors in the units of the Earth radii, and Earth radii/hour. Then, if desired, the vectors are transformed into the base date system.

Called By: INPUTA

Subroutines Called: DMTML, DOMUD, NUTPRE

REFERENCES

1. Sequential Position and Covariance Estimation Trajectory Program (SPACE) Analytic Manual, prepared by Sperry Rand Systems Group for NASA, Contract NAS-5-3509, April, 1965.

2. User's Manual for Goddard Orbit Determination Program (SPACE), prepared by Sperry Rand Systems Group for NASA, Contract NAS-5-3509, April, 1965.

3. Programmer's Manual for Goddard Orbit Determination Program (SPACE), prepared by Sperry Rand Systems Group for NASA, Contract NAS-5-3509, April, 1965.

4. Battin, R.H., Astronautical Guidance, Mc-Graw Hill Book Co., New York, 1964, pp. 11 and 190.

5. Brouwer & Clemence, Methods of Celestial Mechanics, Academic Press, New York, 1961, pp. 117 and 118.

6. Carito, W.A., "The Geopotential and Its Effects Upon Near Earth Satellites", MITRE Technical Report MTR-191, April, 1966, p. 40.

7. U.S. Standard Atmosphere 1962, U.S. Government Printing Office, Washington, D.C., 1962.

8. Ketchum, H.B., Advances in Astronautical Sciences, Plenum Press, 1957, Vol. I, pp. 31-41.

9. Harris, I. & Priester, W., Theoretical Models for the Solar Cycle Variation of the Upper Atmosphere, NASA TND-144, Goddard Space Flight Center, 1962.

10. Baker, R.M.L., Astrodynamics, Academic Press, New York, 1967.

11. Harris, I. & Priester, W., Relation Between Theoretical and Observational Models of the Upper Atmosphere, NASA X-640-63-145, Goddard Space Flight Center, 1963.

12. Wolverton, R.W., ed., Flight Performance Handbook for Orbital Operations, John Wiley & Sons, Inc., New York, 1963, p. 2-389.

13. Gill, S., "A Process for the Step-by-Step Integration of Differential Equations in an Automatic Digital Computing Machine", Proceedings of Cambridge Philosophical Society, Vol. 47, Part 1, pp. 96-108.

14. Explanatory Supplement to the Ephemeris, Her Majesty's Stationery Office, London, 1961.

15. Weisbrod & Anderson, "A Simple Method for Computing Tropospheric and Ionospheric Effects on Radio Waves", Proceedings of the IRE, October, 1959, pp. 1770-1777.

Security Classification

DOCUMENT CONTROL DATA - R & D

(Security classification of title, body of abstract and indexing annotation must be entered when the overall report is classified)

1. ORIGINATING ACTIVITY (Corporate author)	2a. REPORT SECURITY CLASSIFICATION
The MITRE Corporation Bedford, Massachusetts	UNCLASSIFIED
	2b. GROUP N/A

3. REPORT TITLE

THE MODIFIED SPACE-A TRAJECTORY GENERATION PROGRAM

4. DESCRIPTIVE NOTES *(Type of report and inclusive dates)*

N/A

5. AUTHOR(S) *(First name, middle initial, last name)*

William L. Wallace, Richard H. Wiggins, Jr.

6. REPORT DATE	7a. TOTAL NO. OF PAGES	7b. NO. OF REFS
November 1968	163	15

8a. CONTRACT OR GRANT NO.	9a. ORIGINATOR'S REPORT NUMBER(S)
AF 19(628)-5165	
b. PROJECT NO. 7070	ESD-TR-68-288
c.	9b. OTHER REPORT NO(S) *(Any other numbers that may be assigned this report)* MTR-733
d.	

10. DISTRIBUTION STATEMENT

This document has been approved for public release and sale; its distribution is unlimited.

11. SUPPLEMENTARY NOTES	12. SPONSORING MILITARY ACTIVITY
N/A	Director of Planning and Technology, Development Engineering Division, Electronic Systems Division, Air Force Systems Command, L. G. Hanscom Field, Bedford, Massachusetts.

13. ABSTRACT

This report describes the SPACE-A program presently available for operational use. SPACE-A is the trajectory and observation generation portion of the Sequential Position and Covariance Estimation Program (SPACE) which is currently under development. The document contains a detailed analysis of the equations and models used by the program, a brief description of routines used in the program, as well as instructions for its operations. The principal applications of SPACE-A are the prediction of the space-vehicle trajectories and the generation of observational data plus other trajectory related information.

DD FORM 1 NOV 65 1473

Security Classification

14 KEY WORDS	LINK A		LINK B		LINK C	
	ROLE	WT	ROLE	WT	ROLE	WT
ORBITAL PREDICTION						
TRAJECTORY COMPUTATION						
OBSERVATION GENERATION						